

GEOLOGY OF THE NAHCOLITE DEPOSITS AND ASSOCIATED OIL  
SHALES OF THE GREEN RIVER FORMATION IN THE PICEANCE  
CREEK BASIN, COLORADO

by

John Richard Dyni

B.S., Wayne State University, 1953

M.S., University of Illinois, 1955

A thesis submitted to the  
Faculty of the Graduate School of the  
University of Colorado in partial fulfillment  
of the requirements for the degree of  
Doctor of Philosophy  
Department of Geological Sciences

1981


This Thesis for the Doctor of Philosophy Degree by  
John Richard Dyni  
has been approved for the  
Department of  
Geological Sciences  
by



Don L. Eicher



Theodore R. Walker



Bruce F. Curtis

Date May 7, 1981

Dyni, John R. (Ph. D., Geology)

Geology of the Nahcolite Deposits and Associated Oil Shales of the  
Green River Formation in the Piceance Creek Basin, Colorado

Thesis directed by Professor Don L. Eicher

At the depocenter of Eocene Lake Uinta in the northern part of the Piceance Creek Basin, Rio Blanco County, Colorado, the lacustrine Green River Formation contains a saline facies composed of nahcolite and halite commingled with kerogenous marlstones (oil shales). Stratigraphic and lithologic studies of drill cores from 10 exploratory holes reveal that five-eighths of the nahcolite resource, estimated at  $29 \times 10^9$  metric tons, occurs as crystalline aggregates in marlstone. The remainder of the resource consists of laterally continuous zones of disseminated nahcolite in marlstone and beds of mixed nahcolite and halite.

Sedimentologic data indicate that the marlstones and associated sodium minerals were deposited by pelagic, turbiditic, and evaporitic processes in a permanent alkaline lake. About half of the marlstones of the saline facies are laminated and accumulated slowly by pelagic sedimentation of seasonally precipitated carbonate, organic detritus, and fine-grained siliciclastic sediment supplied by surface currents. Organic-rich marly sediments were swept out into the deeper parts of the lake by episodic density currents. These sediments are represented by blebby and streaked kerogenous marlstones that comprise nearly one-half of the marlstones in the saline facies. Bedded nahcolite and halite precipitated during maximum evaporative stages of the lake.

Lower lake waters and sediments were anoxic and favored

high rates of bacterial reduction of sulfate and hydrolysis of fine-grained detrital silicate minerals. These processes resulted in production of bicarbonate and the formation of an authigenic suite of carbonate and silicate minerals devoid of clay and sulfate minerals.

Cyclic, probably seasonal, stratification is recorded by the laminated marlstones and in some units of disseminated and bedded nahcolite and halite. The vertical distribution of total sulfur in the marlstones is also cyclic and may be related to evaporative phases of the lake. Bromine values that increase generally upward through the halitic rocks of the saline facies indicate the existence of residual lake brines and suggest that the lake never evaporated to dryness during Parachute Creek time.

The form and content of this abstract are approved.  
I recommend its publication.

Signed \_\_\_\_\_

Faculty member in charge of thesis

## ACKNOWLEDGMENTS

The writer gratefully acknowledges the help of many people during the course of this investigation. Messrs. Irvin Nielsen, Edward C. Rosar, Joe T. Juhan, and Joe T. Juhan, Jr. made available many of the drill cores on which this study is based. The Laramie Energy Technology Center, Department of Energy, made all of the shale-oil assays except those for core holes C177 and C179 which were made by Tosco Corp., Golden, Colo. The able assistance of P. C. Beck, T. K. Martin, J. W. Blair, Jr., and J. L. Porterfield in making nahcolite and other chemical analyses in the Denver laboratories of the U.S. Geological Survey is acknowledged. Computer plots of the shale-oil analyses were prepared by the Computer Division of the U.S. Geological Survey aided by J. K. Pitman. J. R. Donnell served as Chief of the Oil Shale Section while this study was in progress. Thanks are due Steven Utter and James E. Hawkins, U.S. Bureau of Mines, for arranging a visit to the Bureau's Horse Draw mine to examine nahcolite bed L-4D. Special thanks are due Robert J. Hite, who collaborated with the writer on the early work on the nahcolite deposits, and with whom the writer has had many discussions on the origin of the salines and oil shale over the years that this investigation was in progress.

TABLE OF CONTENTS

	Page
ACKNOWLEDGMENTS.....	iii
LIST OF TABLES.....	vi
LIST OF PLATES AND FIGURES.....	vi
CHAPTER	
I. INTRODUCTION.....	1
Previous Investigations.....	6
Geologic Setting.....	8
Structure.....	14
Methods of Study.....	15
II. GREEN RIVER FORMATION.....	20
III. LITHOLOGY OF THE SALINE FACIES.....	25
Nahcolite Aggregates and Disseminated Nahcolite...	27
Bedded Nahcolite and Halite.....	42
Kerogenous Marlstones.....	50
Micro-Faults and "Loop Bedding".....	61
IV. COMPOSITION OF THE MARLSTONES.....	63
Mineral Distributions.....	78
V. GEOCHEMISTRY OF SULFUR.....	83
VI. LACUSTRINE DEPOSITIONAL MODEL.....	91
Hydrographic Basin and Sediment Sources.....	91
Lake-Basin Morphology.....	96
Lake Waters.....	102
Lateral continuity of beds and laminae.....	102
Vertical succession of sodium minerals	

	and illite.....	103
	Bromine-bearing halite.....	104
VI.	LACUSTRINE DEPOSITIONAL MODEL--continued	
	Lake Waters--continued	
	Geochemical model of lake waters.....	108
	Sources of Bicarbonate.....	111
	Bacterial sulfate reduction.....	111
	Other bicarbonate sources.....	116
	Processes of Sedimentation.....	117
	Turbiditic sedimentation.....	117
	Pelagic sedimentation.....	121
	Evaporitic sedimentation.....	122
VII.	CONCLUSIONS.....	126
	REFERENCES CITED.....	129
	APPENDIX.....	139

## LIST OF TABLES

Table	1. Name and location of 10 core holes.....	16
	2. Amounts of aggregate, disseminated, and bedded nahcolite in 10 core holes.....	26
	3. Frequency of nahcolite aggregates in two core holes.....	31
	4. Quantitative mineralogy of nahcolitic marlstone in core hole C5.....In Appendix	
	5. Inferred composition of surface waters that fed Lake Uinta.....	112

## LIST OF PLATES AND FIGURES

		Page
Plate	1. North-south stratigraphic cross section of the nahcolite deposits of the Green River Formation in the northern part of the Piceance Creek Basin, Colorado.....in pocket	
	2. East-west stratigraphic cross section of the nahcolite deposits of the Green River Formation in the northern part of the Piceance Creek Basin, Colorado.....in pocket	
	3. North-south stratigraphic cross section of nahcolite bed L-4D in the northern part of the Piceance Creek Basin, Colorado.....in pocket	
	Explanation for plates 1 and 2.....in pocket	
Figure	1. Map of the Green River and Flagstaff Formations in Colorado, Utah, and Wyoming.....	9
	2. Map showing the distribution of nahcolitic rocks and halite in the Piceance Creek Basin.....	21
	3. Photographs of nahcolite aggregates in marlstone.	28
	4. Size distribution of nahcolite aggregates in two core holes.....	30
	minerals in nahcolite aggregates.....	33
	6. Photographs of disseminated nahcolite.....	36



Figure	7.	Frequency distribution of the nahcolite content in 11 units of disseminated nahcolite.....	38
	8.	Photographs of laminae in disseminated nahcolite at the top of subzone R-3F in three core holes....	40
	9.	Photographs of bedded nahcolite and halite.....	43
	10.	Subsurface lithofacies map of nahcolite-halite bed R-5C.....	47
	11.	Photographs of couplets of halite and nahcolite..	48
	12.	Photographs of blebby and streaked marlstone.....	51
	13.	Shale-oil content of laminated marlstone and blebby and streaked marlstone.....	56
	14.	Dawsonite content of laminated marlstone and blebby and streaked marlstone.....	57
	15.	Comparison of mineral carbon determined by chemical analysis with mineral carbon computed from table 4.....	68
	16.	Comparison of organic carbon determined from Fischer assays with organic carbon determined by chemical analysis.....	69
	17.	Comparison of water-soluble weight loss with nahcolite determined by thermal method.....	70
	18.	Comparison of acid-soluble weight loss with carbonates calculated from table 4.....	71
	19.	Comparison of acid-insoluble weight with the sum of silicate minerals and kerogen.....	72
	20.	Comparison of the acid-soluble weight loss with the sum of the weights of carbonate minerals from table 4.....	74
	21.	Comparison of acid-soluble calcium with the sum of acid-soluble magnesium and iron.....	75
	22.	Compositional fields for marlstones in core hole C5.....	76
	23.	Stratigraphic distribution of minerals in the saline facies.....	79
	24.	Scanning electron photomicrographs of iron sulfides.....	85

Figure 25.	Vertical profiles of sulfur values in two core holes.....	88
26.	Estimated areas of the hydrographic basin and maximum extent of Lake Uinta.....	92
27.	Vertical profiles of bromine analyses of halite.....	106
28.	Isothermal section for saturated solutions in the system $\text{Na}_2\text{CO}_3\text{-NaHCO}_3\text{-NaCl-H}_2\text{O}$ .....	110

## CHAPTER I

### INTRODUCTION

Saline minerals in lacustrine rocks of the Green River Formation in Colorado and Utah have been known for 50 years through the work of W. H. Bradley. Bradley (1931, pls. 3, 5, and 6; p. 32-36) recognized the former presence of several "saline phases" in outcrops of the formation in Colorado and Utah by empty molds of crystals and crystal aggregates of then unknown saline minerals. He interpreted these "saline phases" as evidence of several evaporative stages of Eocene Lake Uinta during which the Green River Formation was deposited. The salts were identified by Ertl (1947) and Glass (1947) who reported the occurrence of nahcolite ( $\text{NaHCO}_3$ ) in crystalline aggregates scattered through oil shale in the Anvil Points experimental oil-shale mine near Rifle, Colo.

Subsequent stratigraphic studies of outcrops and core from shallow drill holes around the margins of the Piceance Creek Basin north of the Colorado River revealed many thin zones of empty saline crystal cavities ascribed to gypsum-anhydrite(?) in the upper part of the formation (Duncan and Denson, 1949; Waldron and others, 1951; Donnell and others, 1953; and Donnell, 1961). Smith (1963, fig. 3) first noted the occurrence of dawsonite [ $\text{NaAl}(\text{OH})_2\text{CO}_3$ ] in the Colorado oil-shale deposits. However, sodium minerals in the lower part of the formation and their economic potential were not known until the oil-shale deposits in the deeper part of the basin were drilled.

Between 1959 and 1964, 11 core holes were drilled on Federal oil and gas leases in the northern part of the Piceance Creek Basin. These wells encountered a saline facies in the lower part of the Parachute Creek Member of the Green River Formation. Large quantities of nahcolite and halite, commingled with high-grade oil shale, were found; however, this information was not publically available at the time the wells were drilled. Between 1964 and 1966, a series of eight exploratory holes were drilled specifically for sodium minerals in the Green River Formation under Federal sodium permits in the same part of the basin. These wells also encountered large quantities of nahcolite, halite, and dawsonite. The first of these sodium exploratory holes, the Joe T. Juhan core hole 4-1, drilled in 1964 in sec. 4, T. 2 S., R. 98 W., Rio Blanco County, Colorado, is considered the discovery well for sodium minerals in the basin.

The presence of nahcolite and dawsonite has greatly increased the potential economic value of the Colorado oil-shale deposits. The in-place resource of shale oil alone (>63 liters of shale oil per metric ton of rock) is estimated to be  $172 \times 10^9$  metric tons. The in-place nahcolite resource is estimated at  $29 \times 10^9$  metric tons and dawsonite at  $26 \times 10^9$  metric tons which contains  $5.9 \times 10^9$  metric tons of alumina (Federal Energy Administration, 1974, p. 105; Dyni, 1974, p. 120; and Beard and others, 1974, p. 101). The Colorado oil-shale deposits and their associated sodium carbonate minerals constitute an enormous fossil fuel and industrial-mineral resource.

Aside from its economic interest, the Green River Formation

has been studied by many investigators because of its unusual authigenic minerals, fauna and flora, stratigraphy, sedimentology, and geochemistry. From this large body of information, two depositional models have been proposed; a stratified lake model and a playa-lake model. Debate on the merits of each continues today.

The earlier stratified-lake model was developed in a series of papers by Bradley (1930, 1931, 1936, 1948, 1963, and 1964), of which the earliest three pertain to Lake Uinta and the others to Lake Gosiute, the Eocene Lake in which the formation was deposited in southwest Wyoming.

Summarizing the three earliest reports, Bradley proposed that the lacustrine rocks of the Green River Formation in Colorado and Utah were deposited in a shallow (15-30 m), nearly flat-bottomed lake, which formed by tectonic downwarping. The lake waters became thermally stratified, and for long periods of time, varved sediments including the bulk of the oil shale accumulated in a lower anoxic hypolimnion that was devoid of macroscopic burrowing animals or rooted plants. In its early to mature development, when the climate was warm and humid, Lake Uinta was a freshwater lake with an outlet to the sea. There followed a long arid period, accompanied by intermittent volcanism, when the lake contracted in size, lost its outlet, and became saline. Salts, some rich oil shale, thin beds of tuff, and other sediments were deposited. At times, aridity was severe enough to contract the lake to perhaps a series of ponds that approached playa conditions. The climate again became moist, and the lake freshened, expanded, and overflowed. Finally, tectonic downwarping ceased, and the lake

basin filled with tuffaceous fluviatile sediments.

Supposed problems with Bradley's version of a stratified lake model for the deposition of the Green River Formation in Wyoming led Eugster, Surdam, and coworkers to propose a playa-lake model for part of the formation including much of the Tipton and all of the Wilkins Peak Members (Eugster and Surdam, 1971, 1973; Wolfbauer and Surdam, 1974; Eugster and Hardie, 1975; Surdam and Wolfbauer, 1975; and Buchheim and Surdam, 1977). The idea of a playa environment for part of the Green River Formation was proposed previously by White (in Twenhofel, 1926, p. 302-303, fig. 40) who cited evidence of shallow-water or subaerial sedimentary structures in Green River oil shales. Bradley (1925 and 1931) with reference to White's work suggested that playa conditions may have prevailed during arid periods in the history of the Eocene lakes.

The playa-lake model of Eugster, Surdam, and coworkers is likened to Deep Spring playa, California; but on a much larger scale, in which a central, shallow, saline lake is fringed by broad, nearly flat, playa mudflats, with alluvial fans beyond. Calcite and protodolomite formed in the near-surface capillary zone of the playa mudflats. Low-sulfate alkaline waters, evolved in the playa sediments and moved via subsurface drainage and spring seepage toward the central lake. Organic-rich sediments, derived from periphytic blue-green algae, were deposited in the lake. During periods of extreme aridity, lake waters evaporated seasonally, commonly to complete dryness, and deposited trona and halite. During episodic flooding of the basin in pluvial periods, some of the fine-grained carbonate muds were swept into the central

part of the basin. These sediments formed the dolomitic mudstones that are intercalated with the lacustrine oil shales and evaporites. Under a closed-basin regime, shoreline emergence and submergence was highly variable as evidenced by extensive interfingering of playa and lake sediments; 40 or more alternations of such sediments have been noted. Lateral persistence of playa and lake sediments perpendicular to the shoreline indicate low-depositional dips; most estimates range from 0.1 to 0.4 m/km.

Most of the evidence for the playa-lake model was developed from study of surface sections around the margins of the Green River Basin, which contain sedimentary structures that are believed to be indicators of very shallow water deposition and frequent subaerial exposure of sediments. Lundell and Surdam (1975), citing similar evidence from basin-margin sediments, extended the model to include the Parachute Creek Member of the Green River Formation in the Piceance Creek Basin, Colorado.

From evidence gathered mostly from drill cores of the basin-center sediments in the Piceance Creek Basin, probably as many problems are raised by a playa-lake model as those by a stratified permanent lake. As Bradley (1973, p. 1122) succinctly stated, "\* \* \* in the deposits of any extinct lake, one must be mindful of the fact that some sediments represent marginal facies of the former lake, whereas other sediments represent midbasin facies."

This investigation is a subsurface study of the nahcolite deposits in the Green River Formation in the northern part of the Piceance Creek Basin, in northwestern Colorado. The detailed

stratigraphy of the nahcolite deposits is developed from lithologic data from 10 core holes and a surface measured section, and the occurrence and distribution of the evaporites are described. Mineralogical, geochemical, and sedimentological data that bear on the origin of these rocks are presented. From these data, and from published reports, a depositional model for the saline facies is developed.

Processes believed to be important in the origin of these rocks include tectonic control of lake-basin morphometry; a permanent body of strongly alkaline lake water with a high productivity of algal and bacterial biomass; sulfate reduction and production of bicarbonate mediated by bacterial processes; and hydrolysis of silicate minerals resulting in the nearly total destruction of clay minerals and precipitation of authigenic aluminocarbonate and silicate minerals.

#### Previous Investigations

Previous geologic investigations considered here pertain to studies of the rocks of the saline facies of the Green River Formation in the Piceance Creek Basin, Colorado. Smith and Milton (1966) described the mineralogy and widespread stratigraphic occurrence of dawsonite in the formation. The preliminary stratigraphy of the saline facies and the economic geology of the nahcolite and dawsonite resources were reported by Hite and Dyni (1967). DeVoto and others (1970) published maps and cross sections on the distribution of extractable aluminum in the dawsonite-bearing oil shales that occur in the deeper part of the basin.



Generalized stratigraphic cross sections of the Parachute Creek Member including the saline facies were published by Trudell and others (1970). Dyni (1974) correlated many laterally continuous units of nahcolite and halite in a detailed subsurface stratigraphic analysis of the saline facies and reported on the nahcolite resources. Beard and others (1974) summarized the nahcolite and dawsonite resources in the basin.

Numerous mineralogical and geochemical studies have been made of the oil-shale and saline deposits. The occurrence and origin of bromine-bearing halite was discussed by Dyni and others (1970). Brobst and Tucker (1973) used X-ray diffraction methods to study the mineralogy of basin-margin outcrops of lacustrine rocks parts of which are laterally equivalent to the saline facies in the subsurface. Hosterman and Dyni (1972) published a preliminary X-ray diffraction study of the clay mineralogy of the Green River and Wasatch Formations. Williamson and Picard (1974) investigated the carbonate petrology of the formation. Cole (1975) and Cole and Boyer (1978) studied sulfur isotopes and sulfide mineralogy of Green River rocks. Saether (1980) and Stollenwerk (1980) have investigated the distribution of selected elements including fluorine in Colorado oil shale.

A number of workers using a variety of approaches have studied the depositional environments of the Green River Formation in the Piceance Creek Basin. Based on a study of lithofacies, Roehler (1974) envisioned a fresh to saline lake environment with several subenvironments, not unlike the model proposed in broad outline earlier by Bradley (1930). Chemical and sedimentological

evidence indicated to Smith (1974) a similar depositional environment consisting of a chemically stratified sodium carbonate lake. Conversely, Lundell and Surdam (1975) favored a playa-lake environment based on sedimentological evidence from basin-margin exposures. This model was challenged by Desborough (1978) who favored a chemically stratified lake environment based on a microprobe study of the mineralogy and chemistry of the carbonate minerals. Similar conclusions were reached by Cole and Picard (1978) who studied the lateral distribution of detrital and authigenic minerals from shore to basin-center rocks. Many additional papers on the geology of the Green River Formation can be found in a recent bibliography of nearly 900 references by Mullens (1977).

#### Geologic Setting

Lacustrine rocks of the Green River Formation were deposited in a complex of lakes that occupied several early Tertiary structural basins in Wyoming, Utah, and Colorado (fig. 1). North of the Uinta Uplift, in southwestern Wyoming and northwestern Colorado, sediments consisting of carbonates, kerogenaceous marlstones (oil shale), claystones, siltstones, trona ( $\text{NaHCO}_3 \cdot \text{Na}_2\text{CO}_3 \cdot 2\text{H}_2\text{O}$ ), and halite, were deposited in large Gosiute Lake and in small Fossil Lake. South of the uplift in northeastern Utah and northwestern Colorado, lacustrine sediments were deposited in Lake Uinta and in Flagstaff Lake in the Wasatch Plateau of central Utah.

EXPLANATION

Tg, Green River Formation

Tf, Flagstaff Formation

N, Nahcolite

T, Trona

S, Shortlite

H, Halite

M, Mixed sodium carbonate salts

G, Gypsum

U, Unidentified salts

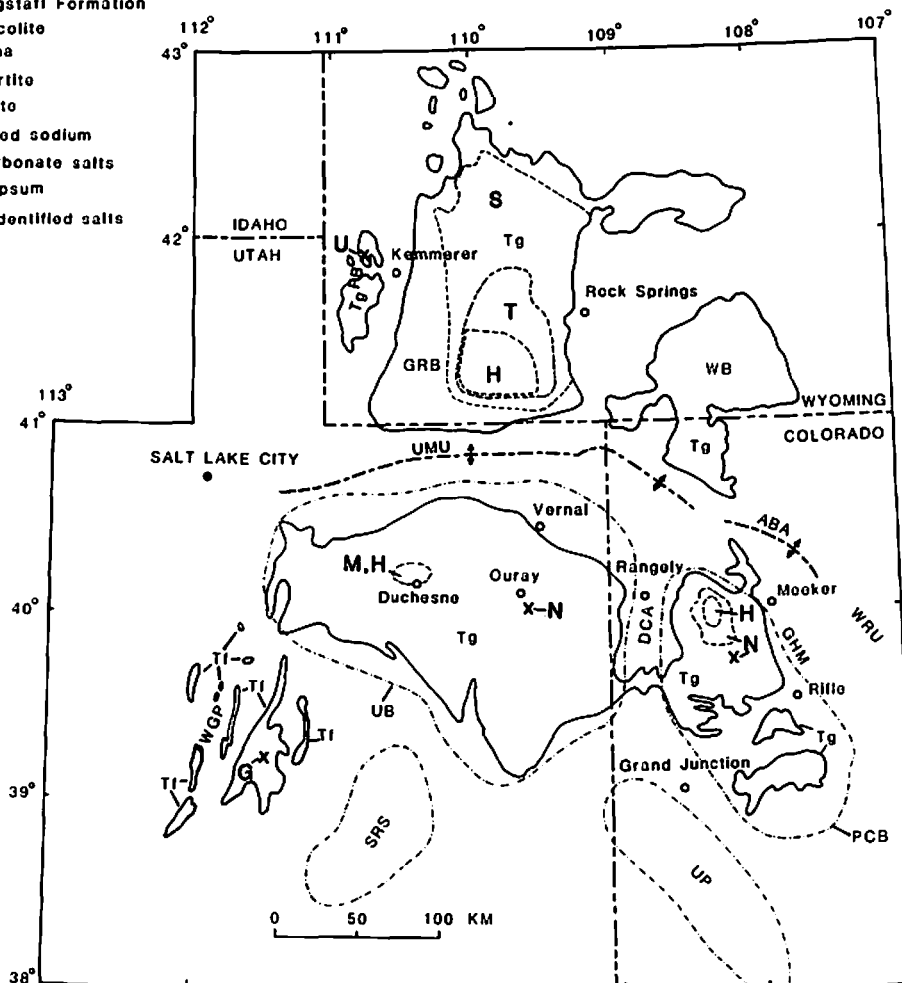


Figure 1.--Map of parts of Colorado, Utah, and Wyoming showing areas occupied by the Green River and Flagstaff Formations, the localities of seven saline facies in the two formations, and some major physiographic and structural features. Where the areal extent of the saline mineral is known, it is shown by a dashed line. If the distribution of the mineral is not known, it is shown by an "X." The distributions of the saline minerals in the Green River Basin, Wyoming, is modified from Culbertson (1971, fig. 1). The areas of outcrop of the Flagstaff Formation are modified from La Rocque (1960, fig. 2). The physiographic and structural features are identified by letters as follows: PCB, Piceance Creek Basin; GHM, Grand Hogback monocline; DCA, Douglas Creek arch; WRU, White River uplift; UP, Uncompahgre Plateau; SRS, San Rafael Swell; WGP, Wasatch and Gunnison Plateaus; UB, Uinta Basin; UMU, Unita Mountain uplift; ABA, Axial Basin anticline; WB, Washakie Basin; GRB, Green River Basin; FB, Fossil Basin.

The earliest sedimentation in the Tertiary-lake complex began with deposition of fossiliferous freshwater limestones, mudstones, and locally, dolomite and gypsiferous evaporites in Flagstaff Lake. This lake occupied a structural basin in the western part of the Rocky Mountain geosyncline along the eastern margin of the Sevier orogenic belt in central Utah (Armstrong, 1968). Sedimentation possibly began in Lake Flagstaff as early as latest Cretaceous (Maestrichtian) time (Ryder and others, 1976, p. 510), and it continued into the Paleocene during the closing phase of the Sevier orogeny (Stanley and Collinson, 1979). Mixed fluvial and lacustrine sediments of about the same and younger age (Claron Formation) were deposited farther south in the southern High Plateaus of southwestern Utah but these strata accumulated probably in a separate basin (Rowley and others, 1979, fig. 1), although Hintze (1973, p. 76-80) suggested that these rocks were once continuous with the Flagstaff Limestone.

In the western part of the Uinta Basin, strata deposited during Paleocene and Eocene time were once continuous with the Flagstaff Formation in the Wasatch Plateau to the south (Abbott, 1957, p. 104; Ryder and others, 1976). During this time, extensive deposits of lacustrine carbonates and claystones, which contain varied amounts of kerogen, and locally sodium carbonate and chloride evaporites, accumulated in Lake Uinta and compose the bulk of the sediments of the Green River Formation. In the Piceance Creek Basin, the earliest Tertiary lacustrine sedimentation is recorded in the upper 275 m of Wasatch Formation, which contains mixed lacustrine and fluvial strata (Snow, 1970, p. 15) that

were deposited simultaneously (but were not continuous) with lower middle Eocene strata (post-Flagstaff Member to "middle marker?") of Ryder and others (1976, fig. 2) in the western part of the Uinta Basin (W. B. Cashion, oral commun., 1979). Uninterrupted lacustrine sedimentation continued in both basins, and eventually, the lake waters joined to form one large lake. In the Piceance Creek Basin, dark fissile clay shale accumulated first, followed by large quantities of kerogen-rich dolomitic rocks (high-grade oil shales). In the northern part of the basin, the dolomitic rocks include a saline facies, which contains large quantities of nahcolite, dawsonite, and halite. When Lake Uinta reached its maximum size in middle Eocene time (Leopold and MacGinitie, 1972) approximately 45 to 46 m.y. ago (Mauger, 1977, p. 32), it spanned an east-to-west distance of about 300 km, and perhaps, as much as 180 km north-to-south. At that time, high-grade oil shale of the Mahogany zone was deposited with small amounts of nahcolite and dawsonite at a depocenter located near the center of Piceance Creek Basin (Smith, 1974, fig. 1). Toward the end of middle Eocene time, mid-lake kerogen-carbonate sedimentation ("open-lacustrine" sediments of Ryder and others, 1976) shifted westward into the eastern part of the Uinta Basin where kerogenous dolomitic rocks, and locally some nahcolite, accumulated. In the Piceance Creek Basin, mid-lake kerogen-carbonate sedimentation gave way to a flood of gravity-flow(?) marly lacustrine siltstones containing carbonized plant fragments (Uinta Formation) (Duncan and others, 1974; O'Sullivan, 1974). The depocenter of mid-lake sedimentation continued to migrate with time toward the western part of the Uinta

Basin. In western Uinta Basin green claystones, dolomitic rocks, minor amounts of siltstone (Evacuation Creek Member of the Green River Formation of Dane, 1955), and an overlying sequence of evaporitic rocks consisting of shortitic and cherty carbonate strata, which contain some kerogen and claystone (saline facies of the Uinta Formation of Dane, 1955) were deposited. At the depocenter near Duchesne, Utah, this evaporite facies contains beds of mixed trona, halite, eitelite  $[\text{Na}_2\text{Mg}(\text{CO}_3)_2]$ , wegscheiderite  $(\text{Na}_2\text{CO}_3 \cdot \text{NaHCO}_3)$ , nahcolite, and other exotic authigenic minerals (J. R. Dyni and Charles Milton, unpublished core hole data). This evaporitic sequence and an overlying sequence of interbedded sandstones and white-weathering limestones containing small amounts of syngenetic(?) gypsum (sandstone and limestone facies of the Uinta Formation of Dane, 1955) form the uppermost lacustrine rocks of the Green River Formation in the Duchesne area (Ryder and others, 1976, fig. 2). Lacustrine sedimentation ended in this area in late middle Eocene time about 40 to 41 m.y. ago (Mauger, 1977, p. 32). Lacustrine sedimentation may have continued episodically into Oligocene time in isolated(?) basins on the Wasatch Plateau (T. D. Fouch, oral commun., 1979), where lacustrine sedimentation had first begun.

Although seven distinct saline facies occur in the lacustrine sediments of Flagstaff Lake, Lake Uinta, and Gosiute Lake, only the oldest facies contains bedded gypsum. In the remaining evaporite facies, syngenetic sulfate minerals are unknown. The significance of this fact will be discussed later in this report.

In middle Eocene time, about 47 m.y. ago, before deposition of the Mahogany oil-shale zone, the first of many volcanic tuffs fell into Lake Uinta. The oldest known tuff lies 62 m below the Mahogany Ledge in Indian Canyon (beds 66-84, fig. 2, Dyni, 1976; W. C. Cashion, oral commun.). Older tuffs are unknown in the Flagstaff Limestone and in the lower part of the Green River Formation in both the Uinta and Piceance Creek Basins (Thomas D. Fouch, oral commun., 1979; Trudell and others, 1974, p. 69; J. R. Dyni, unpublished notes). Volcanism was active throughout the remaining history of Lake Uinta from the time of the first recorded tuff, but there was a pronounced decrease in volcanic activity late in the lake's history as evidenced by fewer tuffs (8) in the upper 340 m of lacustrine rocks exposed in Indian Canyon (J. R. Dyni and W. B. Cashion, unpublished field notes). Volumetrically, the tuffs make up only 1-2 percent of the Green River Formation (Dyani and Cashion, *ibid*; Surdam and Parker, 1972, p. 689) but considering that the tuffs were deposited in the drainage basin fringing the lake as well as in the lake itself, they probably contributed substantial amounts of clastic and dissolved material to the lake. Most tuff beds are altered to alumino-silicate and carbonate minerals; their original composition is thought to have been alkalic rocks such as quartz latite, rhyolite, andesite, and dacite (Griggs in Cashion, 1967, p. 18-19; Bradley, 1964, p. A2; Iijima and Hay, 1968, p. 187). A likely source for some of the tuffs in the Green River Formation in Wyoming is the Absaroka volcanic field, which was active about 45 to 53 m.y. ago. However, in the Uinta and Piceance Creek Basins many of the tuffs are younger than

45 m.y., and they thicken westward to thicknesses (up to 90 cm in Indian Canyon) greater than those in Wyoming. This suggests that much of the tuffaceous material in the Uinta and Piceance Creek Basins was derived from an, as yet, unidentified source located to the west or northwest in the Sevier orogenic belt in northern Utah where volcanic fields 40 to 45 m.y. old might be found (Burke and McKee, 1979, fig. 2).

### Structure

The Piceance Creek Basin is bounded by the Grand Hogback monocline on the east, which forms the west flank of the White River uplift, on the north by folded Cretaceous rocks adjacent to the Uinta-Axial Basin uplift, and on the west by the Douglas Creek arch. Structure maps contoured on markers in the lower and upper parts of the Green River Formation (Dyni, 1969; Austin, 1977) show the strongly asymmetric character of the northern part of the Piceance Creek Basin with the structural low located in T. 1 N., Rs. 97-98 W., Rio Blanco County. Dips are moderate to steep along the northeast and north sides of the basin whereas on the south and west sides of the basin, dips are low. Within the basin, there is a system of northwest-trending folds. Some faults and a few grabens having small displacements trend subparallel to the folds. The similarity of the two structure maps by Dyni (1969) and Austin (1971) indicates the intrabasin folding was post-Green River; although Dyni (1969, p. 64-65), basing his interpretation on isopach data, suggested that some of the folds were in existence during Green River time and may have influenced midbasin



sedimentation, including deposition of the thick saline facies in the lower part of the Green River Formation. Stratigraphic cross sections of the Green River Formation by Trudell and others (1974, fig. 2), Roehler (1974, figs. 1 and 2), and Snow (1970, fig. 8) show pronounced thickening of the formation in the northern part of the basin, and indicate that basin downwarping during Green River time was most active along the Grand Hogback monocline (which may translate into faults at depth) and along the southwest side of the White River on the north side of the basin.

#### Methods of Study

This investigation is based principally on the results of study and laboratory analyses of nearly 6,000 m of drill core obtained from 10 exploratory holes drilled into the thickest part of the saline facies in the Piceance Creek Basin, Colorado (table 1). Most of the core (either 5 or 10 cm in diameter) was cut lengthwise in half, and one of the halves was cut lengthwise into two quarters. One of these quarters of core, commonly in lengths of about 60 cm, was composited, crushed, and powdered to minus 60-mesh. A continuous series of such samples were prepared from each drill core. Portions of each sample were analyzed for their shale-oil and nahcolite contents. The core was examined for lithologic details and was also photographed. The photographs, used in conjunction with lithologic log and shale-oil bar graphs, proved to be useful for stratigraphic correlation of nahcolite units between the drill holes. Many samples were analyzed for qualitative mineralogy by X-ray diffraction. Because of its availability early

Table 1.--Name, location, elevation, depth, and cored interval for 10 drill holes.

USGS identifi- cation number	Name and company	Location	Surface elevation in meters above sea level	Total depth (meters)	Depths of cored intervals (meters)
C1	Irvin Nielsen 20-1  Kaiser Aluminum and Chemical Corp.	298.2 m from south line  112.4 m from east line, SE1/4SE1/4 sec. 20, T. 1 S., R. 97 W.	1894.4	635.2	221.3-635.2
C2	John E. Dunn 20-1  Wolf Ridge Minerals Corp.	365.0 m from north line,  357.3 m from east line, NE1/4NE1/4 sec. 20, T. 1 S., R. 98 W.	1939.2	735.5	457.5-502.3  518.8-735.5
C5	Joe T. Juhan 4-1	566.7 m from north line,  593.3 m from east line, SW1/4NE1/4 sec. 4, T. 2 S., R. 98 W.	2030.1	798.9	360.3-793.4

C34	Colorado core hole 1 U.S. Bureau of Mines-Atomic Energy Comm.	710.5 m from south line, 391.4 m from east line, NE1/4SE1/4 sec. 13, T. 1 N., R. 98 W.	1829.7	957.1	234.7-955.0
C153	Colorado Minerals 28-1 Wolf Ridge Minerals Corp.	82.4 m from north line, 416.1 m from west line, NE1/4NW1/4 sec. 28, T. 1 S., R. 98 W.	1956.0	664.8	3.7-664.8
C154	John Savage 24-1 Wolf Ridge Minerals Corp.	104.5 m from north line, 101.2 m from east line, NE1/4NE1/4 sec. 24, T. 1 S., R. 98 W.	2007.1	852.5	394.3-852.5
C155	Colorado Minerals 14-1 Wolf Ridge Minerals Corp.	195.4 m from north line, 517.8 m from east line, NW1/4NE1/4 sec. 14, T. 1 S., R. 98 W.	1921.2	758.4	3.7-758.4

---

C156	Irvin Nielsen 17-1 Kaiser Aluminum and Chemical Corp.	275.8 m from north line, 782.0 m from east line, NW1/4NE1/4 sec. 17, T. 1 S., R. 97 W.	1998.7	778.6	374.3-778.6
C177	Shell 22X-1 Shell Oil Company	688.8 m from north line, 795.5 m from east line, SW1/4NE1/4 sec. 1, T. 2 S., R. 98 W.	1958.2 <sup>1</sup> (1955.0)	807.4	207.3-807.4
C179	Shell 23X-2 Shell Oil Company	704.4 m from south line, 496.2 m from west line, NE1/4SW1/4 sec. 2, T. 2 S., R. 98 W.	1991.0 <sup>1</sup> (1987.3)	822.7	237.7-822.7

---

<sup>1</sup>Drilling datum is Kelly bushing; ground elevation in parentheses.

in the study, the core from drill hole C5 was analyzed extensively for elemental abundances by optical emission and X-ray spectroscopy and by chemical analyses. Parts of certain cores were analyzed for selected elements including sulfur and bromine; and selected specimens of core were studied in polished and thin section. Some authigenic minerals in oil shale and in nahcolite and halite were examined by scanning electron microscope and energy-dispersive X-ray spectroscopy. The results of much of this work are included in this report.

## CHAPTER II

### GREEN RIVER FORMATION

The Eocene Green River Formation occupies an area of about 4,300 km<sup>2</sup> in the Piceance Creek Basin between the White River and Colorado River in Rio Blanco and Garfield Counties, Colorado (fig. 2). About 2,500 km<sup>2</sup> of this area lies in Rio Blanco County, where the formation reaches its maximum thickness of about 1,100 m (Roehler, 1974, fig. 2). Here, in the northern part of the Piceance Creek Basin, the thickest and highest-grade oil shales are found at depths beginning about 250 to 425 m below the surface. Within the high-grade oil shales are the minerals nahcolite and halite that define the saline facies. The drill cores studied in this investigation penetrate the central part of the saline facies.

In the study area the Green River Formation is divided, in ascending order, into the Anvil Points, Garden Gulch, and Parachute Creek Members. The base of the Garden Gulch Member is poorly defined for lack of drill-hole data, but in core hole C34 (fig. 2), the base of the member is placed at the top of a 9-meter-thick, white, oolitic sandstone at the depth of 913.0 m. The sequence of rocks from this bed to the top of the Parachute Creek Member is 616 m thick and consists mostly of oil shale.

The term oil shale is used in this report only in an economic sense and is defined as a fine-grained sedimentary rock that yields 21 or more liters of oil per metric ton (5 gallons or more of oil per short ton) on pyrolysis. Lithologically, oil shale

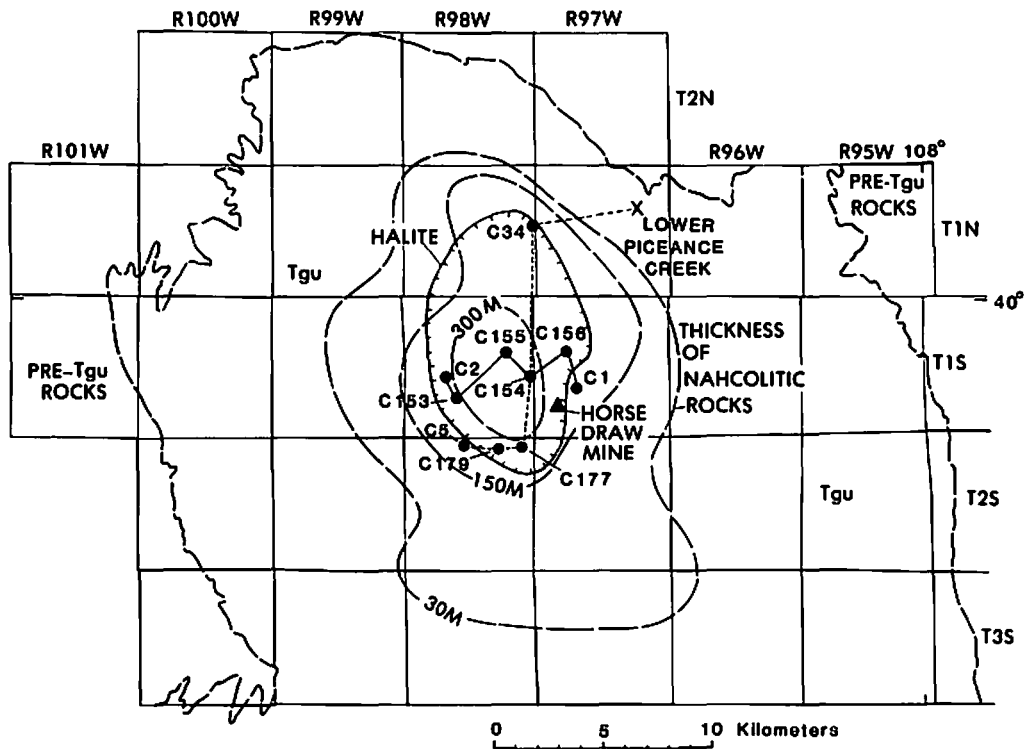


Figure 2.--Map showing the outline of the Green River Formation and the overlying Uinta Formation (Tgu) in the northern part of the Piceance Creek Basin, Colorado. The area of bedded for halite and the 30-, 150-, and 300-meter isopachs for nahcolitic rocks are shown. The locations of the 10 study wells are indicated. The line of section for plate 1 is indicated by the dashed line drawn from core hole C5 to the measured section (X) on lower Piceance Creek. The line of section for plate 2 is shown by the solid line drawn from core hole C2 to core hole C1.

may be marlstone, shale, or siltstone.

The Garden Gulch Member is composed chiefly of fissile, kerogenous illitic shale, whereas the Parachute Creek Member is composed characteristically of massive, tough, kerogenous dolomitic marlstone with little or no illite. In the subsurface, the contact between these two lithofacies is gradational. X-ray diffraction data show the illite content of the upper part of the Garden Gulch shales gradually decreases stratigraphically upward as the rocks become more dolomitic and massive. The Garden Gulch Member is 136 m thick in core hole C34 and thins to 80 m on the outcrop at lower Piceance Creek (fig. 2).

Using bar graphs of shale-oil analyses of cores and cuttings from many wells, the oil-shale deposits of the Parachute Creek and Garden Gulch Members were divided into a series of zones of alternating lean and rich oil shales by J. R. Donnell (Donnell and Blair, 1970; Cashion and Donnell, 1972). The relatively thick, rich oil-shale zones are designated by the series: R-0, R-1, R-2... R-6 and the thinner lean oil-shale zones by the series: L-0, L-1, L-2... L-5. The next three overlying zones are named rather than numbered. These are the B-groove, a thin kerogen-lean zone; the rich Mahogany oil-shale zone; and the A-groove, another thin kerogen-lean unit. The stratigraphically highest oil shales at the top of the Parachute Creek above the A-groove are not designated by name or number.

In the northeastern portion of the Piceance Creek Basin, the kerogenous dolomitic marlstones in the lower part of the Parachute Creek Member grade northward into fissile kerogenous



shales between core hole C34 and the surface section on lower Piceance Creek (pl. 1). In this area, the main body of the Parachute Creek Member below the Mahogany zone, which includes the saline facies, grades northward into massive to platy dolomitic marlstone with little kerogen and with increasing amounts of sandy and silty siliciclastics (Hail, 1972, 1974). Toward lower Piceance Creek on the northeast side of the basin, the main body of the Parachute Creek Member also decreases in kerogen content as analcime, illite, and calcite which are not common in the subsurface in the study area, increase in abundance (Brobst and Tucker, 1973).

In core holes C177 and C179, the Parachute Creek Member is about 490 m thick, and it thins to 360 m on lower Piceance Creek. The maximum known thickness of the Parachute Creek is 539 m in core hole C8.

The saline facies of the Parachute Creek Member extends from near the base upward into the Mahogany oil-shale zone near the top of the member. The lower part of the saline facies contains large amounts of nahcolite and halite, but the upper part has been leached of its water-soluble salts as evidenced by vugs, crystal cavities, and marlstone solution breccias.

Cashion and Donnell (1972) have shown that the oil-shale zones are identifiable on sonic and density geophysical well logs, as well as on shale-oil bar graphs. Some of these zones, and certain rich oil-shale beds, can be traced laterally for as much as 240 km from the southeastern part of the Piceance Creek Basin westward into the southwestern part of the Uinta Basin, Utah. The

shale-oil resources of the Mahogany and R-6 oil-shale zones in the Piceance Creek Basin have been published by Pitman and Johnson (1978) and Pitman (1979).

Toward the saline depocenter in the northern part of the Piceance Creek Basin, the recognition of the oil-shale zones on shale-oil bar graphs becomes difficult because the oil-shale beds are masked by thick beds of nahcolite and halite. However, many continuous units of nahcolite and halite can be physically correlated between core holes and these permit tracing of the oil-shale zonation through the saline facies. Rocks within the saline facies are further divided on the basis of the nahcolite and halite content into subzones or beds, which are designated alphabetically for convenient reference (pls. 1 and 2).

## CHAPTER III

### LITHOLOGY OF THE SALINE FACIES

The lower unleached part of the saline facies of the Parachute Creek Member consists of low- to high-grade oil shale, nahcolite, and halite. This sequence of rocks extends from the middle of oil-shale zone R-2 upward to a well-defined dissolution surface in oil-shale zones R-5 and L-5 (pl. 1). In the core holes studied, the lower unleached part of the saline facies ranges in thickness from 160 m in core hole C198 to a maximum estimated thickness of 328 m in core hole C155. Core hole C155, which is located close to the basin depocenter, did not penetrate the entire thickness of the saline facies; the thickness is estimated from other nearby drill holes.

Nahcolite occurs in (1) nonbedded coarse-crystalline aggregates scattered through oil shale, (2) laterally continuous units of fine-grained crystals disseminated in oil shale, (3) brown microcrystalline laminae and beds, and (4) white coarse-grained beds. Where nahcolite occurs in beds, it is commonly associated with bedded halite.

The relative amounts of aggregate, disseminated, and bedded nahcolite were estimated from the lithologic logs and nahcolite analyses for 10 core holes (table 2). Nahcolite aggregates constitute the largest part of the resource, amounting to about 62 percent of the deposit. About 25 percent of the nahcolite is in disseminated form, and about 13 percent of the nahcolite is

Table 2.--Amounts of aggregate, disseminated, and bedded forms of nahcolite in 10 core holes

Core hole	Mode of occurrence of nahcolite (weight percent)		
	Aggregate	Disseminated	Bedded
C1 <sup>1/</sup>	53.2	29.5	17.3
C2 <sup>1/</sup>	70.4	22.2	7.4
C5	52.8	44.6	2.6
C34	59.6	16.0	24.4
C153 <sup>1/</sup>	71.6	16.3	12.1
C154 <sup>1/</sup>	59.3	26.0	14.7
C155 <sup>1/</sup>	64.2	19.5	16.3
C156 <sup>1/</sup>	72.1	20.2	7.7
C177	54.6	24.7	20.7
C179	64.3	24.7	11.0
Average	62.2	24.4	13.4

<sup>1/</sup> Core hole did not penetrate entire saline facies.

bedded. These values are based on the dominant type of nahcolite found in the subzones shown on plates 1 and 2, although a subzone may actually contain more than one type of nahcolite.

#### Nahcolite Aggregates and Disseminated Nahcolite

Nahcolite aggregates are generally equant, but irregular to spherical in shape. Aggregates commonly occur as scattered individuals in oil shale, but a significant number (14 percent of the aggregates >1 cm in diameter in core hole C177) form coalescent groups of two or more aggregates (fig. 3).

The apparent mean diameter of nahcolite aggregates was measured in slabbed 4-cm-wide drill cores from bore holes C177 and C179 (fig. 4). Where only a part of an aggregate was exposed in the core, its full apparent diameter on the slabbed surface was estimated by projecting the outline of the aggregate beyond the edge of the core. The apparent diameter of the aggregates ranges from 0.3 to 168 cm. Two-thirds of the aggregates are 0.3 to 8 cm in diameter, and almost 90 percent of them are 0.3 to 16 cm in diameter.

The frequency of occurrence of nahcolite aggregates in core holes C177 and C179 was also determined (table 3). The number of aggregates >1 cm across exposed on the slabbed 4 cm wide surface per 0.6 m length of core was determined through the nahcolite-bearing sequence of oil shale in each bore hole. On this basis, about one-half of the nahcolitic oil shale contains fewer than one nahcolite aggregate per 0.6 m length of drill core. About 77 percent of the remaining oil shale contains 1 to 3 aggregates per

Figure 3.--Photographs of slabbed drill cores of typical nahcolite aggregates in Green River oil shale. A. Irregularly shaped to nearly spherical aggregates of nahcolite about 2 to 7 cm in diameter in laminated oil shale. The aggregates are rimmed with pyrite and marcasite that have oxidized and blackened on exposure to air. B. Parts of two nearly spherical rosettes of nahcolite in well-laminated oil shale. The white patch at the center of the lower aggregate is microcrystalline quartz. C. Coalescent clumps of large brown nahcolite crystals in nearly structureless oil shale. D. Coalescent aggregates of nahcolite in well-laminated oil shale. E. Small nahcolite aggregates in the lower part of the core diminish upward in size and grade into disseminated nahcolite crystals in faintly laminated oil shale. A well defined unit of disseminated nahcolite forms the top 2 cm of the core. F. Nearly spherical nahcolite aggregate rimmed with iron sulfide in blebby and streaked oil shale. The white coating on the nahcolite aggregate in this photograph and in photograph A is sodium sulfite. The iron sulfide rim has oxidized, swelling and cracking the drill core. Bedding in photographs A, B, D, and F clearly bends around the aggregates.



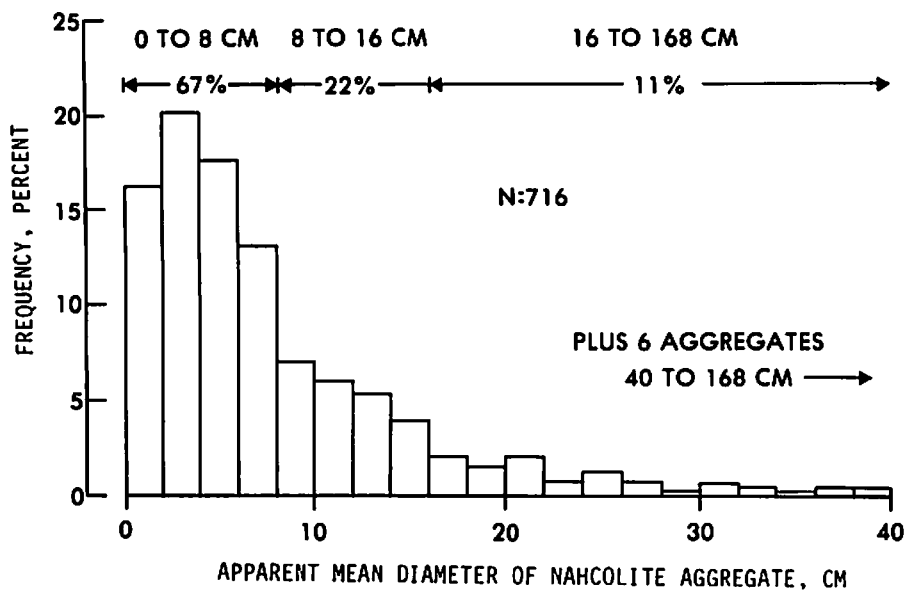


Figure 4.--Size distribution of nahcolite aggregates in core holes C177 and C179.

Table 3.--Frequency of nahcolite aggregates in core holes C177 and C179

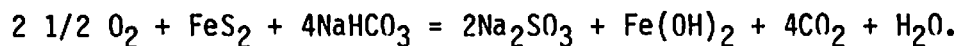
<u>Number of aggregates per 0.6 m length of core</u>	<u>Frequency</u>	<u>Percent</u>
0	420	47.3
1	164	18.5
2	120	13.5
3	75	8.4
4	44	5.0
5	29	3.3
6	18	2.0
7	9	1.0
8	6	0.7
9	3	0.3
	<u>888</u>	<u>100.0</u>



0.6 m length of drill core.

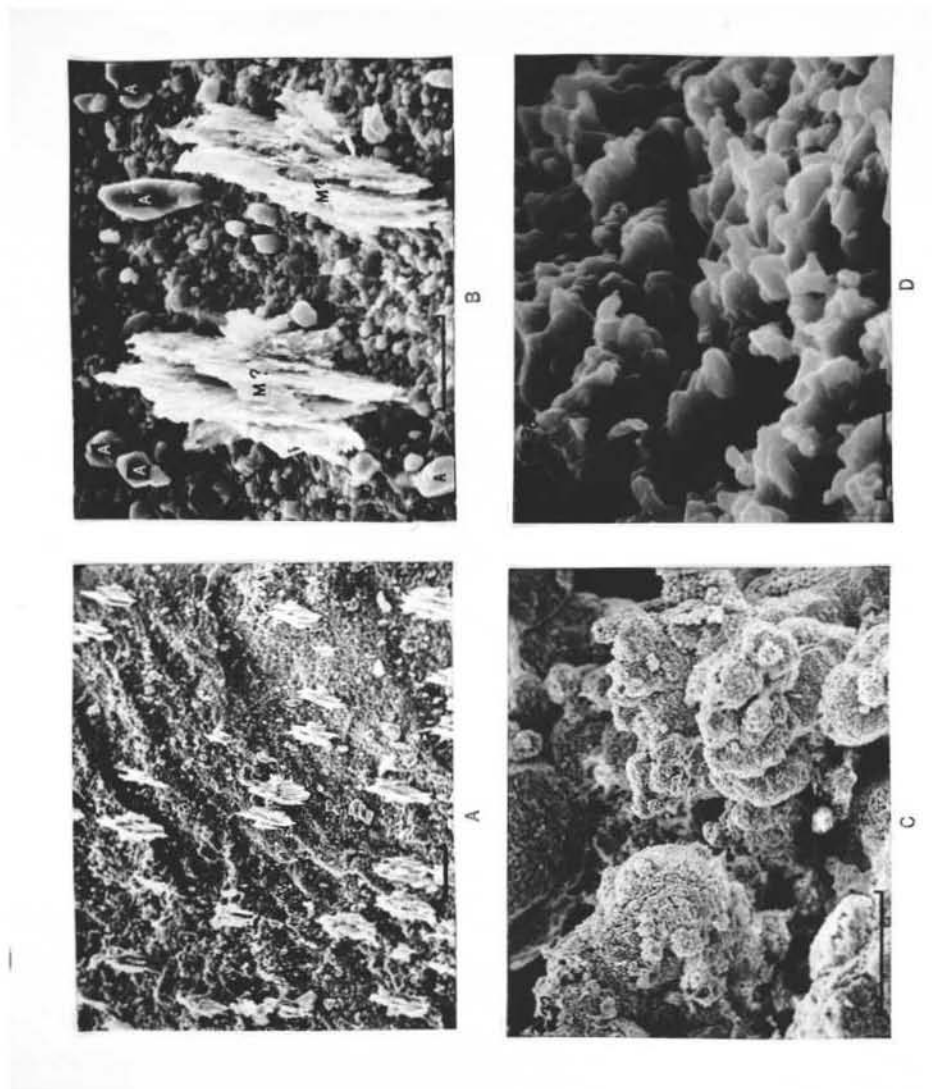
Some aggregates are composed of fine-grained nahcolite crystals, but more commonly, the crystals are medium- to very coarse-grained. The nahcolite crystals are usually bladed and quite thin, measuring about 0.5 to 2.5 cm in length by about 0.2 to 2 mm in thickness. In some aggregates, the crystals are arranged in a rosette-like pattern (fig. 3B). In many, if not most aggregates, the nahcolite crystals form clumps of parallel crystals where the orientation of the crystals differs from one clump to the next (fig. 3C). Individual crystals within an aggregate are usually separated by paper-thin kerogen-rich septa coated with a variety of iron sulfide, carbonate, and silicate minerals most of which are probably authigenic (fig. 5). The nahcolite is generally colored brown by organic impurities. Irregular globs and concentric shells of white microcrystalline quartz are found in many aggregates (fig. 3B).

Pyrite and marcasite commonly form thin rinds around many nahcolite aggregates (fig. 3A, F). On exposure to air, these iron sulfide minerals oxidize rapidly, turn black, and expand. Slabbed surfaces of nahcolite aggregates rimmed with pyrite and marcasite commonly develop a secondary coating of sodium sulfite, probably by reaction of the sulfide minerals with nahcolite:



Nahcolite aggregates occur in laminated as well as in blebby and streaked oil shale. Bedding in both types of oil shale clearly bends around the aggregates and appears to be contorted due to growth of the aggregates by precipitation from interstitial

Figure 5.--Scanning electron photomicrographs of accessory minerals in nahcolite aggregates. A. Water-insoluble kerogenous septum coated with authigenic minerals from a nahcolite aggregate. The light-colored oriented crystal clusters, about 70 to 120  $\mu\text{m}$  long, are iron sulfide (marcasite?). These clusters are oriented parallel to the long dimension (c crystallographic axis) of the bladed nahcolite crystals in the aggregate. Bar scale = 100  $\mu\text{m}$ . B. Close-up view of two marcasite(?) clusters (M?) just to the lower right of the pair of sulfide clusters in the center of SEM photomicrograph A. The larger subhedral grains are probably ankerite (A) and the smallest grains ( $\sim$  4  $\mu\text{m}$ ) coating the septum are euhedral crystals of quartz and subhedral crystals of potassium feldspar. Bar scale = 30  $\mu\text{m}$ . C. Spherulitic blobs of authigenic microcrystalline quartz in the water-insoluble residue of a nahcolite aggregate similar to that in figure 3B. Bar scale = 300  $\mu\text{m}$ . D. Close-up view of the surface of one of the globs in SEM photomicrograph A. Individual quartz crystals are about 1 to 4  $\mu\text{m}$  in length. Bar scale = 10  $\mu\text{m}$ .

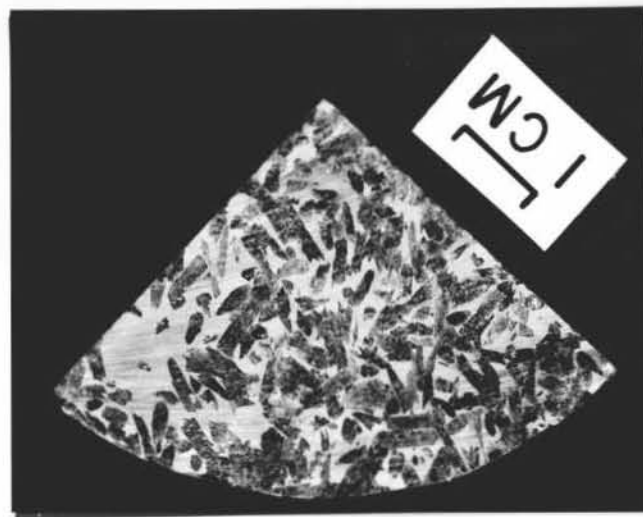


sodium bicarbonate waters during early diagenesis while the enclosing sediments were still soft (fig. 3A, B, D, and F).

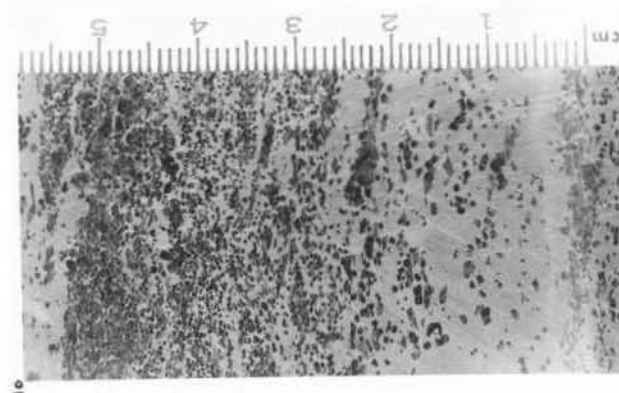
Disseminated nahcolite consists of discrete crystals of nahcolite embedded in a matrix of kerogenous marlstone. The concentration of nahcolite crystals ranges from a densely packed mass of crystals separated by paper-thin marlstone septa, to widely spaced crystals and clumps of small crystals scattered through marlstone (fig. 6A). Nahcolite crystals are commonly fine to medium grained, although larger and smaller crystal sizes were observed. Individual nahcolite crystals are prismatic, elongate, and roughly square to rectangular in cross section. "Swallowtail" twins are common (fig. 6B).

Fifteen units of disseminated nahcolite, ranging from 0.3 to 6.8 m, are shown on plates 1 and 2. Many of these units contain not only disseminated nahcolite crystals, but nahcolite aggregates and lenses, and thin beds of brown microcrystalline nahcolite. Some units show much lateral variation in nahcolite type. Disseminated nahcolite may grade laterally into bedded brown microcrystalline nahcolite or nahcolite aggregates (for example, see unit R-3J on pl. 2). For this reason, the nahcolite content varies by as much as 15 to 20 percent between drill holes near the basin depocenter. On the average, the thicker units of disseminated nahcolite range between 40 and 60 weight percent nahcolite (fig. 7), and contain about 15 to 25 percent more nahcolite than the best of those zones of oil shale that contain only scattered nahcolite aggregates.

Figure 6.--Photographs of disseminated nahcolite in nearly structureless kerogenous marlstone. A. Core slab cut perpendicular to bedding. The apparent size of the nahcolite crystals is about 0.2 to 3 mm. The crystals grade from rather widely scattered to a close-packed fabric toward the top of the photograph. B. Core slab cut parallel to bedding. Randomly oriented prismatic nahcolite crystals lie with their longest dimension (c crystallographic axis) parallel to bedding. Some "swallowtail" twinned crystals can be seen.



B



A

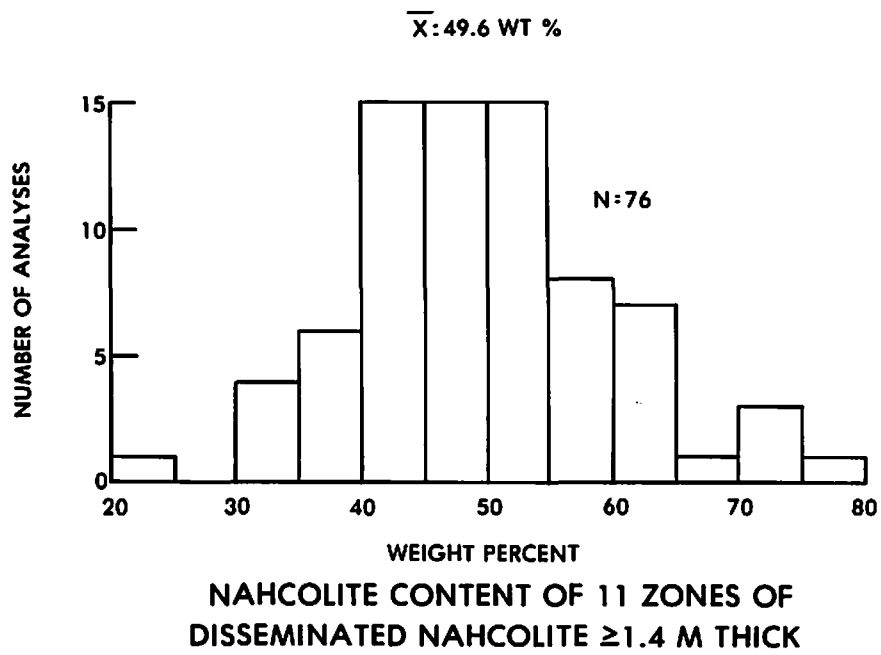


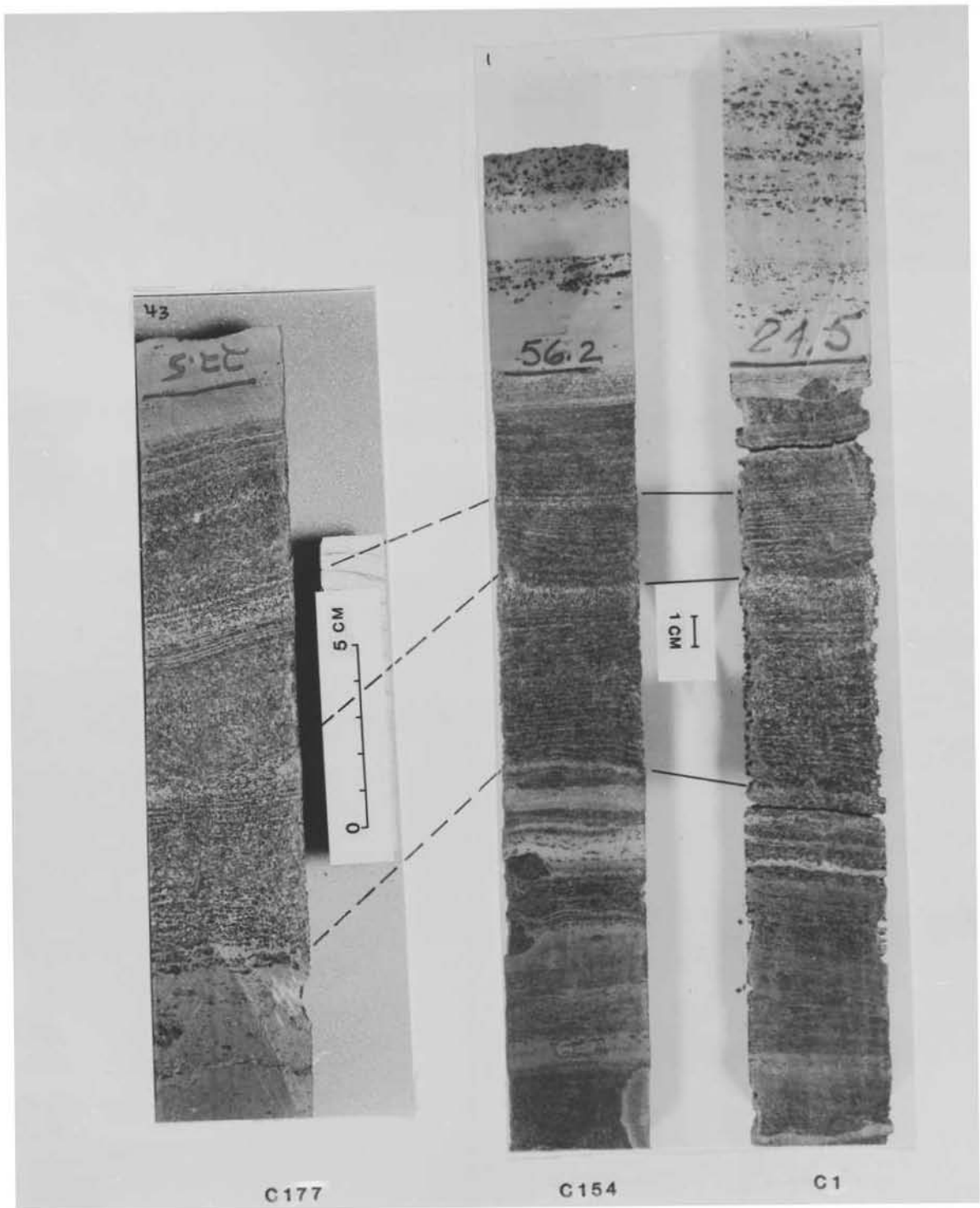
Figure 7.--Frequency distribution of the nahcolite content in 11 units of disseminated nahcolite 1.4, or more meters thick shown on plates 1 and 2. The total number of analyses is 76, and the mean value for all analyses is 49.6 weight percent nahcolite.

Despite vertical and lateral variation in nahcolite types and fabrics, many units of disseminated nahcolite are remarkably persistent laterally. Some units underlie several hundred square kilometers.

With few exceptions, disseminated nahcolite is found in association with only laminated to structureless kerogenous marlstone, and not with blebby and streaked kerogenous marlstone. Some units of disseminated nahcolite are distinctly laminated. The laminae consist of alternating layers of marlstone and disseminated nahcolite. Groups of laminae can be correlated between wells as much as 6 km apart (fig. 8). The laminae suggest annual cycles of sedimentation, or varves. If this is true, the depositional rate for the laminated unit in figure 8 is about 0.5 to 2 mm per year.

The depositional environment of disseminated nahcolite appears to be intermediate between that of nahcolite aggregates, which clearly formed after deposition of the enclosing marlstones, and that of bedded nahcolite which precipitated directly from the parent lake brine. Apparently, the brine was not quite saturated for sodium bicarbonate to precipitate nahcolite but required only slight dewatering of the sediment to cause precipitation and growth of nahcolite crystals. The rate of deposition of marlstone kept pace with precipitation of disseminated nahcolite close to the brine-sediment surface to form a "semibedded" type of nahcolite.

Figure 8.--Photographs of slabbed drill cores of laminated disseminated nahcolite at the top of subzone R-3F from core holes C1, C154, and C177. Alternating laminae of disseminated nahcolite (dark layers) and kerogenous marlstone (light layers) can be easily correlated between core holes C1 and C154, but with less certainty between core holes C154 and C177.



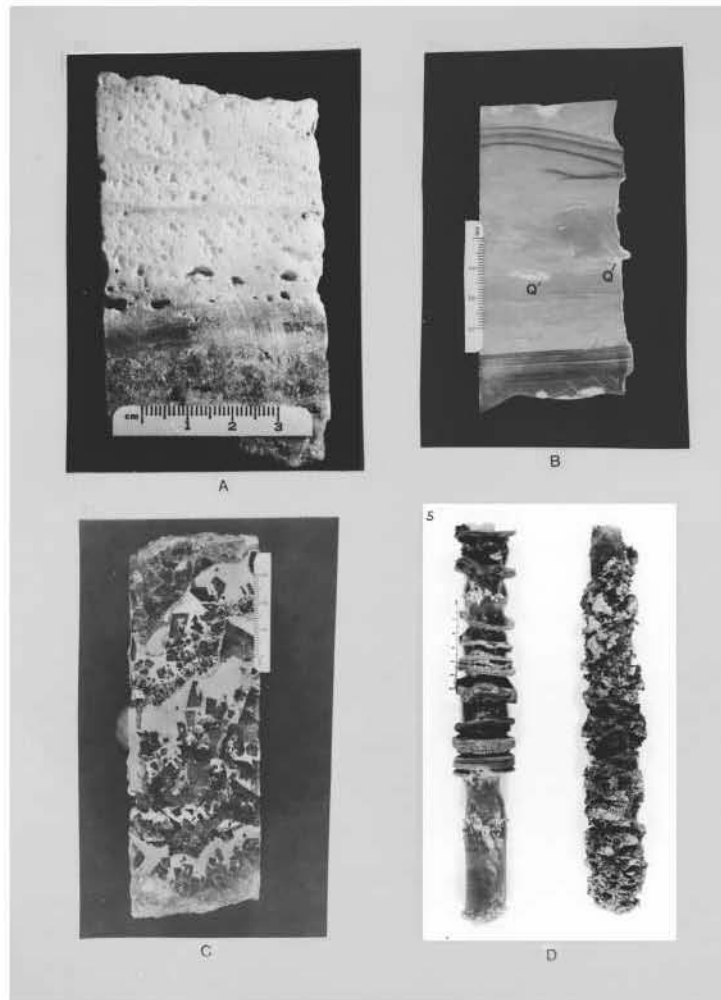
## Bedded Nahcolite and Halite

Bedded nahcolite occurs in two distinct types. The first type consists of porous, white to tan, fine- to dominantly coarse-grained (about 0.2-10 mm) nahcolite having a granular texture. Light-brown and white color-banding and mottling is common in many beds. Most beds of white nahcolite contain scattered laminae and thin layers of marlstone as much as 10 cm thick. Some of these marlstone layers are moderately to highly contorted. Angular fragments of laminated marlstone as much as 4 cm across were noted in one bed of white nahcolite. The contorted marlstone layers and clasts indicate that some of the white nahcolite was locally subjected to considerable slumping and deformation probably during early diagenesis. Aside from the marlstone interbeds, the white nahcolite is relatively free of impurities, although halite is found in some beds close to the basin depocenter. Most beds of white nahcolite are porous and contain irregularly shaped interconnected cavities that are generally about 1 to 7 mm across, and occasionally 15 mm across (fig. 9A). Secondary veins of coarse-grained white nahcolite cut vertically across some beds.

Six of seven beds of white nahcolite ranging from 1.7 to 10 m in thickness are shown on plates 1 and 2. These beds grade into mixed halite and nahcolite toward the chemical depocenter of the basin. The nahcolite content of these beds ranges from 44 to 90 weight percent. One of the thickest beds of white nahcolite, bed L-5A, lies just below the dissolution surface at the top of the lower unleached part of the saline facies and probably contains brine from the overlying leached zone.



Figure 9.--Photographs of drill core of bedded nahcolite and halite. A. Porous, white, and brown coarse-grained nahcolite. Porosity is about 34 volume percent. B. Brown microcrystalline nahcolite showing faint flow structure. A well-laminated layer of kerogenous marlstone 1 cm thick is near the base of the core. The three dark laminae near the top are also marlstone. The contorted white stringers in the center of the specimen are authigenic microcrystalline quartz (Q). C. Poorly developed alternating layers of halite (dark areas) and nahcolite and halite (light areas). The halite is very coarse grained and includes crystals as large as 1 cm. Brine-filled negative crystals and inclusions of irregular shape are abundant in the halite. The light areas consist of a mush of very fine grained (<0.1 mm) prismatic crystals of nahcolite with the interstices between crystals filled with halite. D. Water-eroded pieces of whole drill core of halite and nahcolite. The core to the left shows well developed laminae to very thin beds of alternating halite (deeply eroded layers) and brown microcrystalline nahcolite (thin wafer-like laminae and layers). The core to the right is mixed halite (deeply eroded parts of the core) and nahcolite that shows no distinct bedding.



The second type of bedded nahcolite is brown, fine-grained to microcrystalline, dense, and nonporous (fig. 9B). The nahcolite is commonly interstratified with laminae to thin beds of kerogenous marlstone about 0.2-5 cm thick. The nahcolite is commonly faintly laminated to structureless. Some beds are contorted and folded and show internal flow structures, which were probably formed prior to lithification when the nahcolite and enclosing kerogenous marlstones were still soft and subject to slumping. Much of the nahcolite is colored light to medium brown by small amounts of organic impurities. Creamy patches and irregular stringers of microcrystalline quartz and scattered tiny blebs of pyrite about 0.25 mm across are common accessories; these minerals amount to probably less than a few percent of the nahcolite.

Brown microcrystalline nahcolite forms beds about 1 cm to 8.6 m thick in the upper part of the lower unleached saline facies in oil-shale zones L-4, R-5, and L-5. Few such beds are found below the base of oil-shale zone L-4. Some beds make excellent stratigraphic markers because of their lateral continuity and correlatable sedimentary structures.

One of the most widespread thick beds of brown microcrystalline nahcolite is bed L-4D which underlies a minimum area of 155 km<sup>2</sup>, ranges in thickness from 1.9 to 3.6 m, and averages about 57 weight percent nahcolite. The detailed stratigraphy of nahcolite bed L-4D is shown on plate 3. The nahcolite bed is also the stratigraphic datum for plates 1 and 2. It is one of the principal beds under consideration for mining nahcolite. The U.S. Bureau of Mines Horse Draw Facility has opened

a small entry on bed L-4D at a depth of 562 m in the SW1/4 sec. 29, T. 1 S., R. 97 W.

Some beds of brown microcrystalline nahcolite, like white nahcolite, grade laterally into halite toward basin center (beds R-5G and R-5S), whereas other beds such as L-4D and R-5J appear to be free of halite. Although relationships are still not clear, available stratigraphic evidence suggests that some beds of brown microcrystalline nahcolite grade basinward into white nahcolite and in turn into mixed halite and nahcolite at basin center (fig. 10).

Halite, interstratified with nahcolite and kerogenous marlstone, forms beds 0.6 to 19.5 m thick in the upper part of the unleached saline facies in oil-shale zones R-5 and L-5. These rocks are concentrated in two sequences of several thick beds--one in the lower part of oil-shale zone R-5 and the other in the upper part of zone R-5 and the lower part of zone L-5, with a few thin halite beds between. The halitic rocks are composed commonly of alternating thin layers of halite and nahcolite (fig. 11). Couplets of halite and nahcolite range from paper-thin laminae to layers several centimeters thick. The halite is usually clear to light-smoky gray and medium- to coarse-grained. The nahcolite is tan to light brown, dense, and fine-grained to microcrystalline. Paired layers of nahcolite and halite may be seasonal units of sedimentation akin to the varved marlstone of the Green River Formation (Dyini and others, 1970). Parts of some beds show no clear rhythmic bedding as described above, but consist of an irregular mixture of halite and nahcolite (fig. 9D). Scattered through the halitic beds are interbeds of kerogenous marlstone and

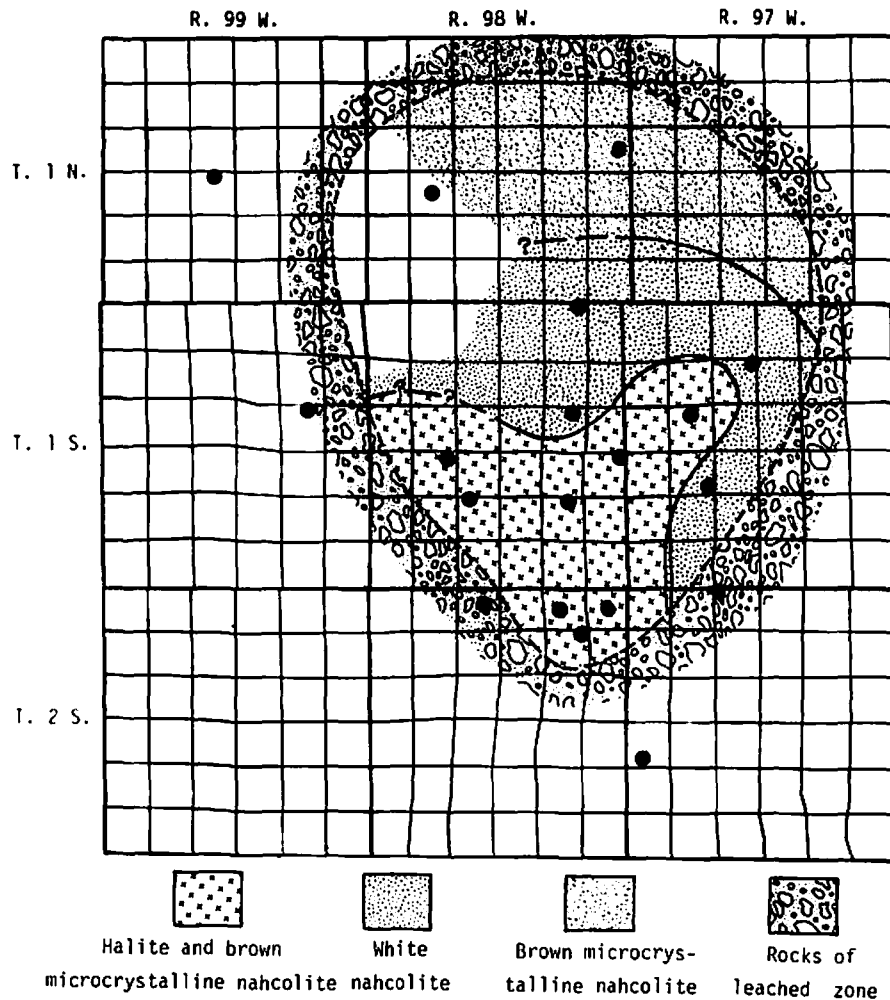
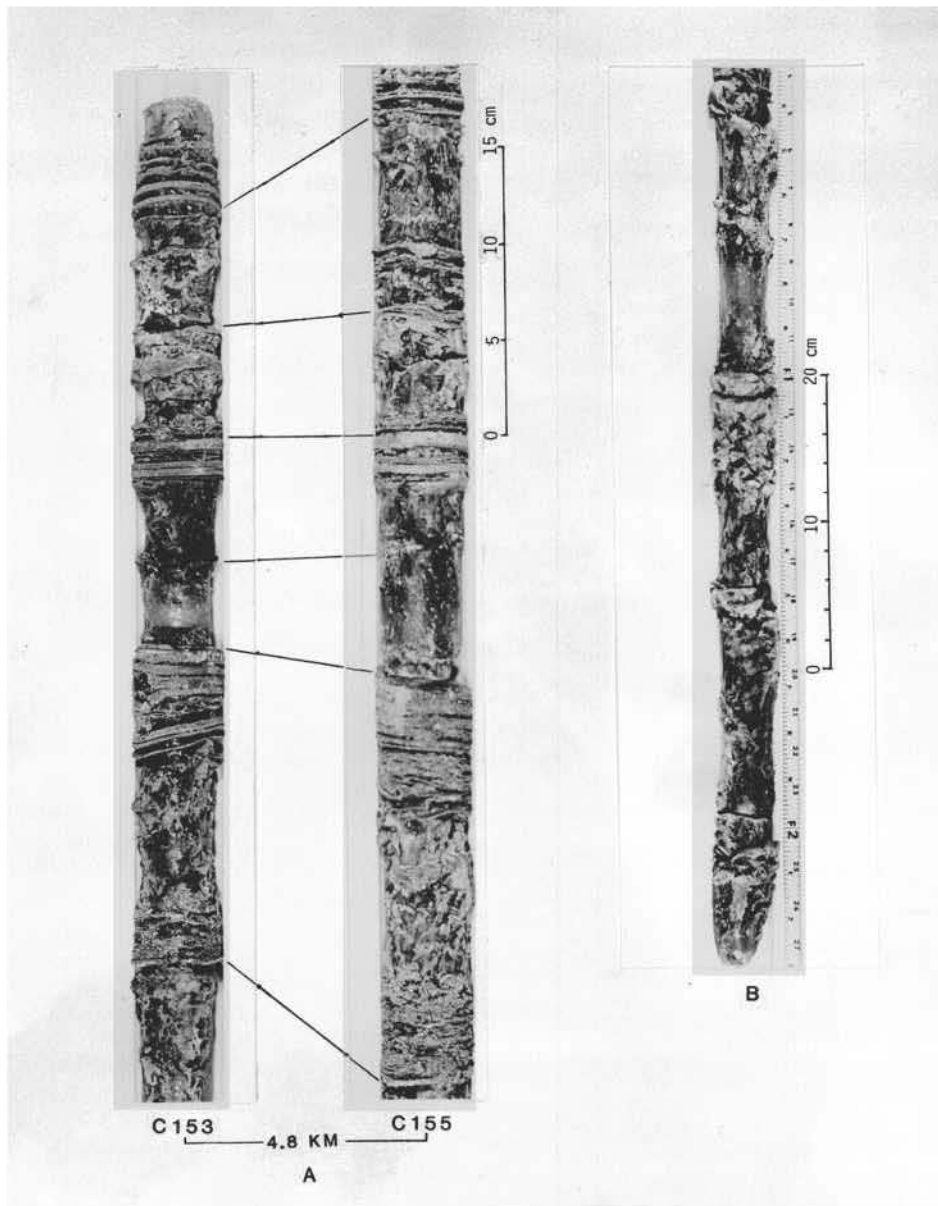


Figure 10.--Subsurface lithofacies map of nahcolite-halite bed R-5C. The lateral extent of the bed is determined by the dissolution surface at the top of the unleached part of the saline facies. As interpreted here, brown microcrystalline nahcolite grades basinward (southward) into white coarse-grained nahcolite which grades into interbedded halite and nahcolite at the basin depocenter. Control wells are indicated by black dots.

Figure 11.--Photographs of rhythmic couplets of halite (eroded dark layers) and nahcolite (resistant light layers). A. Correlation of laminae in drill cores in the top part of bed R-5G from core holes C155 (specimen on right) and C153 (specimen on left) which are 4.8 km apart. Note the small-scale folded nahcolite laminae presumably formed during early diagenesis when the sediments were still soft. B. Thick cyclic units of halite and nahcolite. Here, a typical couplet consists of a lower unit of light-smoky gray coarse-grained halite that grades upward into light-brown microcrystalline nahcolite. The top of the nahcolite layer forms a sharp contact with the next couplet above.



kerogen-poor marlstone that range from laminae to 0.6 m in thickness. The beds of interstratified halite and nahcolite thin away from basin center and grade laterally into white coarse-grained nahcolite and brown microcrystalline nahcolite. The lower sequence of halitic rocks is thickest in the vicinity of core holes C153, C177, and C179, whereas the upper sequence of halitic rocks is thickest in the vicinity of core holes C154 and C155, suggesting that the chemical depocenter for these evaporites shifted several kilometers to the northeast during deposition of these rocks.

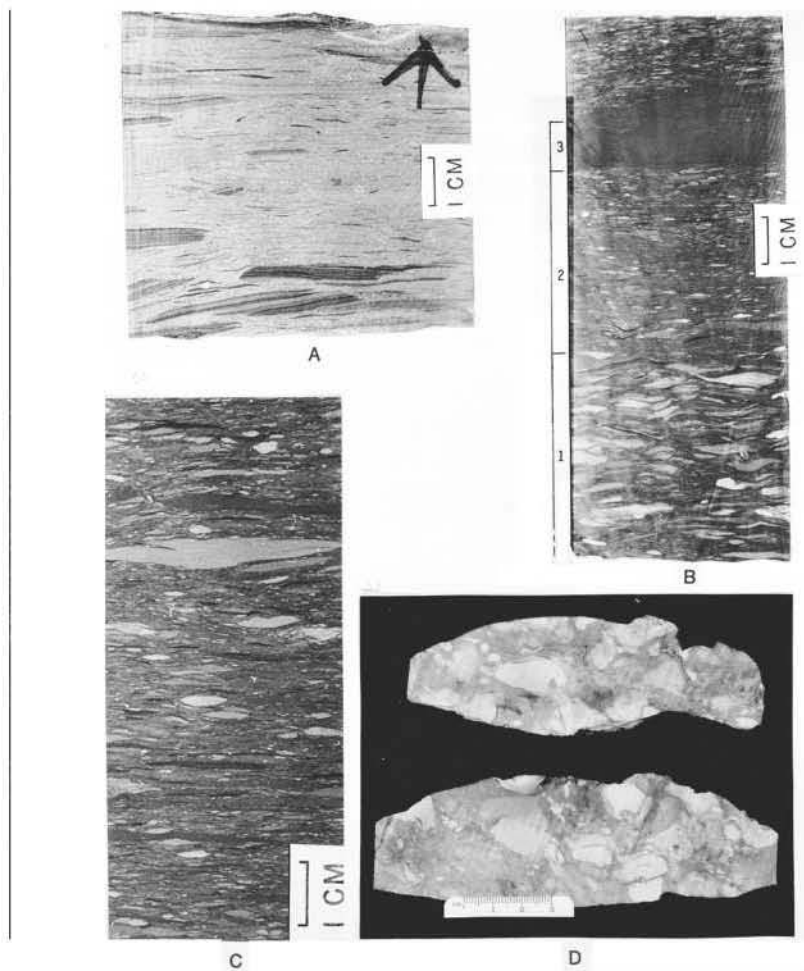
#### Kerogenous Marlstones

The rocks enclosing the nahcolite and halite deposits in the Piceance Creek Basin are predominantly dark yellowish brown kerogenous dolomitic marlstones (oil shales). Based on sedimentary structures, these rocks can be divided into two basic types: (1) laminated marlstone and (2) blebby and streaked marlstone. Some marlstone appears to be nearly structureless, but on close examination, most can be assigned to one or the other of the two types (fig. 12).

The laminated marlstones of the Green River Formation have been described at length by Bradley (1930, 1931). These rocks consist of alternating dark kerogen-rich and light mineral-rich laminae which Bradley believed to be varves. About 50 to 60 percent of the marlstone in the lower unleached part of the saline facies is laminated; the remaining marlstone is blebby and streaked.

Blebby and streaked marlstone was first described as oil

Figure 12.--Photographs of slabbed drill cores and mine rock of blebby and streaked kerogenous marlstone. A. Streaked kerogenous marlstone containing large flat clasts of laminated marlstone that lie nearly parallel to bedding. Some clasts taper to thin wispy edges or have delicate serrated edges. The thin dark streaks may be algal mat material or marly shale. B. Blebby kerogenous marlstone showing well-graded bedding. Units 1, 2, and 3 may comprise a single sedimentation unit (turbidite) which is about 10 cm thick. Units 1 and 2 are composed of clasts of nonlaminated dolomitic marlstone in a kerogen-rich marlstone martix. Unit 3 is nearly structureless pelitic marlstone that contains minute black bedding-parallel streaks of kerogenous material. C. Blebby kerogenous marlstone containing unsorted clasts of nonlaminated marlstone. D. Blebby kerogenous marlstone cut parallel to bedding. The larger nonlaminated marlstone clasts seem to show a preferred east-west orientation.



shale breccias by Bradley (1931, p. 28), who believed that they were derived from subaerially exposed mud flats during low-water stages of Lake Uinta. Trudell and others (1970) and Dyni (1974) noted large amounts of blebby and streaked marlstone in drill cores from the Colorado oil-shale deposits. Dyni and Hawkins (1981) recently reinterpreted these rocks to be lacustrine turbidites that were deposited by lake-bottom currents.

Typical blebby marlstone consists of clasts of light-tan to brown dolomitic marlstone in a matrix of dark-yellowish-brown kerogenous dolomitic marlstone. Most clasts are matrix-supported, thin and flat to lenticular, and lie with their long dimension parallel to bedding. Many clasts have delicately preserved finely serrated or wispy edges whereas others have round to tapered edges (fig. 12A and B). Most clasts are nonlaminated, but some are faintly to well laminated. The laminae within a clast are commonly parallel to the long dimension of clast, but in a few clasts, the laminae are transverse to the long dimension. A few X-ray diffraction analyses indicate that the clasts of lighter hues are composed chiefly of fine-grained dolomite and lesser amounts of quartz and the fine-grained marlstone matrix is composed of dawsonite, dolomite, quartz, sodium and potassium feldspars, and pyrite. Judging from colors, the marlstone matrix contains much more kerogen than the clasts. The longest dimension of the clasts ranges from a few millimeters to 5 or more centimeters by a maximum thickness of about 1 cm. Some blebby marlstone shows distinct graded bedding (fig. 12B); in other units, the clasts show no obvious sorting or graded bedding (fig 12C). In plan view, the



long dimension of some large elongate clasts show a subparallel orientation that may be useful in determining the direction of turbidity currents (fig. 12D). Ripple marks and inverse graded bedding have not been observed in these rocks.

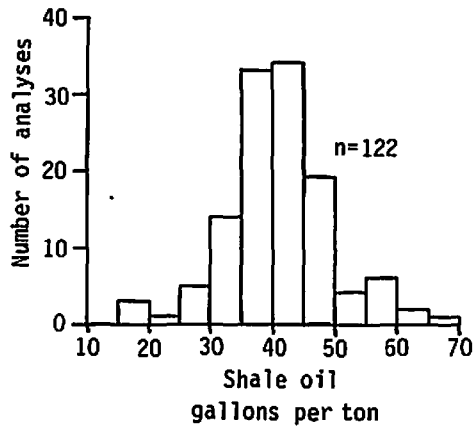
Many nonlaminated marlstones contain thin dark-brown to black flakes that parallel bedding and give the rock a streaked appearance. These flakes do not appear to be carbonized fossil debris of vascular plants. Perhaps, they are algal-mat detritus or simply clasts of kerogen-rich marl. All gradations between blebby and streaked structures occur, and commonly, both structures are intermixed. Many bands of kerogenous marlstone are nearly structureless, but even in these units tiny black bedding-parallel flakes can be detected. Some marlstone shows rhythmic alternation of blebby and streaked layers. Figure 12B shows upward fining of clasts through a 10-cm thick sequence of marlstone. This sequence, which may represent a single depositional unit, can be divided into a lower layer containing relatively large clasts of dolomitic marlstone, a middle layer with distinctly smaller clasts than the one below, and an upper pelitic layer containing a few tiny bedding-parallel flakes.

The blebby and streaked marlstones, on the whole, are massive and tough, and show little tendency to split along bedding planes. Where units of blebby and streaked marlstone are underlain by laminated marlstone, the contact is usually sharp and undulating. The uppermost few centimeters of laminated marlstone commonly displays slumped and contorted bedding and probable drag folds.

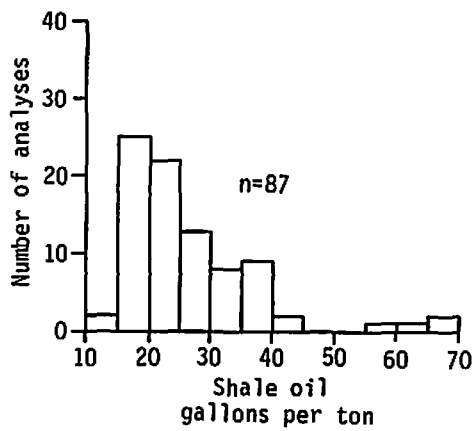
The blebby and streaked marlstones are higher in kerogen content than the laminated marlstones (fig. 13). Frequency distributions of the shale-oil content of core samples of blebby and streaked marlstone and laminated marlstone from the saline facies shown in figure 13 are clearly different. The hypothesis that both sets of shale-oil values are drawn from the same population is rejected at the 0.001 significance level by a Kolmogorov-Smirnov two-sample statistical test. This nonparametric test is sensitive to any differences (skewness, central tendency, and dispersion) in the populations from which the samples were drawn (Siegel, 1956, p. 127-131).

The bulk mineralogy of the blebby and streaked marlstone may also be significantly different from that of the laminated marlstone. The dawsonite content of samples of both types of marlstone was calculated on a nahcolite-free basis from mineral percentages listed in table 4. The frequency distributions of the dawsonite values of samples representing both types of marlstones are shown in figure 14. The hypothesis that the dawsonite values for each type of marlstone are from the same population was rejected at the 0.01 significance level by a Kolmogorov-Smirnov two-sample test. The dawsonite values for laminated marlstone show greater dispersion about the mean than the values for blebby and streaked marlstone. Perhaps, dawsonite was formed under a more uniform and narrower range of chemical conditions in blebby and streaked marlstone than in laminated marlstone.

Blebby and streaked marlstone forms units a few centimeters to 11 m thick. Many units are commonly 1 to 6 m in thickness



Blebby and streaked marlstone



Laminated marlstone

Figure 13.--Shale-oil content of laminated marlstone and blebby and streaked kerogenous marlstone in core holes C177 and C179 calculated on a nahcolite-free basis. Samples containing 30 or more percent nahcolite were omitted.

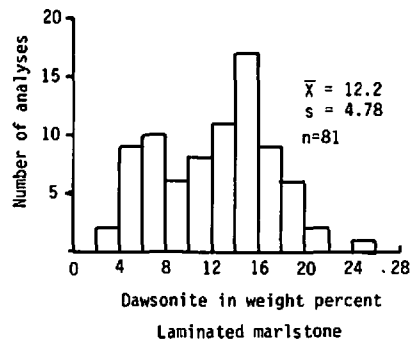
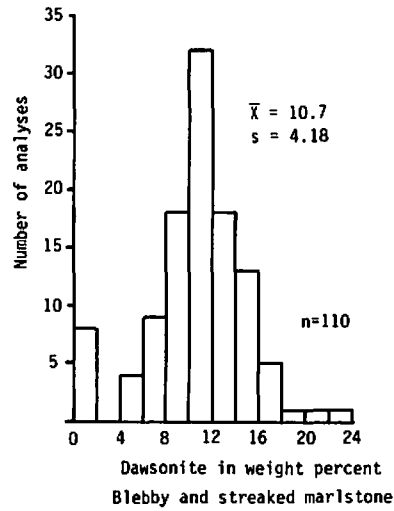


Figure 14.--Dawsonite content of laminated marlstone and blebby and streaked kerogenous marlstone in core hole C5 calculated on a nahcolite-free basis. Data are from table 4.

(pls. 1 and 2). There is evidence that some units of blebby and streaked marlstone form laterally continuous units in the Piceance Creek Basin. For example, the "sixty" oil-shale bed, named in reference to its shale-oil content (Dyner, 1974), is a unit of blebby marlstone near the base of oil-shale zone R-4. This unit is easily identified on shale-oil histograms by its high shale-oil content as well as by its blebby structure in drill cores. The "sixty" bed is about 0.6 to 1.2 m thick, and it occupies a minimum area of 175 km<sup>2</sup> in the northern part of the basin. Other beds of blebby and streaked marlstone will probably be traceable over considerable distances in the basin.

Within the lower unleached part of the saline facies, laminated marlstone contains all three types of nahcolite (aggregates, disseminated, and bedded). However, blebby and streaked marlstone usually contains nahcolite only in aggregates and discontinuous lenses and pods. From study of the vertical distribution of blebby marlstone on plates 1 and 2, the most evaporative phases of Lake Uinta, as represented by bedded halite and nahcolite, appear to have favored the deposition of laminated rather than blebby and streaked marlstone.

The blebby and streaked marlstones were identified as oil shale with pebbles, nodules, or pods of dolomite by Brobst and Tucker (1973), as "flat-pebble conglomerate" by Lundell and Surdam (1975), and as "mosaic breccia" by Bradley (1931, p. 28). Bradley believed these rocks originated during subaerial exposure of kerogen-rich sediments in a mudflat environment. On exposure to the sun, these sediments dried, cracked, and formed many clasts and

flakes that were subsequently incorporated with more mud supplied by the next rise in lake level. This explanation, however, is not consistent with the results of this study.

The clasts in the blebby marlstones have a different composition than the enclosing marly matrix. If both clasts and matrix originated essentially in situ, as Bradley suggested, the composition of the clasts and matrix would not be different. Furthermore, most clasts are flat, not curled as would be expected for sun-cracked fragments. Many clasts taper to thin edges or are delicately serrated indicating that the clasts were soft fragments when they were incorporated within the marly matrix and did not dry and curl. The high degree of parallelism of the flat clasts seems unlikely in a subaerially exposed mudflat environment. The subparallel orientation of the larger elongate clasts (fig. 12D) is strongly indicative of water currents. The fact that some clasts are internally structureless and others are laminated suggests different sediment source areas in the lake basin.

Most of the evidence suggests that the blebby and streaked marlstones are turbidites, rather than desiccation breccias formed in a mudflat environment (Dyner and Hawkins, 1981). The lower contacts of blebby and streaked marlstones which overlie laminated marlstone suggest scouring accompanied by slumping and drag folding of soft laminated marls by strong currents. Graded bedding, a typical sedimentary structure of turbidites, is prominently displayed in some blebby marlstones. The three-fold division of a graded bed of blebby and streaked marlstone in figure 12B suggests a partial Bouma sequence (Blatt and others, 1980, fig. 5.7).

Blebbly units 1 and 2 may correspond to upper flow-regime division A, or perhaps divisions A and B of the Bouma sequence. Pelitic unit 3 in figure 12B is possibly equivalent to Bouma divisions D and E and was deposited by the low density part of the turbidity current when its velocity was low.

Graded bedding is not obvious in some units of blebby and streaked marlstone, and the clasts show little sorting vertically through a bed. Possibly, such units were deposited by relatively short-lived turbidity currents where the clasts had insufficient time to be segregated by size.

The geometry of individual marlstone turbidites is still largely unknown, but their occurrence, indicated on plates 1 and 2, suggests that they are nonchannelized blanket-like beds. Two beds of siltstone in oil-shale zone R-6, and another just above A-groove (pls. 1 and 2) contain large clasts of laminated marlstone. These beds are also believed to be turbidites. In the lower part of the Parachute Creek Member and underlying Garden Gulch Member, a number of thin silty layers about 0.3 to 12 cm thick have been identified on plates 1 and 2 as tuffs; some or all may be turbidites.

Certain tuffaceous beds may be turbidites. The "wavy bedded analcitized tuff" bed lies 14-34 m above the Mahogany marker tuff bed which in turn lies 1-4 m above the Mahogany oil-shale bed contains "irregular stringers of marlstone" and varies from 25 to 150 cm in thickness (Donnell, 1961, p. 858 and pl. 53). The marlstone clasts, and variation in thickness and stratigraphic position suggest a turbiditic origin for this bed. A similar tuffaceous bed, the "Curly bed," which is about 21-36 m below the

Mahogany bed (Cashion and Donnell, 1972; Desborough and others, 1973, fig. 1) may also be a turbidite. Cashion (1967, p. 18-19) noted two general types of tuffs in the Green River Formation in the southeastern part of the Uinta Basin, Utah. The first type has smooth upper and lower surfaces and no internal bedding or grain orientation. The second type has undulatory surfaces, displays internal flowage structures and oriented crystals, and contains inclusions of oil shale and marlstone. Most likely, tuff beds of the first type were deposited directly into the lake with little or no subsequent movement after the sediments came to rest on the lake bottom. Tuffaceous sediments of the second type show evidence of turbiditic and/or grainflow origin (see Middleton and Hampton, 1973, for discussion of gravity-flow sediments including turbidites and grainflow sediments).

#### Micro-Faults and "Loop Bedding"

Most of the laminated marlstones contain a network of pre-lithification curvilinear fractures that cut across bedding at low to high angles. Commonly, laminae on either side of the fracture are slightly offset a few millimeters. These fractures are mostly healed with little or no permeability. Some fractures curve downward into an irregular vertical zone a few millimeters wide that is filled with more-or-less structureless marlstone. Other fractures curve into a surface parallel to bedding and appear to die out. These fractures extend for several centimeters and cut across as much as 2-cm-thick sequences of laminated marlstone. Laminae adjacent to a fracture commonly show slight drag



structures. Similar fractures in blebby and streaked marlstone have not been observed.

"Loop bedding," first described by Bradley (1930, p. 29, pl. 17,B), is another common structure in the laminated marlstones. In rock slabs cut vertical to bedding, "loop bedding" consists of groups of laminae a few millimeters thick, that appear to have been locally constricted, as if one had pinched them together, and other groups of laminae appear to simply pinch out laterally. When examined on slabs cut at angles of 45° or less across bedding, these structures were found to have been formed by a pre-lithification fracture that cut across the laminae at a low angle accompanied by a slight offset of the laminae on either side of the fracture. Some fractures are locally filled with material that appears to have been originally fluidized sediment that was squeezed into the fracture.

The extensive network of pre-lithification fractures suggests they played a role in sediment lithification processes. They are interpreted to be water-escape structures that formed after the sediment was deposited and buried to some unknown depth.

## CHAPTER IV

### COMPOSITION OF THE MARLSTONES

The quantitative mineralogy of 279 core samples which represent the the saline facies in core hole C5 was determined by a variety of analytical methods. The results are listed in table 4.

The analyzed sequence of rocks in core hole C5 is 176.78 m thick and extends downward from the dissolution surface a few meters above the base of oil-shale zone R-5 into the lower one-half of oil-shale zone R-2. This sequence includes nahcolite- and dawsonite-bearing oil shales below the stratigraphically lowest halitic rocks in oil-shale zone R-5 and above the stratigraphically highest occurrence of illitic oil shale in the lower part of zone R-2.

Samples for the depths listed in table 4 were prepared for analysis by compositing one-quarter of 0.6 m lengths of drill core (5 cm in diameter) from core hole C5. The amounts of minerals and kerogen were calculated from the following analyses: acid-soluble sodium (in 6 percent HCl solution) was determined by flame photometry by Wayne Mountjoy and John Blair; elemental aluminum, silicon, potassium, and calcium were determined by wave length-dispersive X-ray fluorescence analysis of pressed pellets of powdered whole-rock samples by J. S. Wahlberg and M. W. Solt. Nahcolite was determined quantitatively by P. C. Beck, who used the thermal method of Dyni and others (1971). The amount of kerogen was calculated from Fischer assays made by the Laramie Energy

Technology Center, Department of Energy, Laramie, Wyoming.

Estimates of the range of precision for the analytical data were made by comparison of the data with duplicate analyses and with analyses made by other methods on small sets of samples, mostly those from table 4. The ranges in precision for the data were determined by regression methods at 95 percent confidence limits. For sodium, duplicate analyses for a set of 13 samples gave an estimated range in precision of  $\pm 1$  to 6 percent of the reported value. For aluminum, the estimated range in precision is  $\pm 5$  to 15 percent for aluminum values of 1.9 or more percent (91 percent of the samples listed in table 4) on the basis of comparing the X-ray data with atomic absorption analyses made on a set of 13 samples by I. C. Frost. The estimated range in precision for silicon is  $\pm 6$  to 15 percent for values of 6.8 or more percent (91 percent of the samples listed in table 4), based on the comparison of the X-ray values with silicon values determined colorimetrically by G. T. Burrow on a set of 14 samples. Potassium values of 1.0 or more percent (80 percent of the samples listed in table 4) have an estimated range in precision of  $\pm 6$  to 22 percent, based on a comparison of the X-ray values with potassium values determined in duplicate by flame photometry by Wayne Mountjoy on a set of 16 samples. For calcium, the estimated range in precision is  $\pm 5$  to 15 percent for values of 2.8 or more percent (90 percent of the samples listed in table 4) based on a comparison of the X-ray data with calcium values determined in duplicate by atomic absorption analyses of a set of 16 samples by Wayne Mountjoy. The accuracy of the elemental data is undetermined. For nahcolite, the estimated

range in precision for samples containing 5.0 or more percent nahcolite is  $\pm 0.3$  to 2.4 percent. The estimated accuracy of the nahcolite values in amounts of 5.0 or more percent ranges from  $\pm 1$  to 10 percent of the reported value.

The mineralogy of each sample was determined qualitatively by X-ray diffraction analyses of pressed pellets of whole-rock specimens. The minerals and their chemical formulas used in calculating mineral percentages were: nahcolite ( $\text{NaHCO}_3$ ), dawsonite [ $\text{NaAl}(\text{OH})_2\text{CO}_3$ ], dolomite [ $\text{CaMg}(\text{CO}_3)_2$ ], calcite ( $\text{CaCO}_3$ ), albite ( $\text{NaAlSi}_3\text{O}_8$ ), potassium feldspar ( $\text{KAlSi}_3\text{O}_8$ ), and quartz ( $\text{SiO}_2$ ). No allowances were made for small amounts of other minerals, including illite and pyrite, which are known to be present in many samples. These minerals probably amount to no more than a few percent in most samples. Additionally, no allowances were made for compositional variations, especially in dolomite, which is known to contain substantial quantities of iron. The steps used to calculate the percentages of the minerals and kerogen follow:

1. The amount of nahcolite was determined by the thermal method, and the amount of sodium in nahcolite was calculated.
2. The amount of sodium assignable to dawsonite was calculated by subtracting nahcolite sodium from the analytically determined value of acid-soluble sodium, and this value was used to calculate the amounts of dawsonite and dawsonitic aluminum.
3. Feldspar aluminum was taken as the difference between total aluminum and dawsonitic aluminum.
4. The amounts of potassium feldspar and aluminum in

potassium feldspar were calculated from the value for potassium.

5. Sodium feldspar was determined from the difference between the amount of feldspar aluminum and the amount of aluminum in potassium feldspar.

6. The difference between the amount of silicon assignable to the feldspars and total silicon was used to calculate percent quartz.

7. Dolomite was calculated from total calcium. For those samples containing both calcite and dolomite, peak-height ratios from X-ray diffractograms were used to calculate relative amounts of each mineral by the method of Royse and others (1971), then percentages of each mineral were calculated from the value for total calcium.

8. The amount of kerogen was calculated from the Fischer assay of the sample, in gallons per ton, multiplied by an empirically derived factor of 0.58 developed by Smith (1966) for oil shale in the Mahogany zone. It is assumed that this factor remains constant through the saline facies, whereas, it probably changes somewhat with depth.

The total amount of minerals plus kerogen for the samples listed in table 4 ranges from 83.2 to 119.6 weight percent. Almost 90 percent of the values range between 94 and 112 weight percent. The grand mean for all 279 samples is 103.4 weight percent.

A series of experiments were made to determine the validity of the methods used to determine the amounts of minerals and kerogen in table 4 and to determine, if possible, the major sources of error in the calculations. The amounts of mineral and organic

carbon (figs. 15 and 16) were compared with values for mineral and organic carbon calculated from the data listed in table 4 for a suite of 46-47 samples selected from those listed in the table 4. The figures show a fairly wide scatter of data points. Correlation coefficients for both data sets is 0.92. Most samples in both figures are biased toward higher calculated rather than analytically determined values for mineral and organic carbon. If the latter values are accurate, the data suggest that the carbonate minerals or kerogen, or both, were overestimated in table 4.

The calculated amounts of minerals and kerogen from table 4 were compared to water-soluble, acid-soluble, and acid-insoluble fractions of small sets of samples listed in table 4 (figs. 17, 18, and 19). In figure 17, the weight loss in water of 16 samples of nahcolitic marlstone was compared to nahcolite values determined by the thermal method. A high degree of correlation ( $r^2=0.997$ ) was found with very little bias, indicating that the thermal method used to determine nahcolite values in table 4 yields accurate results. Similarly, in figure 19, the weight of the acid-insoluble fraction of 28 samples was compared with the total weight of feldspars, quartz, and kerogen from table 4. Again, a high degree of correlation ( $r^2=0.969$ ) was found with only a small bias between data sets, indicating that the sum of the weights of the silicate minerals and kerogen is reasonably accurate. A high degree of correlation ( $r^2=0.997$ ) was also found when the weight loss of the acid-soluble fraction of 29 samples in figure 17 was compared with the sum of the weights of acid-soluble calcium, magnesium, iron, and sodium calculated as metal carbonates. From these data and

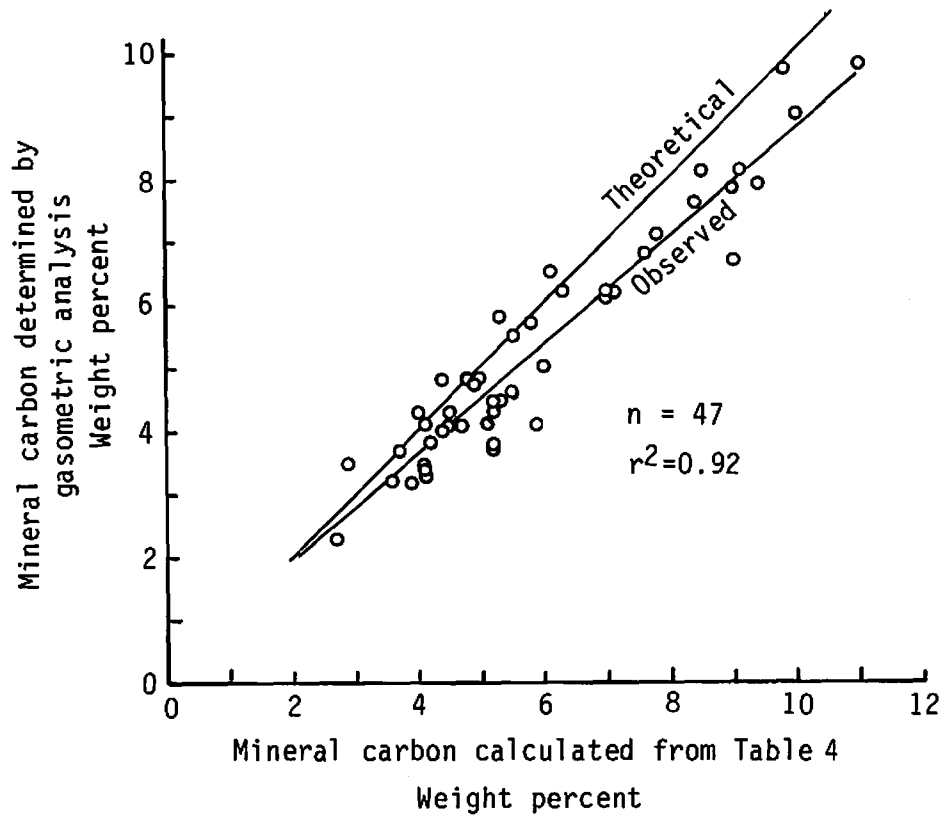


Figure 15.--Comparison of the amount of mineral carbon determined by gasometric analysis with total mineral carbon calculated from the amounts of the carbonate minerals in table 4 for 47 samples of marlstone from table 4. The carbon analyses were made by I. C. Frost.

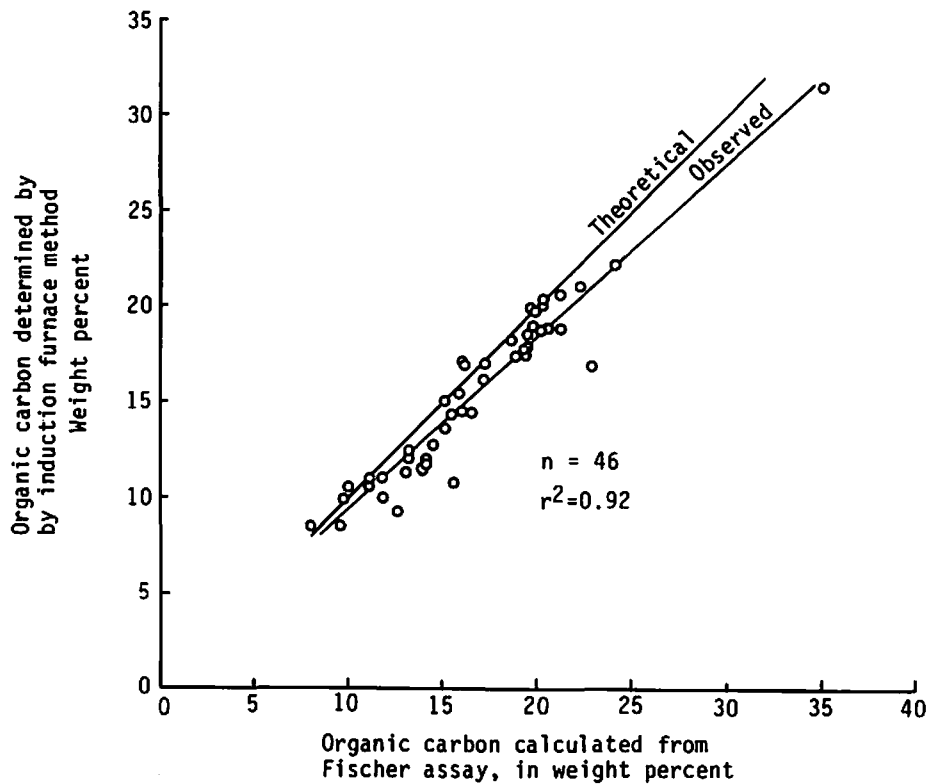


Figure 16.--Comparison of the amount of organic carbon calculated from Fischer assays with the amount of organic carbon determined by chemical analyses for 46 samples from table 4. Organic carbon was calculated by difference from total carbon determined by induction furnace and mineral carbon determined by gasometric analysis. The carbon analyses were made by I. C. Frost, and the Fischer assays were made by the Laramie Energy Technology Center, U.S. Department of Energy.



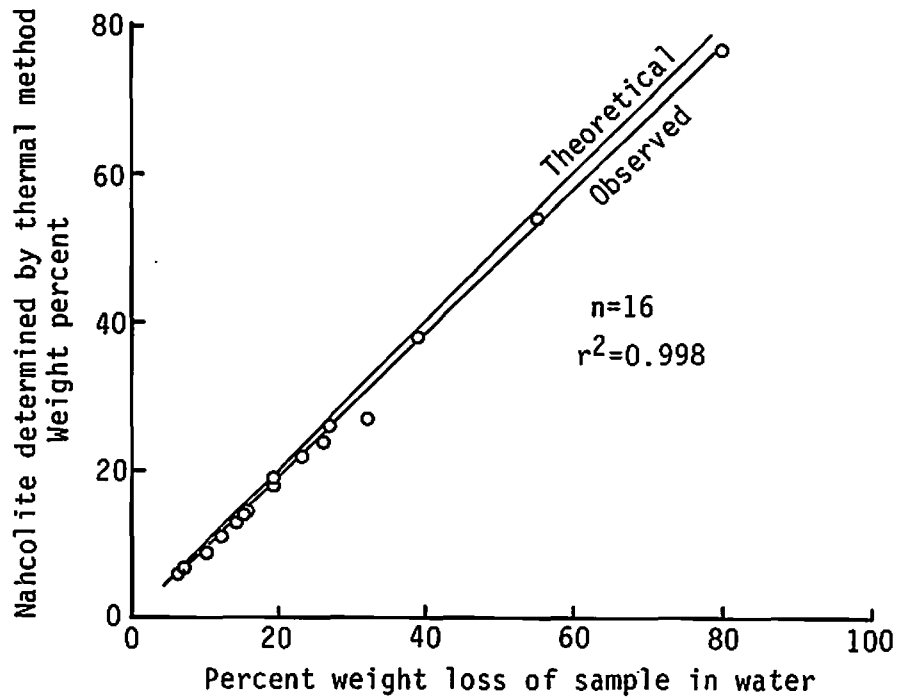


Figure 17.--Comparison of weight loss in water and nahcolite determinations made by the thermal method of Dyni and others (1971) for 16 samples of nahcolitic marlstone selected from table 4.

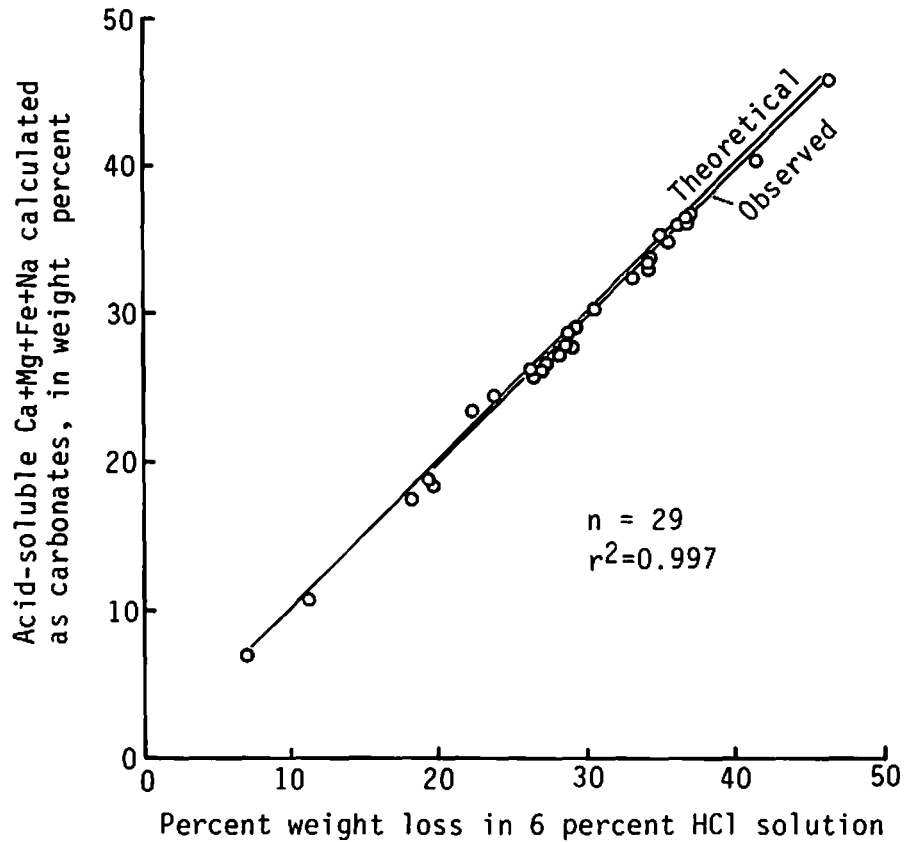


Figure 18.--Comparison of the weight of the acid-soluble fraction with the sum of acid-soluble calcium, magnesium, iron, and sodium calculated as carbonates for 29 samples of nahcolite-free marlstone from table 4. The amount of acid-soluble sodium was calculated as dawsonite, and the other cations were calculated as simple metal carbonates.

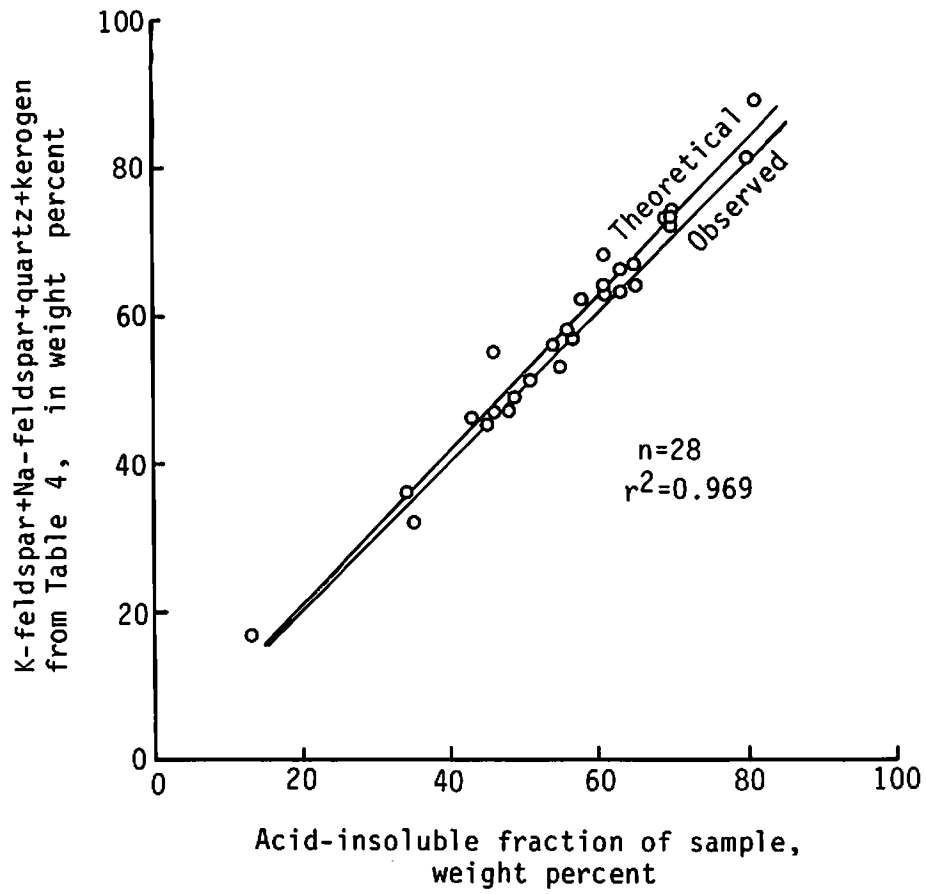


Figure 19.--Comparison of the acid-insoluble weight with the sum of the calculated weights of the silicate minerals and kerogen for 28 samples of marlstone from table 4.

X-ray diffraction analyses, it can be reasonably assumed that the acid-soluble cations occur in dolomite, ankerite, calcite, dawsonite, and possible siderite. When the sum of the weights of the acid-soluble carbonate minerals calculated from table 4 are compared with the acid-soluble weight loss for 28 samples of marlstone in figure 20, the correlation of the data ( $r^2=0.77$ ) is relatively poor, but with no significant bias. Furthermore, the sum of magnesium and iron in atomic percent correlates poorly ( $r^2=0.62$ ) with calcium in the acid soluble fraction of 26 samples in figure 21 calculated on a calcite-free basis from data in table 4. Excess calcium is found in a number of samples suggesting that calcite is underestimated in many samples in table 4, probably because the diffraction lines for calcite and siderite are difficult to see at low concentrations (<10 percent).

The conclusion drawn from the foregoing experimental data is that, with the exception of dawsonite, the principal source of error in computing mineral percentages lies with the acid-soluble carbonate minerals. The percentage of dawsonite was determined from acid-soluble sodium values and should be independent of the other carbonate minerals.

The values for minerals plus kerogen for the samples listed in table 4 were normalized to equal 100 weight percent except those for nahcolite, dawsonite, and kerogen, which were assumed to be measured without substantial error. These normalized values, summed as silicates, carbonates, and kerogen are plotted on ternary diagrams in figure 22. Figure 22A shows the compositional field for samples calculated with nahcolite, and figure 21B shows the

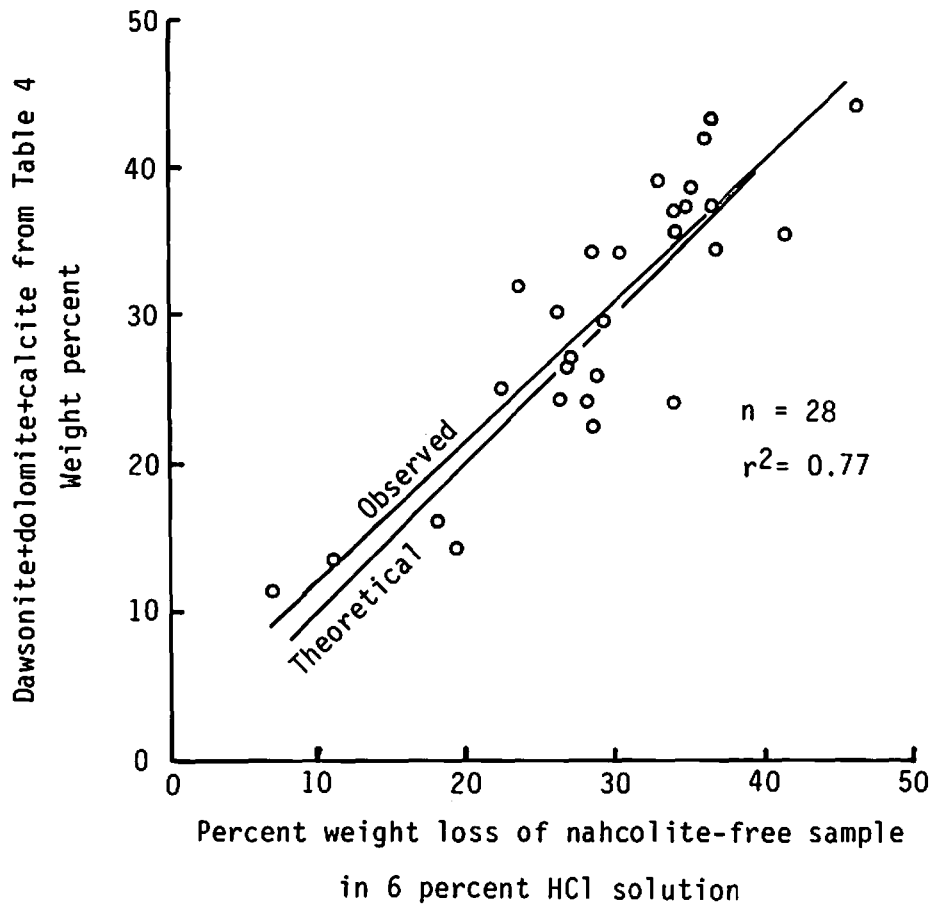


Figure 20.--Comparison of the acid-soluble weight loss with the sum of the calculated amounts of the carbonate minerals for 28 samples of nahcolite-free marlstone from table 4.

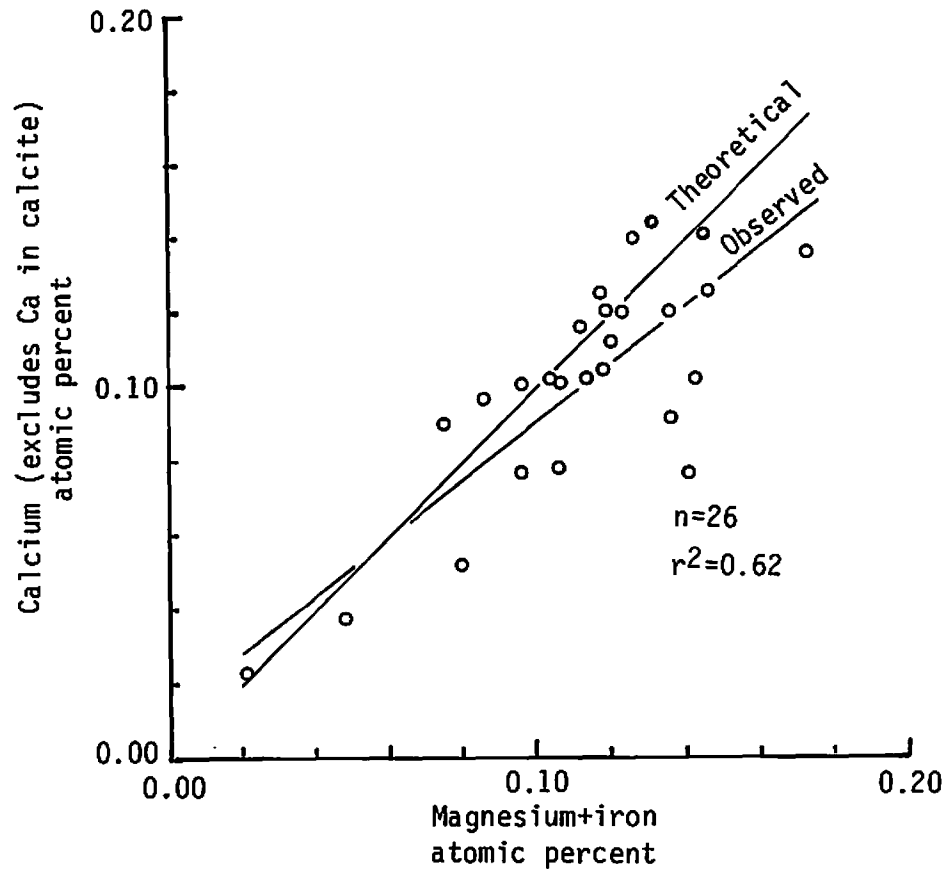
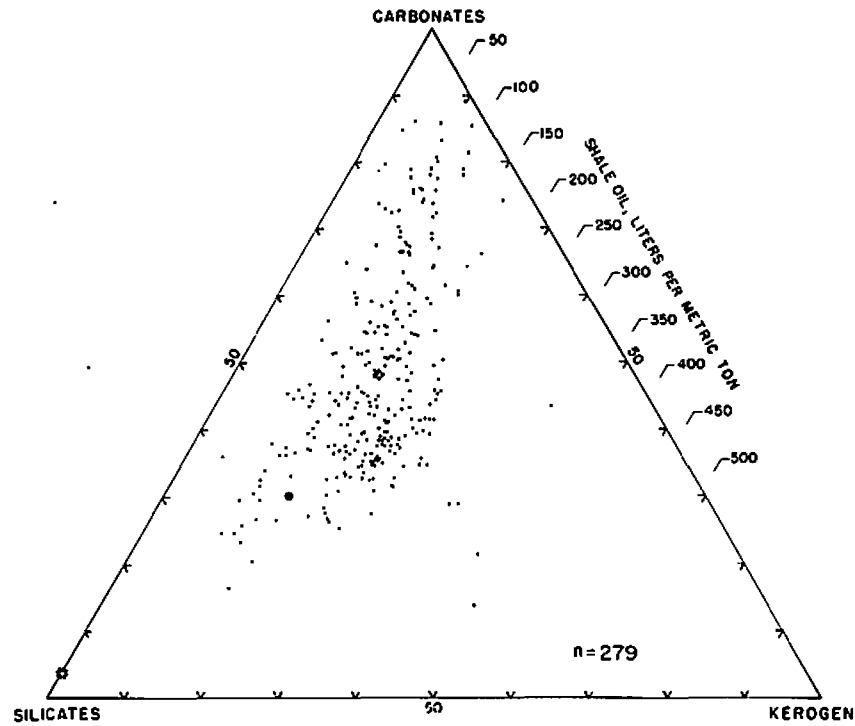


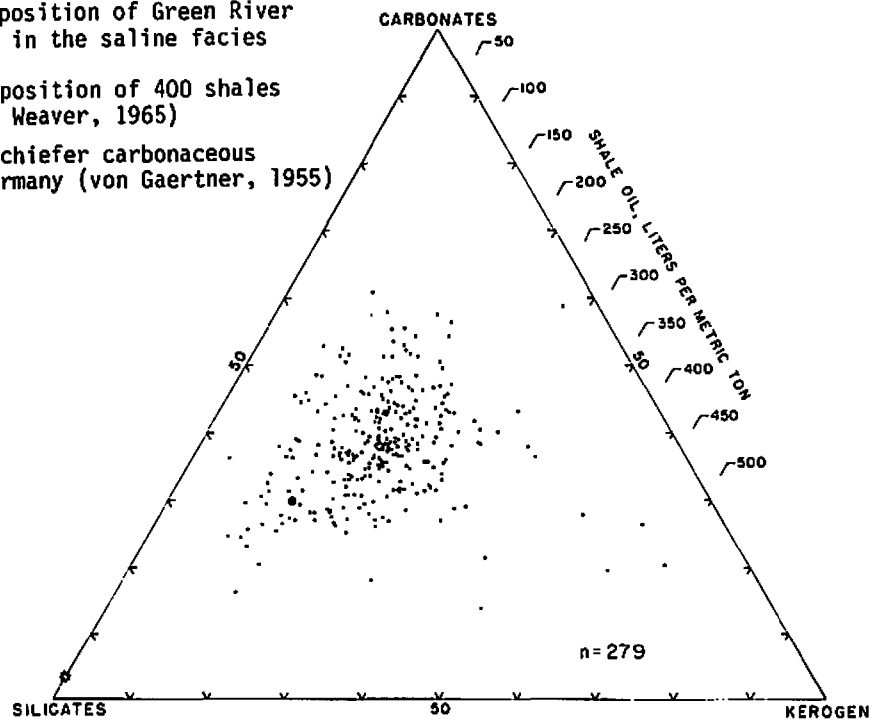
Figure 21.--Comparison of the amount of acid-soluble calcium with the sum of the amount of acid-soluble magnesium and iron for 26 samples of marlstone selected from table 4.

Figure 22.--Compositional fields for kerogenous marlstone from the saline facies in core hole C5 between the depths of 561.14 and 737.92 m. Normalized data are from table 4. Carbonates include dawsonite, dolomite, calcite, and nahcolite in diagram A and exclude nahcolite in diagram B. Silicates include K-feldspar, Na-feldspar, and quartz in both diagrams.



A. Compositional field of nahcolitic marlstone

- ◊ Average composition of Green River marlstone in the saline facies
- ▣ Average composition of 400 shales (Shaw and Weaver, 1965)
- Posidonienschiefer carbonaceous shale, Germany (von Gaertner, 1955)



B. Compositional field of nahcolite-free marlstone



field excluding nahcolite. The average mineral composition for the 279 samples including nahcolite is 48.1 weight percent carbonate minerals, 33.1 percent silicate minerals, and 18.8 percent kerogen. Figure 21A shows a wide scatter of data points reaching toward the carbonate end of the diagram, which reflects nahcolite-rich units and beds. With the removal of nahcolite, the compositional field contracts to a rather small area with mean values for the entire sample suite of 38.1, 38.6, and 23.3 weight percent for carbonates, silicates, and kerogen, respectively.

The composition of a carbonaceous marine shale from Germany in terms of carbonate and silicate minerals and organic matter is not greatly different from that of saline Green River marlstone, although the two kinds of rocks differ in mineral types and origin, whereas the average composition for 400 samples of Phanerozoic marine shales lies completely out of the compositional field for Green River marlstone.

#### Mineral Distributions

Figure 23, a simplified version of plate 1, shows the stratigraphic distribution of some minerals in the Green River oil-shale deposits from the depocenter to the outcrop on lower Piceance Creek. The stratigraphic distributions for nahcolite, dawsonite, halite, analcime, illite, and "exotic" minerals including northupite, searlesite, shortite, and wegscheiderite are shown. These mineral distributions are based on X-ray diffraction analyses of samples from core hole C5 (table 4), C177 (writer's unpublished data), C34 (Robb and others, 1978), and from the surface section on lower Piceance Creek (Brobst and Tucker, 1973).

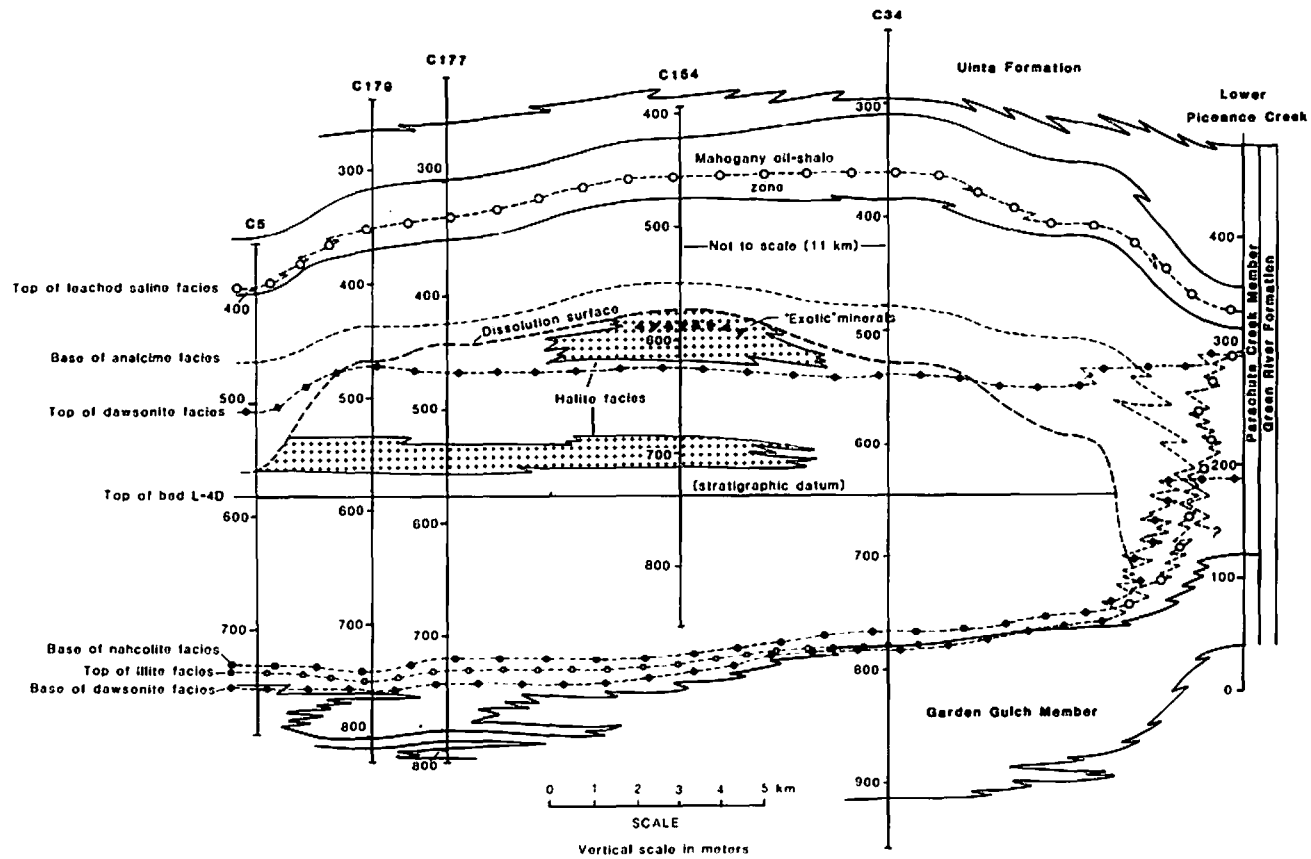


Figure 23.--Stratigraphic distribution of some minerals in the saline facies of the Green River Formation.

The mineral distributions shown on figure 23 form a series of concentric overlapping zones beginning with illite and analcime and progressing basinward through dawsonite, nahcolite, halite, and finally to the unusual minerals searlesite, northupite, shortite, and wegscheiderite found in the youngest halitic rocks at basin center. Relatively small amounts of minerals that lie outside their boundaries on the cross section are not shown.

In the subsurface, illite is the principal clay mineral in the fissile kerogenous shales that comprise the Garden Gulch Member. The top of the illite facies is shown in the wells, but data are too few to show the distribution of illite elsewhere on the cross section. Illite is present throughout most of the Parachute Creek Member on the outcrop at lower Piceance Creek (Brobst and Tucker, 1973, p. 30-32), but it is not yet clear how the mineral is distributed in the rocks from the outcrop to core hole C34.

Mineral facies relationships between core hole C34 and the surface at lower Piceance Creek are complex. Abrupt changes in mineral facies occur in a distance of a few kilometers of the outcrop, and the relationships shown on the cross section are partly speculative.

Analcime appears to be restricted to the upper leached part of the saline facies and overlying rocks. The base of the analcime facies lies rather persistently about 60-90 m below the Mahogany oil-shale zone in the subsurface and is found in progressively older rocks toward lower Piceance Creek. On the outcrop, analcime occurs essentially throughout the Parachute Creek Member.

Analcime, other than in minor amounts, is not found in the lower part of the oil-shale deposits in the subsurface.

In the subsurface, dawsonite first appears about 5-15 m below the top of the illite facies and is distributed vertically through as much as 280 m of kerogenous marlstone in the lower part of the saline facies. Dawsonitic rocks thin abruptly in the vicinity of lower Piceance Creek, and on the outcrop, dawsonitic rocks have thinned to a 110-m-thick sequence below the Mahogany zone.

The lower boundary for nahcolite lies consistently several meters above the top of the illite facies and extends upward to the dissolution surface. Most likely, nahcolite originally extended upward to the top of the leached part of the saline facies in the middle of the Mahogany zone. The nahcolitic rocks were originally at least 420 m thick as estimated in core hole C154, thinning to a leached 40-m-thick sequence in and just below the Mahogany zone on the surface at lower Piceance Creek.

Halite is limited to the lower part of the saline facies above nahcolite bed L-4D and below the dissolution surface, but like nahcolite, it probably was once present in the upper leached part of the saline facies, perhaps as high as B-groove and the lower part of the Mahogany zone which contain several solution breccias. Halite is restricted to subsurface rocks at the depocenter of the basin.

Searlesite, northupite, shortite, and wegscheiderite are found in small quantities in the upper group of halitic rocks just below the dissolution surface. Some of these minerals may have

been present in the upper leached part of the saline facies but have since been dissolved by ground water.

## CHAPTER V

### GEOCHEMISTRY OF SULFUR

Sulfur is believed to have played an important role in the origin of the sodium carbonate deposits of the Green River Formation. Dyni (1977) reported that sulfur in the nahcolitic oil shales in the Piceance Creek Basin is found almost entirely in reduced form chiefly in iron sulfide minerals and combined in small amounts with kerogen. Primary sulfate minerals are almost wholly unknown in any of the saline facies of the Green River Formation. Milton (1971) reported the occurrence of several authigenic sulfate minerals, but these are found only in trace amounts.

Within lacustrine rocks of the Tertiary lake system of Utah and Colorado, gypsum in beds as thick as 2.9 m are present in the Flagstaff Limestone on the Wasatch Plateau of central Utah (fig. 1) (Gill, 1950, p. 105). The only other occurrence of authigenic(?) gypsum in rocks of the Tertiary lake system of Utah and Colorado is in surface exposures of the upper one-half of the saline facies and the overlying limestone and sandstone facies of the Uinta Formation of Dane (1955), which form the youngest lacustrine rocks of the Tertiary lake system in western Uinta Basin (unpublished data). Brobst and Tucker (1973, p. 24) reported gypsum in outcrops of the Parachute Creek Member in the Piceance Creek Basin, but these are minor products of weathering. Surdam and Stanley (1980, fig. 2) show an occurrence of gypsum just below the Mahogany oil-shale bed in the eastern part of the Uinta Basin, but it is questionable,

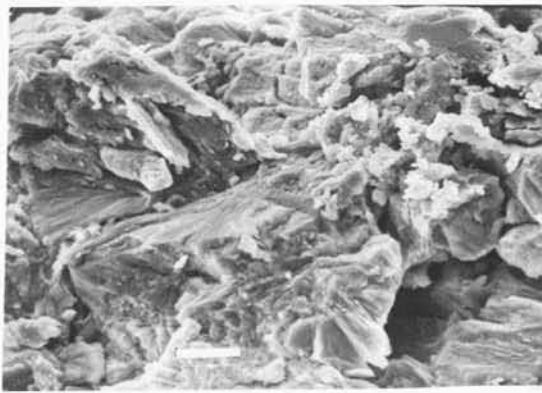
without substantiating evidence, whether this occurrence is primary or the product of weathering. Evidently, only reduced sulfur in sulfide minerals and small amounts combined with kerogen survived in the Tertiary lake system of Utah and Colorado after Flagstaff time until late in the history of Lake Uinta. The evidence indicates a large-scale three-fold geochemical cycle of dominantly oxidizing conditions represented by bedded gypsum in the Flagstaff Limestone, reducing conditions indicated by sulfide minerals during most of Green River time, followed by a return to oxidizing conditions late in Green River and Uinta time with the reappearance of authigenic(?) gypsum.

Cole and Boyer (1978) found that pyrite is the most abundant iron sulfide mineral in the Parachute Creek Member in the Piceance Creek Basin followed by marcasite, and pyrrhotite: small amounts of sulfur occur as sulfate and in kerogen. The sulfide minerals occur mostly in blades, blebs, streaks, lenses, discontinuous laminae, and patches in kerogenous marlstone. Within the saline facies, lesser amounts of mixed pyrite and marcasite form coatings around nahcolite aggregates (fig. 3A, F). Clumps of delicate blades of marcasite (?) and cubes of pyrite occur in small amounts in halite and nahcolite (fig. 24).

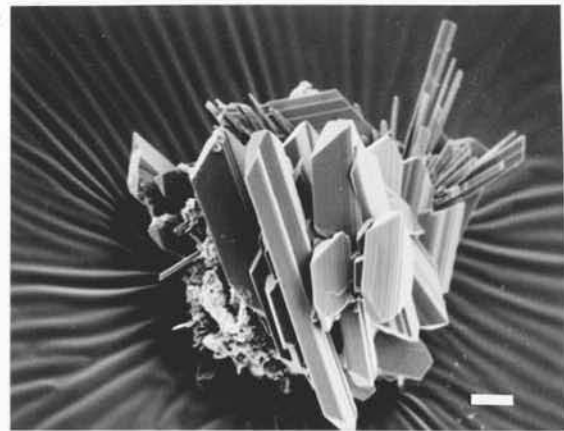
The average sulfur content in kerogen ranges from 1 to 2 percent (Smith, 1963) and represents only a small portion of the total sulfur in the Parachute Creek Member. Cole and Boyer also reported a small amount of sulfate in the Parachute Creek Member, but it is not known if this is weathered or authigenic material.

The sulfur content of 874 samples of oil shale

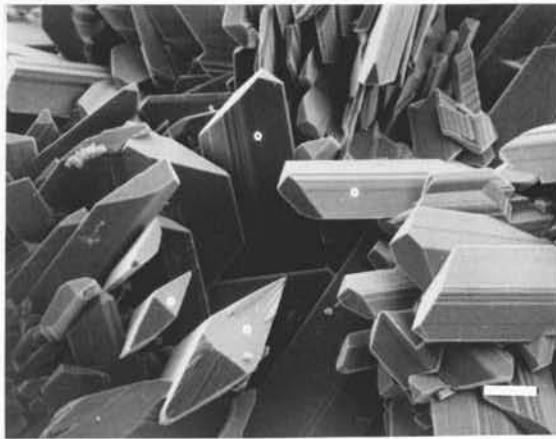
Figure 24.--Scanning electron photomicrographs of iron sulfide minerals in kerogenous marlstone, nahcolite, and halite. A. Fresh, unoxidized massive pyrite and marcasite from a discontinuous stringer subparallel to bedding in kerogenous marlstone. The pyrite-marcasite coatings around nahcolite aggregates are similar to this photomicrograph. B. A cluster of delicate prismatic crystals of marcasite(?) about 0.25 mm across from the water-insoluble residue of halite in a kerogenous matrix. X-ray diffraction analyses of such clusters found both marcasite and pyrite, although the crystal forms in photomicrographs B and C suggest marcasite. C. Close-up view of longitudinally striated crystals from a cluster similar to that in photomicrograph B. D. A group of penetration-twinned cubes of pyrite from the insoluble residue mentioned above. The bar scales on all the photomicrographs are 30  $\mu\text{m}$  long.



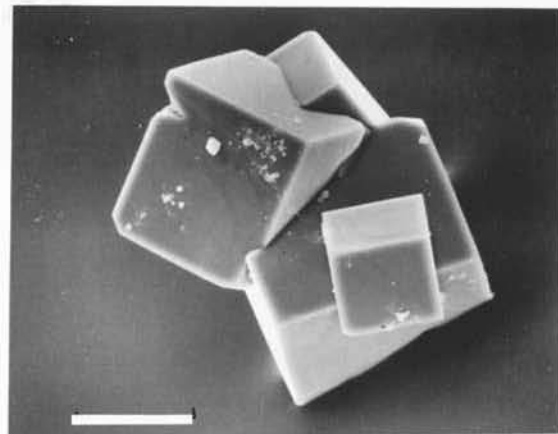
A



B



C



D

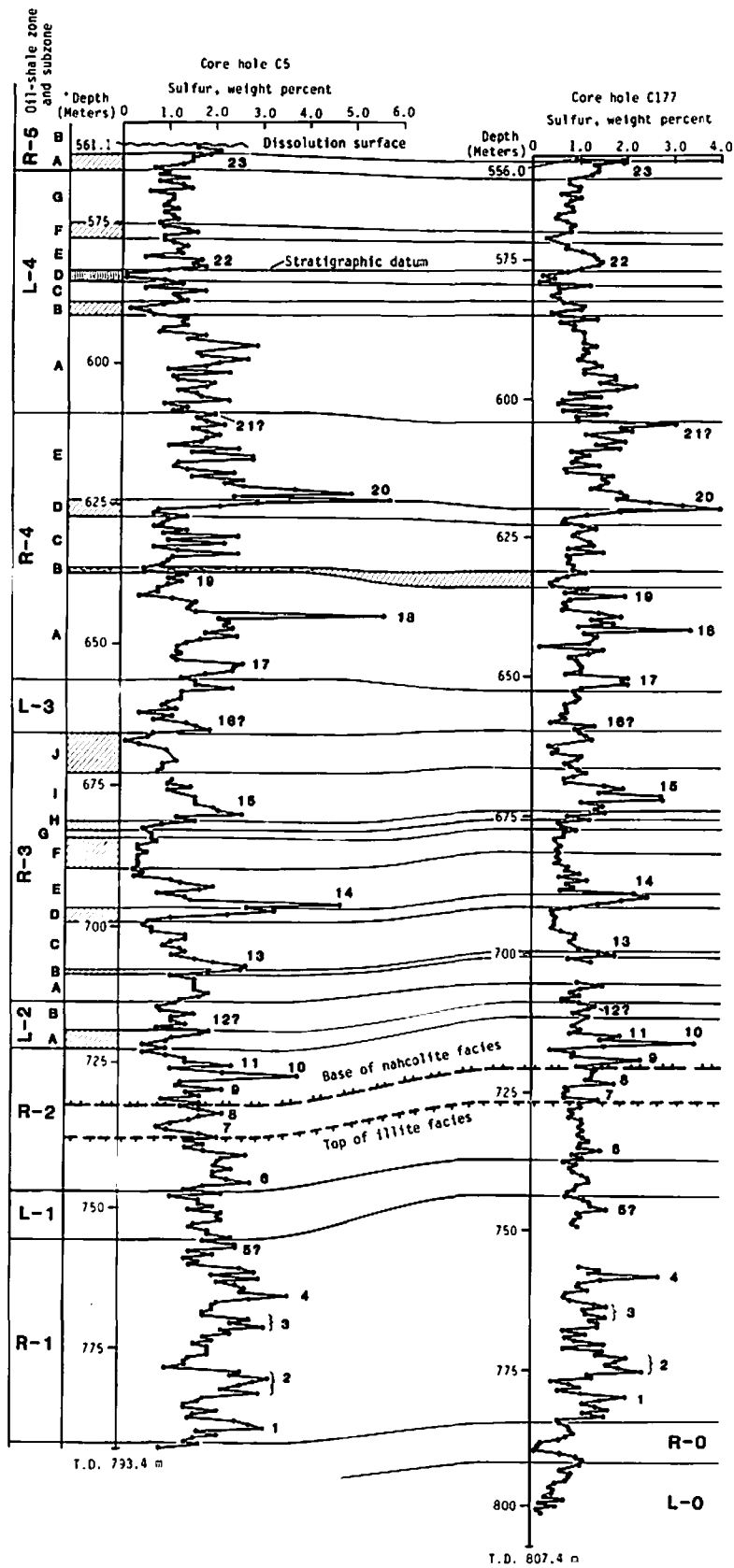


which represents nearly the entire sequence in core hole C177 was determined by wavelength-dispersive X-ray spectroscopy. The analyzed sequence of rocks extends from 232.9 to 801.9 m below the surface. The average sulfur content of this interval was 0.75 weight percent, and ranges from 0.01 percent in samples of bedded halite to 4.9 percent in nahcolitic oil shale. Dyni (1977) reported that the vertical distribution of sulfur through these rocks is cyclic with pronounced sulfur maxima in nahcolitic rocks occurring at or immediately above units of disseminated and bedded nahcolite (fig. 25).

Figure 25 shows vertical plots of sulfur values for 714 samples from core holes C5 and C177 which represent the upper part of the Garden Gulch Member and the lower unleached saline facies below the lowest occurrence of halite. The samples were prepared from 0.6 m lengths of quartered drill core which were crushed, powdered, and pelletized. The analyses were made by wavelength-dispersive X-ray spectrometry. The lower instrumental limit of detection is about 60 ppm. Analytical precision ranges from  $\pm 10$  percent for average values to  $\pm 25$  percent for the lowest values. The sulfur analyses in the figure are calculated on a nahcolite-free basis to eliminate the effect of dilution of the marlstone matrix in which most of the sulfur occurs.

The mean sulfur values (nahcolite-free) for the sequence of kerogenous marlstone from the base of oil-shale zone R-1 to the top of zone L-4 in core holes C-5 and C-177 are 1.49 and 1.03 weight percent, respectively. A Mann-Whitney U-test and a Kolmogorov-Smirnov two-sample test at a significance level of 0.01 both reject

Figure 25.--Vertical profiles of sulfur determinations of oil shale in core holes C5 and C177. The sulfur values are given on a nahcolite-free basis.



the hypothesis that the two sets of sulfur values were drawn from the same population. This suggests that there is significant lateral variation in total sulfur for the same stratigraphic sequence of rocks. The data suggest that the amount of total sulfur decreases toward the depocenter of the basin.

The sulfur values show much variation vertically through each of the core holes with local buildups of as much as 4 to 6 percent sulfur. As many as 23 of these sulfur cycles can be correlated between the two core holes. These cycles are identified by number on the profiles. Five sulfur cycles are in illitic kerogenous shales in oil-shale zone R-1. In the nahcolite facies, 8 of the 15 numbered sulfur cycles reach their maximum values at or just above the top of a unit of disseminated or bedded nahcolite, suggesting a genetic relationship between nahcolite and sulfide deposition. Preliminary petrographic study suggests that the sulfur in the numbered sulfur cycles occurs chiefly in the forms described by Cole and Boyer (1978) which Dyni (1977) suggested were deposited during early diagenesis. Parts of the sulfur profiles in the nahcolitic rocks are not readily correlatable between the core holes, perhaps due, as suggested by Dyni (1977), to an overprint of sulfide coatings deposited on nahcolite aggregates during late diagenesis which obscures the earlier-formed sulfide. The numbered sulfur cycles seem to show no preference for laminated or blebby and streaked marlstone.

## CHAPTER VI

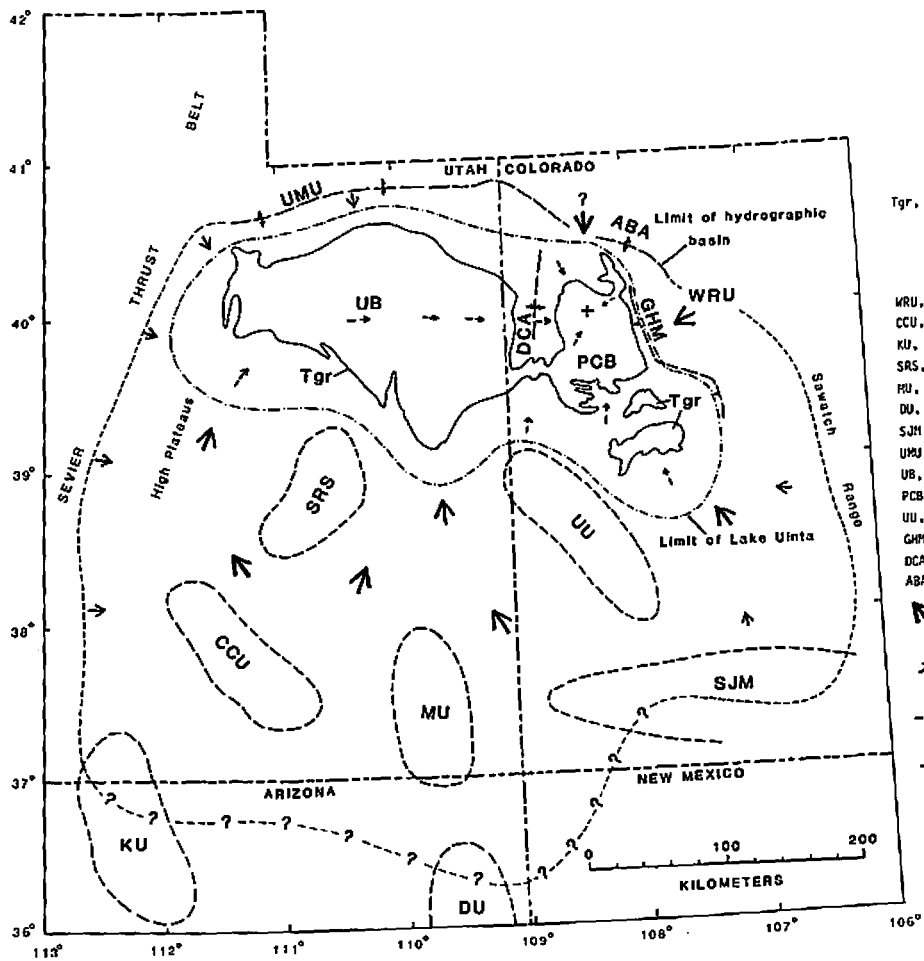
### LACUSTRINE DEPOSITIONAL MODEL

In the following depositional model for the nahcolite deposits in the Piceance Creek Basin, five factors are evaluated: (1) extent of the basin and sources of sediments, (2) lake-basin morphology, (3) permanency and chemistry of lake waters, (4) sulfate-bicarbonate reactions, and (5) processes of sedimentation. The depositional model described herein may be termed the permanent lake model.

#### Hydrographic Basin and Sediment Sources

Eocene Lake Uinta must have drained a large part of the Colorado Plateau in Utah, Colorado, and adjacent states. The estimated area of the hydrographic basin of Lake Uinta, shown in figure 26, is 223,000 km<sup>2</sup>. In contrast, the area of the hydrographic basin of Eocene Lake Gosiute in Wyoming is estimated at 126,000 km<sup>2</sup> (Bradley and Eugster, 1969, p. 321). Probably conservative in size, the hydrographic basin of Lake Uinta is adapted from paleogeographic maps of the Eocene Epoch by Hunt (1956, fig. 56) and McDonald (1972, fig. 7). Parts of the hydrographic basin are poorly defined for lack of definitive physiographic features, especially on the south side where topographic relief was low. Here, the basin could have extended far into central Arizona and western New Mexico (see Hunt, 1956, fig. 56). Other parts of the basin are more clearly defined

Figure 26.--Estimated areas of the hydrographic basin and the maximum extent of Lake Uinta during middle Eocene (Mahogany zone time). The hydrographic basin, probably conservative in size, may have extended southward into central Arizona and western New Mexico. The queried arrow north of Piceance Creek Basin is about the location of an ancestral stream proposed by Bradley (1931, p. 89-90, fig. 14) that drained Eocene Lake Gosiute to the north and emptied into Lake Uinta.



#### EXPLANATION

Tgr, Area occupied by the Green River Formation in the Uinta and Piceance Creek Basins. Outcrops in the Wasatch Plateau are omitted.

WRU, White River uplift  
 CCU, Circle Cliffs upwarp  
 KU, Kaibab upwarp  
 SRS, San Rafael Swell  
 MU, Monument upwarp  
 DU, Defiance upwarp  
 SJM, San Juan Mountains  
 UMU, Uinta Mountain uplift  
 UB, Uinta Basin  
 PCB, Piceance Creek Basin  
 UU, Uncompahgre upwarp  
 GJM, Grand Hogback monocline  
 DCA, Douglas Creek arch  
 ABA, Axial Basin anticline

↖ Major source of fine-grained sediments and soluble salts

↗ Minor source of fine-grained sediments and soluble salts

→ Direction of water movement in Lake Uinta

+ Depocenter for salines in the Parachute Creek Member

by positive Laramide structural elements that were being vigorously eroded and were contributing sediments to the lake basin during Green River time.

The boundary of the hydrographic basin follows approximately the crest of the Uinta Mountains, extends eastward along the Axial Basin anticline, then bends southward following the White River uplift and Sawatch Range to the San Juan Mountains. All of these features were positive structural elements during early and mid-Tertiary time (Tweto, 1975) and are assumed here to have formed the drainage divide between the hydrographic basin of Eocene Lake Uinta with other Tertiary drainage areas to the north and east. The western edge of the basin is assumed to be somewhat west of the High Plateaus region of central Utah. Coarse clastics consisting of Precambrian and early Paleozoic quartzites and Paleozoic carbonates were being deposited eastward off a highland in the Sevier thrust belt that bordered the High Plateaus region on the west (Stanley and Collinson, 1979).

Sources and direction of movement of sediments are indicated by arrows on figure 26. The small arrows indicate source areas that contributed coarse clastics because of high relief and a relatively small drainage area and because of resistant types of sedimentary rocks that were being eroded. Such areas are suggested along the south flank of the Uinta Mountains (Picard, 1957, fig. 8) and in the eastern part of the Sevier thrust belt (Stanley and Collinson, 1979; Ryder and others, 1976). Source areas and direction of movement of fine-grained sediments (sands and muds) and soluble salts are indicated by the large arrows. Large areas



in southeastern Utah were underlain by Mesozoic sedimentary rocks that probably supplied large volumes of fine-grained sediments to the basin. Sediments derived from sandstones and shales of the Mesaverde Formation and the underlying Mancos Shale, both of Late Cretaceous age, possibly made up a major part of the total volume of these sediments, although younger Paleocene and older Mesozoic sedimentary rocks no doubt contributed significant amounts. Solutes derived from these formations, especially from the Mesaverde and Mancos Formations, probably included substantial quantities of sulfate, which formed from weathering of pyrite in carbonaceous and coaly shales in the Mesaverde Formation and in marine shales of the Mancos Shale. There is no compelling evidence to suggest that the source rocks, or the streams that emptied into Lake Uinta, were sulfate deficient. On the contrary, sulfate was probably an abundant solute in surface waters that drained the areas of low relief south of Lake Uinta.

Volcanism contributed varied amounts of silicic air-fall ash to the hydrographic basin and to the lake during deposition of the saline facies. Brobst and Tucker (1973, p. 15-18) recorded a total of 1.5 volume percent of volcanic ash as discrete beds in 177.1 m of kerogenous marlstone in the upper part of the Parachute Creek Member exposed along lower Piceance Creek from the base of oil-shale zone R-5 to the top of the Mahogany zone. The same amount of volcanic ash was found in beds in 953 m of middle and upper Green River lacustrine rocks in Indian Canyon by the writer and W. B. Cashion (unpublished notes). However, only a few scattered beds of volcanic tuff have been found in the lower part

of the Parachute Creek and underlying Garden Gulch Members in Piceance Creek Basin (pl. 1). Possibly, as much as three times, or more, of the volume of ash recorded as discrete beds in the lake sediments were deposited in the hydrographic basin and transported to the lake and were deposited as widely disseminated components of the marls.

Leaching of volcanic ash probably contributed substantial amounts of sodium and other alkali and alkaline earth metals to the dissolved sediment load of Lake Uinta especially in the last half of Parachute Creek time.

#### Lake-Basin Morphology

Throughout its existence, Eocene Lake Uinta occupied the northern part of its hydrographic basin in the Uinta and Piceance Creek sedimentary-structural basins (fig. 26). Bradley (1931, p. vi and 54) envisioned the lake basin as a nearly flat, shallow, pan-shaped depression with gently sloping shores and topographic gradients within the basin of less than 0.2 m/km (<1 ft/mi). Similar lake-basin morphology was inferred for Lake Uinta in the Piceance Creek Basin by Lundell and Surdam (1975). These authors concluded that primary dips of depositional surfaces were low and ranged from 0.2 to 0.6 m/km (1 to 3 ft/mi) based in part on sedimentological studies of outcrops. However, the subsurface stratigraphy presented in this report (pl. 1), and other published subsurface stratigraphic data clearly show that the basin was strongly asymmetric, and that primary dips must have varied significantly in different parts of the basin.

Along the eastern and northeastern sides of the Piceance Creek Basin, much of the fine-grained basinal lacustrine rocks of the Green River Formation interfinger abruptly eastward with shoreward sandy clastic rocks deposited in what Roehler (1974, p. 57) termed a "mountain-front" environment. The subsurface basinal rocks, as revealed in wells on the east side of the Piceance Creek gas field (Duncan and Belser, 1950), consist of 300 m of mostly gray to black kerogenous shale of the Garden Gulch Member overlain by 330 to 400 m of gray to black fine-grained kerogenous dolomitic rocks of the Parachute Creek Member. The lower three-quarters of this sequence interfingers laterally eastward within a distance of 7 to 10 km with the Anvil Points Member, a shoreward sequence of rocks, 425 to 580 m thick, composed of dominantly sandstone and sandy shale, which contains much oolite, locally abundant ostracodes, some conglomerate, and fossil wood (Duncan and Denson, 1949; Duncan and Belser, 1950; Donnell, 1961, pls. 50, 51, and 53; O'Sullivan, 1974; Snow, 1970). Elsewhere in the basin, the interfingering of basinal lacustrine rocks with shoreward rocks is much less abrupt in a lateral sense and interbedded units of basin, and shore rocks persist laterally for considerable distances (for example, see Roehler, 1974, southwest portion of fig. 1).

The facies relationships described above indicate continuous, moderately rapid, downwarping during early to middle Eocene time along the east and northeast sides of the basin, in response to tectonic movement along possible deep-seated high-angle faults (not documented) flanking the Grand Hogback and perhaps along the northeast side of the Red Wash syncline (Murray and Haun,

1974, fig. 8). In the southern and western parts of the basin, lithofacies relationships indicate that the rate of subsidence was much less. Consequently, depositional slopes along the east, northeast, and north(?) sides of the Piceance Creek Basin must have been significantly higher than in other parts of the basin.

Taking into account the effects of regional structure and differential compaction of sediments, Bradley (1964, p. A16-A17) concluded that shoreward outcrops of the Green River Formation in the western part of the Green River Basin in southwestern Wyoming displayed "abnormally high" primary dips of 1-10°. Abrupt interfingering of conglomeratic fluvial rocks of the Wasatch Formation with fine-grained lacustrine marlstones of the Green River Formation along the structurally active northern flank of the Uinta Mountains also suggests high initial dips northward into Eocene Lake Gosiute (Bradley, 1964, p. A9-A16; Anderman, 1955; Culbertson and others, 1980, pl. 1).

Lithofacies relationships between the Anvil Points Member and basinward sediments of the Parachute Creek and Garden Gulch Members in the Piceance Creek Basin suggest that primary dips were not as high as those reported by Bradley in the Green River Basin, but perhaps were as much as 1-2° (17-35 m/km). In other parts of the Piceance Creek Basin, primary dips may have been as low as 0.2-0.6 m/km as suggested by Bradley (1931) and Lundell and Surdam (1975). If a 1-2° lake basin slope is assumed, and assuming that the width of the slope from shore to the lowest point in the basin was about 6 km, a depth of water of about 100 to 200 m is indicated. The point of these calculations is that if the lake

basin was asymmetric with relatively steeper primary dips along the east and north sides (Snow, 1970, fig. 8), the lake could have been considerably deeper than has been suggested by Lundell and Surdam (1975).

The configuration of the lake bottom may not have been as flat as Bradley (1931, p. vi) surmised. Isopach data for the Parachute Creek and Garden Gulch Members (Dyner, 1969, fig. 3, p. 64-65) suggest the presence of several subbasins in the northern part of the Piceance Creek Basin. The principal depocenter for the nahcolite and halite deposits is in the east one-half of T. 1 S., R. 98 W. A small subbasin lies to the north in T. 1 N., Rs. 97-98 W. as suggested by Dyner's isopach data. In this area, several bedded units of nahcolite in the lower part of oil-shale zone R-5 locally thicken northward. Another subbasin, in which salines may have accumulated, is along the Hunter Creek syncline in Tps. 2-3 S., R. 97 W. according to Dyner (ibid.). These subbasins were probably interconnected during deposition of the salines, and they had a local control on the thickness and lithology of some beds.

The Piceance Creek Basin itself is the easternmost of two sedimentary (and structural) subbasins of Lake Uinta, the other being Uinta Basin in Utah. The Piceance Creek and Uinta Basins are separated by the Douglas Creek arch (fig. 26). During the time of deposition of the saline facies of the Parachute Creek Member in the Piceance Creek Basin (ca. 46-50? m.y.; Mauger, 1977), the "delta facies" (Bradley, 1931, p. 18) consisting of 570 m of shallow lacustrine and fluvial gray and green sandy mudstones and channel-form sandstones was being deposited in the southwestern

part of Lake Uinta. At the same time a 600-meter-thick lithofacies consisting of interbedded planar-form sandstones, siltstones, gray and green shales, and oolitic, algal, and ostracodal limestones of the Douglas Creek Member was being deposited in shallow shoreward waters in the southern part of Lake Uinta in southeastern Uinta Basin (Cashion, 1967, p. 8-12). Rocks of the delta facies and the Douglas Creek Member grade northeastward and northward toward the depocenter of Lake Uinta into open-lacustrine marlstones and kerogenous marlstones of the Parachute Creek Member. No evaporites equivalent in age to the saline facies of the Parachute Creek Member in the Piceance Creek Basin are known in the Uinta Basin. This suggests that the waters of Lake Uinta during Parachute Creek time flowed eastward toward the Piceance Creek Basin.

The Douglas Creek arch (fig. 26) was a sublacustrine positive structural element that separated the Uinta and Piceance Creek Basins during much of Parachute Creek time. Shallow-water mudstones, sandstones, and siltstones that are laterally equivalent to the saline facies of the Parachute Creek Member were deposited in a mudflat environment on the southern end of the arch (Roehler, 1974, fig. 1). At the same time probably deeper water lacustrine sediments were being deposited across the middle or northern end of the arch, but these rocks have since been eroded away. Cashion and Donnell (1972) show that oil-shale zones R-4 through the Mahogany oil-shale zone and other selected beds were probably once continuous between the two basins although they thin across the middle part of the Douglas Creek arch. From this evidence, it seems probable the Uinta and Piceance Creek Basins were connected

through most if not all of Parachute Creek time, and that lake waters flowed eastward across the Douglas Creek arch carrying solutes that were concentrated by evaporation and deposited in the northern part of the Piceance Creek Basin.

The size of Lake Uinta must have varied in response to changing rates of water inflow and evaporation which were controlled by climate. During much of Parachute Creek time, the lake was estimated to be about one-third to one-half in size (20,000-30,000 km<sup>2</sup>) to that shown in figure 26. Following the deposition of the saline facies, Lake Uinta expanded to its maximum size, estimated to be about 56,000 km<sup>2</sup>, in middle Mahogany zone time. The maximum size of the lake is represented by the Mahogany oil-shale bed, the most widespread unit of the Green River Formation.

Transgressive and regressive lake stages are recorded by siliciclastic and carbonate rocks that formed laterally widespread planar beds in the southern part of the lake basin where depositional slopes were generally very low (<0.2-0.4 m/km). Such rocks include those of the Douglas Creek Member described by Cashion (1967) in the southeastern part of the Uinta Basin. Along the steeper eastern and northern parts of the Piceance Creek Basin, lake-basin to shore changes in lithofacies are relatively abrupt and shoreward clastic rock units are relatively thick compared to their lateral extent, reflecting steeper depositional dips as exemplified by rocks of the Anvil Points Member (Snow, 1970). As these rocks were being deposited on the margins and in shallower parts of the lake, the dissolved salts were being concentrated in the

deepest part of Lake Uinta in one or several small depressions in the northern part of the Piceance Creek Basin.

#### Lake Waters

Whether Lake Uinta was a permanent or playa lake during deposition of the saline facies of the Parachute Creek Member has been a controversial subject among researchers. In this section, stratigraphic, sedimentologic, and geochemical data are submitted as evidence in support of the permanent lake model and a model of the geochemical evolution of the lake waters is summarized.

#### Lateral continuity of beds and laminae

Within the saline facies, many beds of nahcolite and halite can be traced over scores of square kilometers in the Piceance Creek Basin. These beds were precipitated directly from a parent brine rather than having been formed within the sediments from interstitial brines. Individual couplets of halite and nahcolite and laminations within units of disseminated nahcolite can be correlated between core holes for distances of several kilometers (figs. 8 and 11). Such features seem best explained by fluctuations of salinity and salting stages of a permanent lake brine, which were controlled by episodic (possibly seasonal) variations in lake-water inflow and evaporation.

Interbedded with the evaporites are many units of kerogenous marlstone that can be correlated for tens, even hundreds, of kilometers in and between the Piceance Creek and Uinta Basins (Cashion and Donnell, 1972; Pitman and Johnson, 1978; and



Pitman, 1979). Within some beds, individual laminae of marlstone can be correlated in cores for many kilometers (Trudell and others, 1970, fig. 3, and Curry, 1964, fig. 2). These widespread beds and laminae of marlstone suggest deposition in quiet, unagitated, relatively deep waters in a large lake.

Within the saline facies in the northern part of the Piceance Creek Basin, oololiths, pisoliths, oncololiths, stromatolites, crossbedding, ripple-marks, mudcracks, oxidized (red) sediments, rafted sand or coarser grains, and other features that would indicate shallow-water sedimentation and/or subaerial exposure of sediments have not been found.

#### Vertical succession of sodium minerals and illite

Figure 23 indicates an ordered vertical succession of minerals in the saline facies at the basin depocenter beginning with illite in the upper part of the Garden Gulch Member. As the abundance of illite decreases through an interval of marlstone and shale about 15 m thick, dawsonite first appears and gradually increases in abundance upward through the interval. About 20-25 m above the lowest occurrence of dawsonite, the lowest nahcolite occurs as aggregates scattered through marlstone. About 10 m above the base of the nahcolitic rocks, the lowest of five zones of disseminated nahcolite occurs (L-2A, R-3B, R-3D, R-3F, and R-3H). The next higher unit of nahcolite, subzone R-3J, about 66 m above the base of the nahcolitic rocks, contains the lowest occurrence of bedded nahcolite. Bedded halite first appears in the lower part of oil-shale zone R-5, 172 m above the lowest occurrence of nahcolite.

This vertical sequence of mineral occurrences indicates a progressive evolution of lake and interstitial brine in terms of increasing salinity through Parachute Creek time.

#### Bromine-bearing halite

Dyni and others (1970) found that the bromine content of bedded halite in the Parachute Creek Member ranges from 15 to 182 ppm, and that the bromine values increased progressively upward, with many local variations, through the halitic rocks. Because the bromide ion is very soluble in the system  $\text{NaCl-NaBr-H}_2\text{O}$ , most of it remains in solution during precipitation of halite. However, a small amount of bromide ion substitutes for chloride in the crystal lattice of halite in proportion to the amount of bromine in the parent brine (Braitsch, 1971, p. 135-145). Bromide ion may also be present in fluid inclusions, but the amount compared to that in solid solution in halite is probably insignificant. Adsorption of bromine by kerogen and matrix minerals of the marlstones in the saline facies of the Parachute Creek Member is not significant. (Dyni and others, 1970, table 1, p. 175). Therefore, the vertical distribution of bromine in halitic rocks in the Parachute Creek Member appears to be a function of the original bromine content of the waters entering (and leaving) the basin and the evaporation history of Lake Uinta.

An upward increase in bromine content through a bed or sequence of beds of halite is interpreted to mean that the salinity of the parent brine increased in terms of bromine and other salts more soluble than halite. An upward decrease in bromine suggests

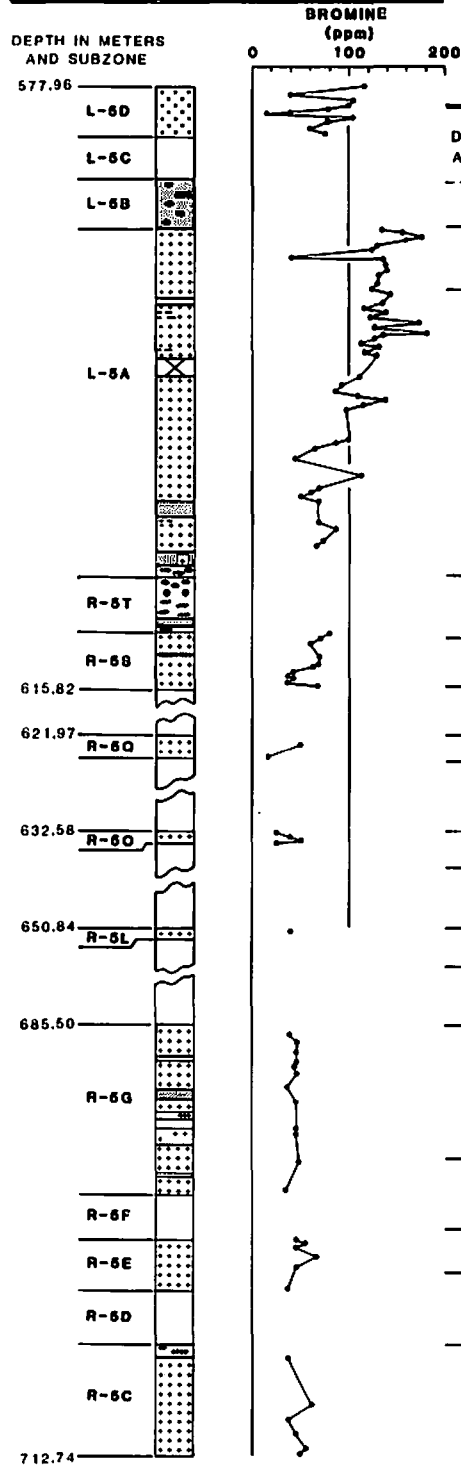
dilution of the brine with inflowing waters of relatively low-bromine content, perhaps accompanied by dissolution of some previously deposited halite. A sequence of halite beds that show no change in bromine content might suggest complete desiccation of the lake from one salting stage to the next, or possibly a barred basin setting in which the volume of influx waters matched reflux waters during salting stage with no net increase in the salinity of the brine. These interpretations of the bromine profiles assume no change in the bromine content of the waters entering Lake Uinta.

Bromine profiles for halitic rocks in two core holes that penetrate the saline facies in the Piceance Creek Basin are shown in figure 27. The bromine profile for core hole C154 is modified from Dyni and others (1970, fig. 7), and includes minor changes in depths based on new information. Another bromine profile through the same sequence of rocks is shown for core hole C8 which is located 2.6 km southwest of core hole C154.

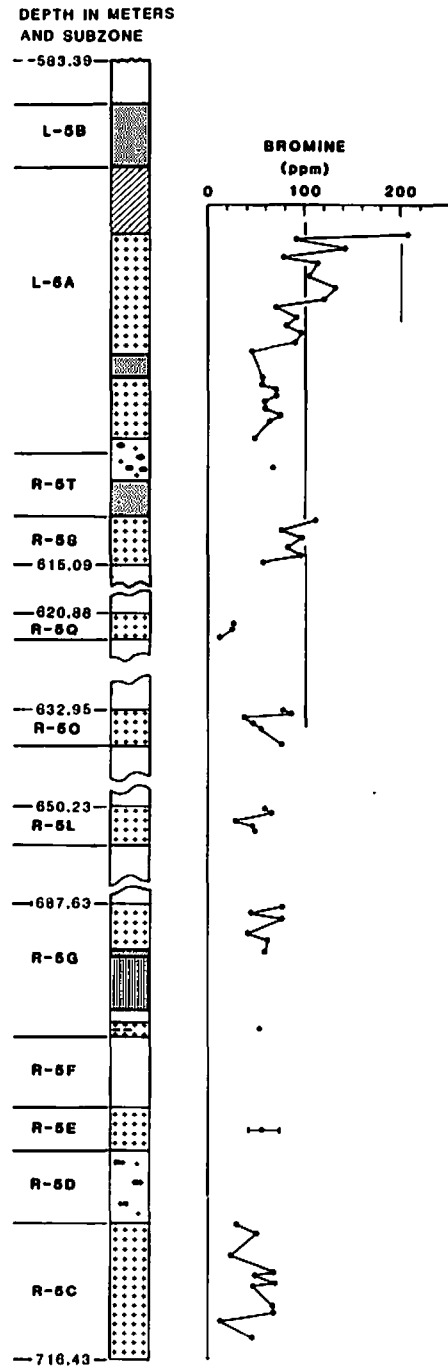
Both bromine profiles show a gradual increase in bromine from the base of subzone R-5C to the top of subzone L-5A. The profiles seem to show little change from subzone R-5C to R-5D and average about 50 ppm Br; however, the analytical error for these low values may be too large to clearly detect trends in the bromine profiles. From subzone R-5D to the top of L-5A, the bromine values clearly increase to as much as 200 ppm, then decrease to below 100 ppm in the highest subzone L-5D. The overall increase in bromine through the halitic rocks is interpreted to mean that there was a permanent body of water in the basin. Even during a period of maximum evaporation in subzone L-5A time, the parent lake brine

Figure 27.--Vertical profiles of bromine analyses of halite in core holes C154 and C8. Core hole C8 (Sinclair Oil Co. Skyline 1) is located in the NW1/4NE1/4 sec. 26, T. 1 S., R. 98 W., 2.6 km southwest of core hole C154. The data for core hole C154 are revised from Dyni and others (1966) with minor corrections. The bromine analyses for both core holes were made by wavelength-dispersive X-ray fluorescence spectrometry on pelletized samples of halite by O. B. Raup, H. L. Groves, Jr., and J. S. Wahlberg of the U.S. Geological Survey. One hundred data points shown for core hole C154 represent 168 bromine analyses. Where samples were closely spaced, two or more analyses were averaged and are shown by a single datum point. Similarly, 63 data points represent 70 bromine analyses for core hole C8. Because the drill core for subzone R-5E was probably mixed, the bromine values for the entire subzone are shown by a single datum point, which represents the average of eight analyses (53 ppm Br); the bar shows the range of values (41-74 ppm Br). Each of the remaining data points represents one analysis.

Core hole C154



Core hole C8



continued to accumulate bromine. Decreases in bromine content such as between subzones R-50 and R-50 and between L-5A and L-5D probably represent periods of freshening when the lake waters were replenished by relatively large quantities of inflowing water of low-bromine content before the next halite salting stage was reached.

#### Geochemical model of lake waters

Bradley and Eugster (1969) developed a quantitative geochemical model to explain the origin of the trona deposits in the Green River Formation in southwestern Wyoming. They showed that the precipitation of trona and nahcolite from saturated solutions in the system  $\text{Na}_2\text{CO}_3\text{-NaHCO}_3\text{-NaCl-H}_2\text{O}$  is controlled by the "bicarbonate quotient"  $(g\text{HCO}_3)/(g\text{HCO}_3 + g\text{CO}_3)$ , partial pressure of  $\text{CO}_2$  ( $P_{\text{CO}_2}$ ), temperature, and chloride content of the salting solution. Precipitation of nahcolite rather than trona is favored by a high bicarbonate quotient ( $>0.45$ ), high  $P_{\text{CO}_2}$ , cooler rather than warmer water, and a lower rather than higher chloride content. Probably the key factor is a high  $P_{\text{CO}_2}$ , which would increase the bicarbonate quotient. Lundell and Surdam (1975, p. 495) suggested that the  $P_{\text{CO}_2}$  of interstitial waters in the organic-rich sediments in the Piceance Creek Basin was probably high because large quantities of  $\text{CO}_2$  were generated by the anaerobic decay of organic matter. Bradley and Eugster (1969, table 15) found that sodium carbonate brines in contact with the atmospheric reservoir of  $\text{CO}_2$  have bicarbonate quotients of about 0.15 and precipitate trona at salting stage. These calculations suggest

that interstitial and lake brines from which the nahcolite in the Piceance Creek Basin precipitated were not in contact with the atmosphere, and that they maintained a high  $P_{CO_2}$  because of biogenic processes in an anaerobic environment.

Mineral equilibria for saturated solutions in the system  $Na_2CO_3$ - $NaHCO_3$ - $NaCl$ - $H_2O$  for trona, nahcolite, and halite in terms of sodium and chloride contents and bicarbonate quotient are shown on an isothermal section at 30°C in figure 28.

The solid line ABCD represents the hypothetical evolution of lake brine in the northern part of the Piceance Creek Basin during deposition of the saline facies. Point A represents a fresh to somewhat brackish water at the onset of closed-basin conditions during deposition of the black kerogenous clay shales of the Garden Gulch Member. Point B represents a dilute brine stage of the lake prior to the first precipitation of nahcolite (point A° from Bradley and Eugster, 1969, fig. 26). This point may be about the composition of interstitial waters when hydrolysis of silicate minerals began as evidenced by the gradual upward decrease in illite and by the first appearance of authigenic dawsonite and quartz at the base of the saline facies (Hite and Dyni, 1964, fig. 4). At point C, the lake brine was becoming nearly saturated for nahcolite. Only a slight reduction in water content due to compaction of the sediment containing such brine would have resulted in precipitation of disseminated nahcolite within the sediment (e.g., subzones L-2A, R-3B, etc.). When the lake brine itself became saturated for nahcolite, bedded microcrystalline nahcolite (R-3J and younger units) was deposited during nahcolite-

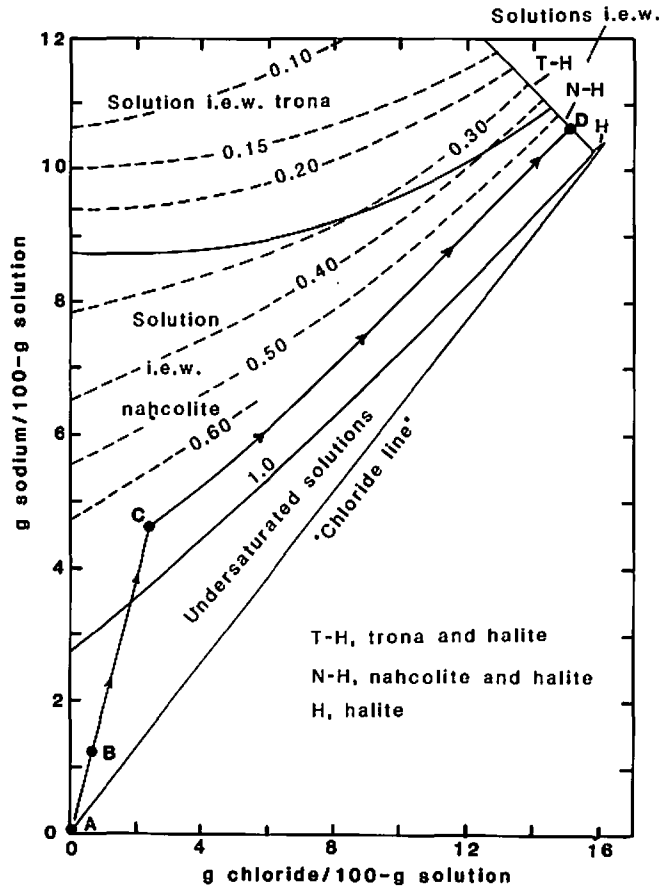


Figure 28.--Isothermal section at 30°C for saturated solutions in the system  $\text{Na}_2\text{CO}_3\text{-NaHCO}_3\text{-NaCl-H}_2\text{O}$  (modified from Bradley and Eugster, 1969, fig. 26). Solid lines are phase boundaries and dashed lines are bicarbonate quotients  $[\text{gHCO}_3/(\text{gHCO}_3+\text{CO}_3)]$  in the nahcolite+solution and trona+solution fields; i.e.w. = in equilibrium with. The "chloride line" represents a 1:1 mole ratio of sodium to chloride.



salting stages of the lake. The lake brine continued to slowly increase its chloride content at the expense of precipitating nahcolite until point D was reached when the brine became saturated for halite and nahcolite. At this point, the first of numerous beds of mixed halite and nahcolite starting with subzone R-5C was precipitated directly from the lake brine. During deposition of the saline facies, the composition of the lake brine undoubtedly changed repeatedly through time from an undersaturated condition to nahcolite- and nahcolite/halite-precipitating stages, but there was an overall increase of more soluble solutes including bromide in the parent brine. During the time oil-shale zones R-5 and L-5 were being deposited, the composition of the lake brine was probably close to that of point D.

#### Sources of Bicarbonate

##### Bacterial sulfate reduction

Syngenetic sulfate minerals are virtually absent in the several saline facies of the Green River Formation in Colorado, Wyoming, and Utah, yet considering the likely sources of sediment for Lakes Uinta and Gosiute, sulfate was probably a major ion in the waters entering these lakes. Bradley and Eugster (1969, table 7) used a composite chemical analysis of several water samples from the Green River at Jensen, Utah, as a model for runoff water (including springs) that fed Lake Gosiute during the time of trona and halite deposition. The same water is assumed to be the average of that supplying Lake Uinta during Parachute Creek time. The chemical composition is given in table 5.

Table 5.--Inferred composition of surface waters that fed Lake Uinta during deposition of the saline facies in Parachute Creek

time

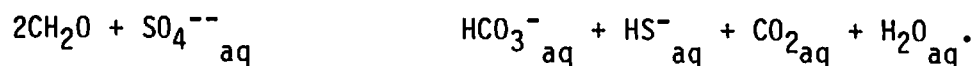
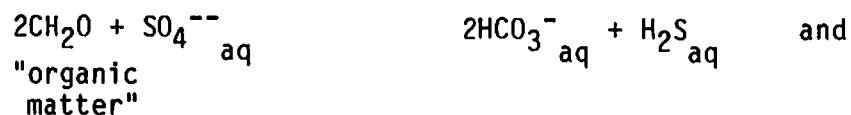
[Adapted from Bradley and Eugster, 1969, table 7]

Dissolved species	Parts per million	Equivalent parts per million
Fe <sup>++</sup>	0.1	0.004
Ca <sup>++</sup>	61.4	3.064
Mg <sup>++</sup>	20.7	1.703
Na <sup>+</sup>	44.5	1.936
K <sup>+</sup>	3.3	0.084
		<hr/> 6.791+
HCO <sub>3</sub> <sup>-</sup>	227.0	3.721
SO <sub>4</sub> <sup>--</sup>	120.5	2.509
Cl <sup>-</sup>	18.0	0.508
F <sup>-</sup>	0.4	0.021
NO <sub>3</sub> <sup>-</sup>	1.5	0.024
BO <sub>3</sub> <sup>---</sup>	0.2	0.010
		<hr/> 6.793-

Fahey (1962, p. 38) attributed the virtual absence of sulfate salts in the Green River Formation to biogenic reduction of sulfate in the euxinic environment of Lake Gosiute. Bradley and Eugster (1969, p. B24 and B30) favored this mechanism, but they also considered the possibility that the surface waters feeding the lake may have been sulfate deficient. However, low-sulfate waters seem unlikely in view of the probable sources of sediment as discussed earlier.

The absence of sulfate salts in the Green River Formation is attributed to biogenic reduction of sulfate by sulfate-reducing bacteria in interstitial waters of euxinic sediments of Lakes Uinta and Gosiute, and the reduced sulfur was lost to the atmosphere as  $H_2S$  and/or was precipitated as iron sulfide minerals. In this process, probably large quantities of bicarbonate were produced which eventually precipitated as carbonate minerals, including nahcolite. A prerequisite for the precipitation of sodium carbonate minerals is that the mole ratio of Na:Cl in the evolving waters from runoff to lake brine must exceed unity (table 5 and fig. 28).

The bacterial reduction of sulfate is a metabolic process mediated by sulfate-reducing bacteria (e.g., Desulfovibrio and Desulfotomaculum). The process involves the oxidation of metabolizable organic matter to carbon dioxide and bicarbonate and the reduction of sulfate to reduced sulfur species  $H_2S$  and  $HS^-$  while maintaining electrical neutrality of the water. The generalized reactions (Berner, 1971, p. 123) are



The reduced sulfur reacts with available iron (and other metals) to form pyrite and marcasite (or metastable iron monosulfides that convert later to iron disulfides) or escapes to the atmosphere as H<sub>2</sub>S. Since iron is present in dolomite and ankerite as well as in pyrite/marcasite in the marlstones of the saline facies, sufficient iron may have been available to precipitate all of the reduced sulfur, thereby lowering the amount of H<sub>2</sub>S to nontoxic levels for maintaining a high rate of bacterial sulfate reduction. The complete reduction of sulfate, rather than availability of organic matter, was the probable limiting factor that caused cessation of activity of sulfate-reducing bacteria in the sediment.

Evidence for fossil bacteria (trichobacteria) in the Green River Formation was reported by Bradley (1925, p. 257; 1931, p. 40 and pl. 19). Bradley suggested that the large amounts of structureless kerogen found in Green River oil shales was the result of extensive bacterial activity. Tissot and others (1978) reported that the types and distribution of organic substances of biogenic origin they found in the Green River Formation in the Uinta Basin also indicated that the kerogen, especially in the lower part of the formation, was synthesized and/or extensively reworked by micro-organisms.

Studies of fractionation of sulfur isotopes by Cole (1975), Jensen (1963), and others show a gradual increase of  $\delta^{34}\text{S}$  values in pyrite stratigraphically upward through the Green River Formation as well as from shore to basin-center rocks. These trends suggest preferential reduction of  $^{32}\text{S}$  by sulfate-reducing bacteria and loss of this sulfur as  $\text{H}_2\text{S}$  and/or pyrite while basin-center waters gradually increased in  $^{34}\text{S}$  through time.

The numbered sulfur maxima in the profiles of total sulfur for core holes C5 and C177 (fig. 25) may represent peak periods of bacterial reduction of sulfate accompanied with a high rate of production of bacterial bicarbonate. Many of these sulfur maxima coincide with zones of disseminated and bedded nahcolite which mark evaporative salting stages of Lake Uinta. During these stages, sulfate ion would be concentrated in the lake and interstitial waters permitting increased activity of sulfate-reducing bacteria. Some of the numbered sulfur cycles associated with nahcolite-rich units (subzones L-2A; R-3B; D, H; and R-4D) show a gradual upward increase in sulfur through the nahcolite-rich unit and reach a maximum value at or just above the top of the unit. This relationship may simply reflect the increase in concentration of sulfate in the evaporating lake water with a corresponding increase in the rate of sulfate reduction as these waters become incorporated in the accumulating sediments.

The numbered sulfur maxima which are not associated with bedded or disseminated nahcolite (sulfur cycles 1-11, 17, 18, and 21?) may represent evaporative phases of the lake that did not reach nahcolite-salting stage. Further study may reveal additional

correlatable sulfur maxima in the Green River Formation. Isotopic sulfur trends through these sulfur cycles have not yet been investigated.

In general, total sulfur varies with the kerogen content in the saline facies. Comparison of the shale-oil bar graphs for core holes C5 and C177 on plate 1 with the sulfur profiles for these core holes (fig. 25) shows that many of the numbered sulfur maxima coincide with units of high-grade oil shale. Cole (1975, fig. 27) found that  $\delta^{34}\text{S}$  values increase with the kerogen content of low- to moderate-grade oil shale. Bradley (1970, p. 995-996) noted that some types of blue-green and green algae (probable major kerogen precursors) synthesize lipids rather than carbohydrates in a stressed environment, and that sulfate-reducing bacteria cultured on lipids in sea water synthesize hydrocarbons.

It seems evident from the foregoing discussion that bacterial processes were important in the origin of kerogen and some of the carbonate minerals of the Green River Formation, especially during saline stages of the lake. The abundance of bacteria in lake and sediment waters in such an environment may be enormous.

#### Other bicarbonate sources

Other sources of bicarbonate include direct additions in runoff waters feeding the lake (table 5), and hydrolysis of aluminosilicate minerals. Hydrolysis reactions were undoubtedly important in the evolution of the alkaline waters of Lake Uinta during Parachute Creek time and in the origin of the unusual suite

of matrix minerals including dawsonite that comprise the marlstones in the saline facies. These reactions and associated geochemistry have been discussed by Smith (1974).

#### Processes of Sedimentation

On the basis of lithologies and sedimentary structures of the kerogenous marlstones and evaporites that make up the saline facies of the Parachute Creek Member in the Piceance Creek Basin, three major processes of sedimentation, turbiditic, pelagic, and evaporitic, are recognized. Deltaic sediments may be present in the saline facies at the north end of the basin, but data are not sufficient to discuss them here.

#### Turbiditic sedimentation

The occurrence of turbidity currents in modern lakes and reservoirs, and the large amounts of fine-grained sediments that can be transported, in some cases for long distances, and deposited by such currents are well known (e.g., Grover and Howard, 1938; Bell, 1942; Gould, 1951, 1960; Ludlam, 1969, 1974; and Sturm and Matter, 1978). However, few turbidites in Tertiary and older lacustrine deposits have been documented. The importance of turbidity currents as a major process of sedimentation in these deposits may have been underestimated.

Turbidity currents are interpreted to have played a major role in the deposition of kerogen-rich marly sediments in the saline facies of the Parachute Creek Member. Turbiditic marlstones comprise as much as 40-50 percent of the marlstone in the saline

facies below the dissolution surface. Individual beds range from a few centimeters or less to 11 m in thickness. Some of the thicker units may be multiple turbidites.

An example of a possible multiple turbidite is the 1-meter-thick "sixty" oil-shale bed in core hole C1. This bed consists of 16 units of alternating blebby marlstone and pelitic marlstone slightly streaked with black flakes. These units are 1.5 to 17 cm thick. The contacts between units are obscure but do not appear to be erosional. The alternating units of blebby and streaked marlstone suggest several successive turbidity currents, one immediately following the other. The base of the "sixty" bed rests with sharp contact on 7-9 cm of light-tan laminated marlstone which displays much internal flowage structure and small drag folds. Evidently, the turbidity current carrying the "sixty" bed sediments was strong enough to disrupt and locally drag along several centimeters of the underlying soft laminated marl.

Some beds underlying turbiditic marlstones in the saline facies show little evidence of disruption. Perhaps these marlstones represent medial or distal parts of the turbidity current under a flow regime too low to scour or disrupt the underlying sediments.

The marly composition of the turbidites in the Parachute Creek Member may partly explain the lack of graded bedding, Bouma sequences, and sole marks, which are well known sedimentary structures of siliciclastic marine turbidites. Turbidity currents during deposition of the saline facies may have been rather high density flows so that settling rates of the flat marlstone clasts



and flakes of kerogenous material were too low to permit significant size-differentiation of particles. A rapid decrease in the speed of the current could also account for poor sorting and lack of graded bedding (Sturm and Matter, 1978, p. 161).

The speeds of turbidity currents measured in lakes and reservoirs range from 7 to 50 cm/sec (0.25-1.8 km/hr) (Grover and Howard, 1938; Gould, 1951; Sturm and Matter, 1978). Assuming a median value of 15 cm/sec (0.57 km/hr), a turbidity current entering Lake Uinta at the south end of Piceance Creek Basin (fig. 26) could have reached the depocenter of the basin in 12 days, assuming a distance of 170 km from the south edge of the lake to the depocenter.

As much as 400 m of turbiditic marlstone in the saline facies below the dissolution surface was deposited near the basin depocenter in core holes C177 and C179. Here, the rate of deposition is probably the highest in the saline facies.

The amount of turbiditic marlstone comprising the sediments in the saline facies of the Parachute Creek Member (40-50 percent) does not seem unreasonably high in light of studies of sediments in modern lakes and reservoirs. For example, 17 to 72 percent of the upper 4 m of sediments in the central basin of Lake Brienz, Switzerland, is turbiditic sediment (Sturm and Matter, 1978, fig. 7). About 50 percent of the sediments in Green Lake near Fayetteville, New York, are carbonate-rich turbidites (Ludlam, 1974).

The sediment sources of turbidity flows in Lake Uinta are still unknown. Whether the turbidity currents originated from one

or several major point sources such as inlets of major streams, or whether the sediment was derived from random points about the lake basin has not yet been determined. The abundance of internally structureless dolomitic clasts in some turbidites suggests that these clasts were possibly derived from homogenous muds that accumulated above the chemocline of the lake, whereas the laminated clasts may have been plowed up from laminated marls in deeper parts of the basin.

Freshly deposited turbiditic marls may have provided an exceptionally favorable environment for growth of anaerobic bacteria, including sulfate-reducers. Sisler (1960, p. 189) reported bacterial populations, including sulfate-reducers, through 30 m of turbiditic Lake Mead sediment was continuously high, from 1 to 10 million per gram, of wet sediment which is comparable to bacterial populations in raw sewage. No doubt the large amounts of nutrient-rich interstitial waters in the turbiditic sediment favor a high rate of bacterial activity.

The direct correlation of  $\delta^{34}\text{S}$  values with organic content of Green River oil shale (Cole, 1975, figs. 27 and 28), the high organic content of turbiditic marlstone compared with laminated marlstone (fig. 13), and the fact that some of the numbered sulfur maxima (8-11) in figure 25 correlate with turbiditic marlstone suggest considerable bacterial activity. If much of the water of a turbidity current was stream runoff, especially stream flood waters, it could have carried large quantities of dissolved nutrients including fresh supplies of sulfate having low  $\delta^{34}\text{S}$  values that would favor increased bacterial sulfate reduction.

Stirring up the underlying sediments by turbidity currents may have allowed escape of bacterial wastes such as hydrogen sulfide.

Some of the thicker, freshly-deposited turbidites had a high water content and were probably subject to slumping and flowage. An example is illustrated on plate 3. The upper few meters of turbiditic marlstone immediately below nahcolite bed L-4D shows evidence of much soft-sediment flowage and slumping. The lenticular units of brown microcrystalline nahcolite at and below the base of nahcolite bed L-4D were originally deposited as continuous layers. While the sediments were still soft and plastic, these layers and the enclosing turbiditic marls were highly contorted by sliding and slumping.

#### Pelagic sedimentation

About 50 to 60 percent of the kerogenous marlstones of the saline facies below the dissolution surface are laminated marlstones, which were deposited in the open waters of the lake. These rocks typically consist of pairs of laminae, one light-hued and mineral-rich and the other dark and organic-rich, that Bradley (1930, 1948) described convincingly as varves deposited in a meromictic (chemically stratified) lake.

On the whole, laminated marlstones are more abundant in the upper part of the saline facies (oil-shale subzone L-4E and above) than in the lower part of the facies. During deposition of the upper part of the saline facies, the lake waters were more saline and possibly dense enough to inhibit the flow of bottom currents.

The laminated marlstones were most likely derived by

precipitation of carbonate minerals from the lake and interstitial sediment waters, and from organic debris of micro-organisms that settled to the lake bottom. Surface currents and undercurrents above the chemocline probably contributed some fine silt- to clay-sized siliciclastic sediment that was altered extensively during diagenesis.

Depositional rates for laminated marlstones were lower than for turbiditic marlstones. Bradley (1930, p. 99) reported the thickness of varves for oil shale of moderate grade (15-35 gallons of oil/ton  $\cong$  63-146 liters of oil/metric ton) ranged from 0.03 to 0.114 mm and averaged 0.065 mm. Assuming an average bulk density of  $2.1 \text{ g/cm}^3$  for the laminated marlstones, the average rate of accumulation of sediment (lithified) was only  $0.014 \text{ g/cm}^2/\text{yr}$ . In contrast, the turbiditic marlstones were deposited at highly varied rates that may have ranged from about the average rate for laminated marlstone to as much as  $200 \text{ g/cm}^2/\text{yr}$ . The duration of Lake Uinta in terms of varve counts per unit thickness of laminated marlstone as made by Bradley (1930) must include allowances for depositional rates for the turbiditic marlstones.

#### Evaporitic sedimentation

Available evidence (e.g., vertical sequence of mineral facies; bromine and  $\delta^{34}\text{S}$  data) suggests that the hydrographic basin of Lake Uinta was closed, and the lake waters became progressively more saline during deposition of the nahcolite and halite. Possibly, there were brief interludes of open-lake conditions represented by marlstones lacking evaporites, such as oil-shale subzone L-2B.

Although hydrolysis of silicate minerals and bacterial sulfate-bicarbonate reactions influenced lake- and sediment-water chemistry, climatically-controlled fluctuations in water salinity and sediment dewatering were primary factors in precipitation of nahcolite and halite.

Coarse-grained nahcolite aggregates clearly formed diagenetically from interstitial waters in the soft marly sediments as indicated by plastic deformation of bedding in laminated and turbiditic marlstones around the growing aggregates and by penetration of coarse-grained crystals into the surrounding marlstone (fig. 3C). The lake waters were probably quite saline but still insufficiently concentrated to precipitate nahcolite when they became incorporated into the sediments. During initial sediment dewatering, nahcolite began to nucleate, probably within a meter or so of the sediment-water interface as suggested by undisturbed thin tuff beds immediately above nahcolite aggregates (Lundell and Surdam, 1975, p. 495). In figure 3A, B, and D, bedding a few centimeters above nahcolite aggregates are relatively even and undisrupted.

At higher lake-water salinities, at or close to nahcolite-salting stage, fine-grained disseminated nahcolite precipitated at or just below the sediment-water interface and kept pace with deposition of kerogen-rich marl to form a "semi-bedded" unit of nahcolite. Some units of disseminated nahcolite are well laminated, displaying alternating nahcolite-rich and marl laminae. A pair of these laminae probably represent a seasonal cycle of deposition (varve) where nahcolite was precipitated during

the driest and hottest part of the summer, when evaporation was highest. Couplets of marlstone and nahcolite in figure 8 measure about 0.5-2 mm in thickness; an average depositional rate for these rocks is about 1 mm per year.

During nahcolite-salting stages of the lake, brown microcrystalline beds of laminated and structureless nahcolite were deposited directly from the brine. Depositional rates are difficult to estimate, but the laminated structure in some beds suggests low rates comparable to that for disseminated nahcolite. Some beds of microcrystalline nahcolite were deposited on soft turbiditic marls. The nahcolite beds were subsequently highly contorted or were disrupted by slumping of the soft underlying sediments and formed lenses and pods. An excellent example of soft-sediment deformation of bedded nahcolite is illustrated on plate 3.

Later in the history of the saline facies, the lake waters became saturated for halite and began to precipitate mixtures of halite, nahcolite, wegscheiderite, and trace amounts of trona. Brine depths during halite-salting stages were probably only a few meters (Dyini and others, 1970, p. 177), but the parent brine never completely evaporated as evidenced by the increasing amounts of bromine in halite upward through the halitic rocks. Parts of the halitic rocks display rhythmically deposited couplets of nahcolite and halite that are believed to be another type of seasonal deposit. An average rate of deposition was found to be about 5 cm/yr (Dyini and others, *ibid*).

The upper 45 m of the saline facies below the dissolution

surface contains local concentrations of northupite, searlesite, and shortite. Boron, a halophile element, was probably concentrated by the parent lake brines, and precipitated later when the brine became saturated for boron salts.

## Chapter VIII

### CONCLUSIONS

A variety of data derived from the study of cores from 10 drill holes that penetrate the sodium-mineral saline facies of the Parachute Creek Member in the Piceance Creek Basin reveals a complex interplay of biologic, chemical, and sedimentational processes that lead to deposition of the world's largest commingled resources of oil shale, nahcolite, and dawsonite.

The northern part of the Piceance Creek Basin acted as a chemical sump for Lake Uinta during Parachute Creek time. The Douglas Creek arch may have formed a submergent barrier between the Parachute Creek subbasin of Lake Uinta from the larger Uinta subbasin to the west, and aided in directing the flow of lake waters toward the deep northern part of the Piceance Creek Basin. Lithofacies relationships in the northern part of the Piceance Creek Basin indicate that the lake waters may have been as deep as 100-200 m, whereas in the southern part of the basin, the lake was much shallower.

During Parachute Creek time, Lake Uinta became a closed meromictic lake. The lake, however, was not ephemeral, but formed a permanent, chemically stratified, body of water that existed throughout the deposition of the saline facies. The lower lake waters (monimolimnion) and sediments were anoxic. Within the sediments, anaerobic bacteria, including sulfate-reducers, thrived.

During deposition of the saline facies, lake stages varied



widely between evaporative phases and less saline phases that were recorded by deposition of "semibedded" units of nahcolite and bedded halite and nahcolite, and indirectly, by cyclic deposition of pyrite and marcasite. Although the lake waters varied in salinity, there was an overall increase in the most soluble ions including those of bromine and boron.

Open-lake sedimentation was not static as previously thought, but involved strong turbidity currents that account for deposition of about one-half of the marlstones in the saline facies below the dissolution surface. The freshly deposited turbiditic marls were a favorable environment for high rates of anaerobic bacterial activity and the formation of exceptionally kerogen-rich sediment. The laminated marlstones were deposited under near-static conditions by seasonal precipitation of carbonate minerals and detritus of aquatic micro-organisms as described earlier by Bradley (1930).

Within the accumulating sediments, sulfate was essentially totally reduced by bacteria and much bicarbonate was produced. This bicarbonate along with that produced by hydrolysis of silicate minerals, precipitated in carbonate minerals including nahcolite. Hydrolysis of silicate minerals, another important process in the lake-sediment system, destroyed most of the original fine-grained siliciclastic detritus and precipitated a new suite of authigenic minerals including quartz, feldspars, and the unusual aluminocarbonate mineral, dawsonite, that make up the fine-grained matrix of the marlstones.

The rates of deposition of sediments in this chemically active environment were highly variable. The laminated marlstones and some of the bedded microcrystalline nahcolite were deposited at low rates measuring 1 mm, or much less, per year. In contrast, turbiditic marlstones and some of the bedded halite and nahcolite were deposited at much higher rates measured in centimeters per year to perhaps as much as a meter, or more, per year for brief durations.

The aggregates of coarse-grained nahcolite, which comprise five-eighths of the total resource of nahcolite, grew in the soft marls near the sediment-water interface. Lithification proceeded by gradual dewatering of the sediment. Sediment waters were expelled initially by diffusion, and finally along a developing system of prelithification microfractures.

## REFERENCES CITED

- Abbott, Ward, 1957, Tertiary of the Uinta Basin in Guidebook to the geology of the Uinta Basin, 8th annual field conference: Intermountain Association of Geologists, p. 102-109.
- Anderman, G. G., 1955, Tertiary deformational history of a portion of the north flank of the Uinta Mountains in the vicinity of Manila, Utah, in Green River Basin, 10th annual field conference: Wyoming Geological Association, p. 130-134.
- Armstrong, R. L., 1968, Sevier organic belt in Nevada and Utah: Geological Society of America Bulletin, v. 79, p. 429-458.
- Austin, A. C., 1971, Structure contours and overburden on the top of the Mahogany zone, Green River Formation, in the northern part of the Piceance Creek Basin, Rio Blanco County, Colorado: U.S. Geological Survey Miscellaneous Field Studies Map MF-309.
- Beard, T. N., Tait, D. B., and Smith, J. W., 1974, Nahcolite and dawsonite resources in the Green River Formation, Piceance Creek Basin, Colorado, in Guidebook to the energy resources of the Piceance Creek Basin, Colorado, 25th field conference: Rocky Mountain Association of Geology, p. 101-109.
- Bell, H. S., 1942, Density currents as agents for transporting sediments: Journal of Geology, v. 50, p. 512-547.
- Berner, R. A., 1971, Principles of chemical sedimentology: New York, McGraw-Hill Book Company, 240 p.
- Blatt, Harvey, Middleton, Gerard, and Murray, Raymond, 1980, [2nd ed.] Origin of sedimentary rocks: Englewood Cliffs, New Jersey, Prentice-Hall, Inc., 782 p.
- Bradley, W. H., 1925, A contribution to the origin of the Green River Formation and its oil shale: American Association of Petroleum Geologists Bulletin, v. 9, p. 247-262.
- \_\_\_\_\_, 1930, The varves and climate of the Green River epoch: U.S. Geological Survey Professional Paper 158-E, p. 87-110.
- \_\_\_\_\_, 1931, Origin and microfossils of the oil shale of the Green River Formation of Colorado and Utah: U.S. Geological Survey Professional Paper 168, 58 p.
- \_\_\_\_\_, 1936, The biography of an ancient American lake: The Scientific Monthly, v. 42, p. 421-430.

Bradley, W. H., 1948, Limnology and the Eocene lakes of the Rocky Mountain region: Geological Society of America Bulletin, v. 59, p. 635-648.

\_\_\_\_\_, 1963, Paleolimnology in Frey, D. G., [ed.] Limnology in North America: University of Wisconsin Press, p. 621-652.

\_\_\_\_\_, 1964, Geology of Green River Formation and associated Eocene rocks in southwestern Wyoming and adjacent parts of Colorado and Utah: U.S. Geological Survey Professional Paper 496-A, 86 p.

\_\_\_\_\_, 1970, Green River oil shale--concept of origin extended: Geological Society of America Bulletin, v. 81, p. 985-1000.

\_\_\_\_\_, 1973, Oil shale formed in desert environment; Green River Formation, Wyoming: Geological Society of America Bulletin, v. 84, p. 1121-1124.

Bradley, W. H., and Eugster, H. P., 1969, Geochemistry and paleolimnology of the trona deposits and associated authigenic minerals of the Green River Formation of Wyoming: U.S. Geological Survey Professional Paper 496-B, 71 p.

Braitsch, O., 1971, Salt deposits, their origin and composition: New York, Springer-Verlag, 297 p.

Brobst, D. A., and Tucker, J. D., 1973, X-ray mineralogy of the Parachute Creek Member, Green River Formation, in the northern Piceance Creek Basin, Colorado: U.S. Geological Survey Professional Paper 803, 53 p.

Buchheim, H. P., and Surdam, R. C., 1977, Fossil catfish and the depositional environment of the Green River Formation, Wyoming: Geology, v. 5, p. 196-198.

Burke, D. B., and McKee, E. H., 1979, Mid-Cenozoic volcano-tectonic troughs in central Nevada: Geological Society of America Bulletin, v. 90, p. 181-184.

Cashion, W. B., 1967, Geology and fuel resources of the Green River Formation, southeastern Uinta Basin, Utah and Colorado: U.S. Geological Survey Professional Paper 548, 48 p.

Cashion, W. B., and Donnell, J. R., 1972, Chart showing correlation of selected key units in the organic-rich sequence of the Green River Formation, Piceance Creek Basin, Colorado, and Uinta Basin, Utah: U.S. Geological Survey Oil and Gas Investigations Chart OC-65.

- Cole, R. D., 1975, Sedimentology and sulfur isotope geochemistry of Green River Formation (Eocene), Uinta Basin, Utah, Piceance Creek Basin, Colorado: University of Utah dissertation, 274 p.
- Cole, R. D., and Boyer, D. L., 1978, Iron-sulfide mineralogy and morphology in oil shale and marlstone, Green River Formation, Piceance Creek Basin, Colorado (abs.): American Association of Petroleum Geologists Bulletin, v. 62, no. 3, p. 505.
- Cole, R. D., and Picard, M. D., 1978, Comparative mineralogy of nearshore and offshore lacustrine lithofacies, Parachute Creek Member of the Green River Formation, Piceance Creek Basin, Colorado, and eastern Uinta Basin, Utah: Geological Society of America Bulletin, v. 89, p. 1441-1454.
- Culbertson, W. C., 1971, Stratigraphy of the trona deposits in the Green River Formation, southwest Wyoming: University of Wyoming Contributions to Geology [Trona Issue], v. 10, p. 15-23.
- Culbertson, W. C., Smith, J. W., and Trudell, L. G., 1980, Oil-shale resources and geology of the Green River Formation in the Green River Basin, Wyoming: U.S. Department of Energy, Laramie Energy Technical Center Report of Investigations LETC/RI-80/6, 102 p.
- Curry, H. D., 1964, Oil-content correlations of Green River oil shales, Uinta and Piceance Creek Basins in Guidebook to the geology and mineral resources of the Uinta Basin, 13th annual field conference: Intermountain Association of Petroleum Geologists, p. 169-171.
- Dane, C. H., 1955, Stratigraphic and facies relationships of the upper part of the Green River Formation and the lower part of the Uinta Formation in Duchesne, Uintah, and Wasatch Counties, Utah: U.S. Geological Survey Oil and Gas Investigations Chart OC-52, 2 sheets.
- Desborough, G. A., 1978, A biogenic-chemical stratified lake model for the origin of oil shale of the Green River Formation: an alternative to the playa-lake model: Geological Society of America Bulletin, v. 89, p. 961-971.
- Desborough, G. A., Pitman, J. K., and Donnell, J. R., 1973, Microprobe analysis of biotites--a method of correlating tuff beds in the Green River Formation, Colorado and Utah: U.S. Geological Survey Journal of Research, v. 1, p. 39-44.

- DeVoto, R. H., Stevens, D. N., and Bloom, D. N., 1970, Dawsonite and gibbsite in the Green River Formation: The Mines Magazine, v. 60, p. 17-21.
- Donnell, J. R., 1961, Tertiary geology and oil-shale resources of the Piceance Creek Basin between the Colorado and White Rivers, northwestern Colorado: U.S. Geological Survey Bulletin 1082-L, p. 835-891.
- Donnell, J. R., and Blair, R. W., Jr., 1970, Resource appraisal of three rich oil-shale zones in the Green River Formation, Piceance Creek Basin, Colorado: Colorado School of Mines Quarterly, v. 65, p. 73-87.
- Donnell, J. R., Cashion, W. B., and Brown, J. H., Jr., 1953, Geology of the Cathedral Bluffs oil-shale area, Rio Blanco and Garfield Counties, Colorado: U.S. Geological Survey Oil and Gas Investigations Map OM-135.
- Duncan, D. C., and Belser, Carl, 1950, Geology and oil-shale resources of the eastern part of the Piceance Creek Basin, Rio Blanco and Garfield Counties, Colorado: U.S. Geological Survey Oil and Gas Investigations Map OM-119.
- Duncan, D. C., and Denson, N. M., 1949, Geology of the Naval oil-shale Reserves 1 and 3, Garfield County, Colorado: U.S. Geological Survey Preliminary Oil and Gas Investigations Map 94, 2 sheets.
- Duncan, D. C., Hail, W. J., Jr., O'Sullivan, R. B., and Pippingos, G. N., 1974, Four newly named tongues of Eocene Green River Formation, northern Piceance Creek Basin, Colorado: U.S. Geological Survey Bulletin 1394-F, 13 p.
- Dyni, J. R., 1969, Structure of the Green River Formation, northern part of the Piceance Creek Basin, Colorado: The Mountain Geologist, v. 6, p. 57-66.
- \_\_\_\_\_, 1974, Stratigraphy and nahcolite resources of the saline facies of the Green River Formation in northwest Colorado in Guidebook to the energy resources of the Piceance Creek Basin, Colorado, 25th field conference: Rocky Mountain Association of Geologist, p. 111-122.
- \_\_\_\_\_, 1977, Distribution and origin of sulfur in Colorado oil-shale deposits (abs.): American Association of Petroleum Geologists Bulletin, v. 61, p. 1376-1377.
- Dyni, J. R., and Hawkins, J. E., 1981, Lacustrine turbidites in the Green River Formation, northwestern Colorado: Geology, v. 9, no. 5, p. 235-238.

- Dyni, J. R., Hite, R. J., and Raup, O. B., 1970, Lacustrine deposits of bromine-bearing halite, Green River Formation, northwestern Colorado in Third Symposium on Salt, Northern Ohio Geological Society, Cleveland, Ohio: p. 166-180.
- Dyni, J. R., Mountjoy, Wayne, Hauff, P. L., and Blackmon, P. D., 1971, Thermal method for quantitative determination of nahcolite in Colorado oil shale: U.S. Geological Survey Professional Paper 750-B, p. B194-B198.
- Ertl, Tell, 1947, Sodium bicarbonate (nahcolite) from Colorado oil shale: American Mineralogist, v. 32, p. 117-120.
- Eugster, H. P., and Hardie, L. A., 1975, Sedimentation in an ancient playa-lake complex: The Wilkins Peak Member of the Green River Formation of Wyoming: Geological Society of America Bulletin, v. 86, p. 319-334.
- Eugster, H. P., and Surdam, R. C., 1971, Bedded cherts in the Green River Formation: Geological Society of America Abstracts with Program, v. 3, no. 7, p. 559-560.
- \_\_\_\_\_ 1973, Depositional environment of the Green River Formation of Wyoming: a preliminary report: Geological Society of America Bulletin, v. 84, p. 1115-1120.
- Fahey, J. J., 1962, Saline minerals of the Green River Formation: U.S. Geological Survey Professional Paper 405, 50 p.
- Federal Energy Administration, 1974, Project independence blueprint final task force report, potential future role of oil shale: prospects and constraints: U.S. Department of the Interior, 495 p.
- von Gaertner, H. R., 1955, Petrographische Untersuchungen am nordwestdeutschen, Posidonienschiefer: Geologisches Rundschau, v. 43, p. 447-463.
- Gill, J. R., 1950, Flagstaff limestone of the Spring City-Manti area, Sanpete County, Utah: The Ohio State University Master of Science Thesis.
- Glass, J. J., 1947, Sodium bicarbonate (nahcolite) from Garfield County, Colorado (abs.): American Mineralogist, v. 32, p. 201.
- Gould, H. R., 1951, Some quantitative aspects of Lake Mead turbidity currents: Society of Economic Paleontologists and Mineralogists Special Publication 2, p. 34-52.

- Gould, H. R., 1960, Turbidity currents in Smith, W. O., Vetter, C. P., Cummings, G. B., and others, Comprehensive survey of sedimentation in Lake Mead, 1948-49: U.S. Geological Survey Professional Paper 295, p. 201-207.
- Grover, N. C., and Howard, C. S., 1938, The passage of turbid water through Lake Mead: American Society of Civil Engineers and Transactions, v. 103, p. 720-732.
- Hail, W. J., Jr., 1972, Preliminary geologic map of the Barcus Creek SE Quadrangle, Rio Blanco County, Colorado: U.S. Geological Survey Miscellaneous Field Studies Map MF-347.
- \_\_\_\_\_, 1974, Preliminary geologic map and section of the Barcus Creek Quadrangle, Rio Blanco County, Colorado: U.S. Geological Survey Miscellaneous Field Studies Map, MF-619.
- Hintze, L. F., 1973, Geologic history of Utah: Brigham University Geology Studies, v. 20, pt. 3, 181 p.
- Hite, R. J., and Dyni, J. R., 1967, Potential resources of dawsonite and nahcolite in the Piceance Creek Basin, northwest Colorado: Quarterly Colorado School of Mines, v. 62, p. 25-38.
- Hosterman, J. W., and Dyni, J. R., 1972, Clay mineralogy of the Green River Formation, Piceance Creek Basin - a preliminary study: U.S. Geological Survey Professional Paper 800-D, p. D159-D163.
- Hunt, C. B., 1956, Cenozoic history of the Colorado Plateau: U.S. Geological Survey Professional Paper 279, 99 p.
- Iijima, Azuma, and Hay, R. L., 1968, Analcime composition in tuffs of the Green River Formation of Wyoming: American Mineralogist, v. 53, p. 184-200.
- La Rocque, Aurele, 1960, Molluscan faunas of the Flagstaff Formation of central Utah: Geological Society of America Memoir 78, 100 p.
- Leopold, E. B., and MacGinitie, H. D., 1972, Development and affinities of Tertiary floras in the Rocky Mountains in Graham, A., ed., Floristics and Paleofloristics of Asia and Eastern North America: Amsterdam, Elsevier Publishing Company, p. 147-200.
- Ludlam, S. D., 1969, Fayetteville Green Lake, New York. III. The laminated sediments: Limnology and Oceanography, v. 14, p. 848-857.



- Ludlam, S. D., 1974, Fayetteville Green Lake, New York. VI. The role of turbidity currents in lake sedimentation: *Limnology and Oceanography*, v. 19, p. 656-664.
- Lundell, L. L., and Surdam, R. C., 1975, Playa-lake deposition: Green River Formation, Piceance Creek Basin, Colorado: *Geology*, v. 3, p. 493-497.
- MacDonald, R. E., 1972, Eocene and Paleocene rocks of the southern and central basins in *Geologic Atlas of the Rocky Mountain Region*: Rocky Mountain Association of Geologists, p. 243-256.
- Mauger, R. L., 1977, K-Ar ages of biotites from tuffs in Eocene rocks of the Green River, Washakie, and Uinta Basins, Utah, Wyoming, and Colorado: *University Wyoming Contributions to Geology*, v. 15, p. 17-41.
- Middleton, G. V., Hampton, M. A., 1973, Sediment gravity flows: mechanics of flow and deposition in Turbidites and deep-water sedimentation: *Society of Economic Paleontologists and Mineralogists, Pacific Section, Los Angeles*, 157 p.
- Milton, Charles, 1971, Authigenic minerals of the Green River Formation: *University of Wyoming Contributions to Geology (Trona Issue)*, v. 10, p. 57-63.
- Mullens, M. C., 1977, Bibliography of the geology of the Green River Formation Colorado, Utah, and Wyoming to March 1, 1977: *U.S. Geological Survey Circular 754*, 52 p.
- Murray, D. K., and Haun, J. D., 1974, Introduction to the geology of the Piceance Creek Basin and vicinity, northwestern Colorado in *Guidebook to the energy resources of the Piceance Creek Basin, Colorado*, 25th field conference: *Rocky Mountain Association of Geologists*, p. 29-39.
- O'Sullivan, R. B., 1974, Chart showing correlation of selected restored stratigraphic diagram units of the Eocene Uinta and Green River Formation, east-central Piceance Creek Basin, northwestern Colorado: *U.S. Geological Survey Oil and Gas Investigations Chart OC-67*.
- Picard, M. D., 1957, Green River and lower Uinta Formations-- subsurface stratigraphic changes in central and eastern Uinta Basin, Utah in *Guidebook to the geology of the Uinta Basin*, 8th annual field conference: *Intermountain Association of Petroleum Geologists*, p. 116-130.

- Pitman, J. K., 1979, Isopach, structure contour, and resource maps of the R-6 oil-shale zone, Green River Formation, Piceance Creek Basin, Colorado: U.S. Geological Survey Miscellaneous Field Studies Map MF-1069.
- Pitman, J. K., and Johnson, R. C., 1978, Isopach, structure contour, and resource maps of the Mahogany oil-shale zone, Green River Formation, Piceance Creek Basin, Colorado: U.S. Geological Survey Miscellaneous Field Studies Map MF-958.
- Robb, W. A., Smith, J. W., and Trudell, L. G., 1978, Mineral and organic distributions and relationships across the Green River Formation's saline depositional center, Piceance Creek Basin, Colorado: U.S. Department of Energy, Laramie Energy Technology Center Report of Investigations LETC/RI-78/6, 30 p.
- Roehler, H. W., 1974, Depositional environments of rocks in the Piceance Creek basin, Colorado in Guidebook to the energy resources of the Piceance Creek Basin, Colorado, 25th field conference: Rocky Mountain Association of Geologists, p. 57-64.
- Rowley, P. D., Steven, T. A., Anderson, J. J., and Cunningham, C. G., 1979, Cenozoic stratigraphic and structural framework of southwestern Utah: U.S. Geological Survey Professional Paper 1149, 22 p.
- Royse, C. F., Jr., Wadell, J. S., and Petersen, L. E., 1971, X-ray determination of calcite-dolomite: an evaluation: Journal of Sedimentary Petrology, v. 41, p. 483-488.
- Ryder, R. T., Fouch, T. D., and Elison, J. H., 1976, Early Tertiary sedimentation in the western Uinta Basin, Utah: Geological Society of America Bulletin, v. 87, p. 496-512.
- Saether, Ola Magne, 1980, The geochemistry of fluorine in Green River oil shale and oil-shale leachates: University of Colorado Ph. D. Thesis, 232 p.
- Shaw, D. B., and Weaver, C. E., 1965, The mineralogical composition of shales: Journal of Sedimentary Petrology, v. 35, p. 213-222.
- Siegel, Sidney, 1956, Nonparametric statistics for the behavioral sciences: McGraw-Hill Book Co., New York, 312 p.
- Sisler, F. D., 1960, Bacteriology and biochemistry of the sediments in Smith, W. O., Vetter, C. P., and Cummings, G. B., and others, Comprehensive survey of sedimentation in Lake Mead, 1948-49: U.S. Geological Survey Professional Paper 295, 254 p.

- Smith, J. W., 1963, Stratigraphic change in organic composition demonstrated by oil specific gravity-depth correlation in Tertiary Green River oil shales, Colorado: American Association of Petroleum Geologists Bulletin, v. 47, p. 804-813.
- \_\_\_\_\_, 1966, Conversion constants for Mahogany-zone oil shale: American Association of Petroleum Geologists Bulletin, v. 50, p. 167-170.
- \_\_\_\_\_, 1974, Geochemistry of oil-shale genesis in Colorado's Piceance Creek Basin in Guidebook to the energy resources of the Piceance Creek Basin, Colorado, 25th field conference: Rocky Mountain Association of Geologists, p. 71-79.
- Smith, J. W., and Milton, Charles, 1966, Dawsonite in the Green River Formation of Colorado: Economic Geology, v. 61, p. 1029-1042.
- Snow, C. B., 1970, Stratigraphy of basal sandstones in the Green River Formation, northeast Piceance [Creek] Basin, Rio Blanco County, Colorado: Mountain Geologist, v. 7, p. 3-32.
- Stanley, K. O., and Collinson, J. W., 1979, Depositional history of the Paleocene-lower Eocene Flagstaff limestone and coeval rocks, central Utah: American Association of Petroleum Geologists Bulletin, v. 63, p. 311-323.
- Stollenwerk, K. G., 1980, Geochemistry of leachate from retorted and unretorted Colorado oil shale: University of Colorado Ph. D. Thesis, 218 p.
- Sturm, Michael, and Matter, Albert, 1978, Turbidites and varves in Lake Brienz (Switzerland): deposition of clastic detritus by density currents: International Association of Sedimentologists Special Publication 2, p. 147-168.
- Surdam, R. C., and Parker, R. B., 1972, Authigenic aluminosilicate minerals in the tuffaceous rocks of the Green River Formation, Wyoming: Geological Society of America Bulletin, v. 83, p. 689-700.
- Surdam, R. C., and Stanley, K. O., 1980, Effects of changes in drainage boundaries on sedimentation in Eocene Lakes Gosiute and Uinta of Wyoming, Utah, and Colorado: Geology, v. 8, p. 135-139.
- Surdam, R. C., and Wolfbauer, C. A., 1975, Green River Formation: a playa-lake complex: Geological Society of America Bulletin, v. 86, p. 335-345.

- Tissot, B., Deroo, G., and Hood, A., 1978, Geochemical study of the Uinta Basin: formation of petroleum from the Green River Formation: *Geochimica and Cosmochimica Acta*, v. 42, p. 1469-1485.
- Trudell, L. G., Beard, T. N., and Smith, J. W., 1970, Green River Formation lithology and oil-shale correlations in the Piceance Creek Basin, Colorado: U.S. Bureau of Mines Report of Investigations 7357, 14 p.
- Trudell, L. G., Beard, T. N., and Smith, J. W., 1974, Stratigraphic framework of Green River Formation oil shales in the Piceance Creek Basin, Colorado in *Guidebook to the energy resources of the Piceance Creek Basin, Colorado*, 25th field conference: Rocky Mountain Association of Geologists, p. 65-69.
- Twenhofel, W. H., 1926, *Treatise on sedimentation*: Baltimore, Williams and Wilkins Company, 661 p.
- Tweto, Ogden, 1975, Laramide (Late Cretaceous-early Tertiary) orogeny in the southern Rocky Mountains in Curtis, B. F. (ed.), *Cenozoic history of the southern Rocky Mountains*: Geological Society of America Memoir 144, p. 1-44.
- Waldron, F. R., Donnell, J. R., and Wright, J. D., 1951, Geology of Debeque oil-shale area, Garfield and Mesa Counties, Colorado: U.S. Geological Survey Oil and Gas Investigations Map OM-114, 2 sheets.
- Williamson, C. R., and Picard, M. D., 1974, Petrology of carbonate rocks of the Green River Formation (Eocene): *Journal of Sedimentary Petrology*, v. 44, p. 738-759.
- Wolfbauer, C. A., and Surdam, R. C., 1974, Origin of nonmarine dolomite in Eocene Lake Gosiute, Green River Basin, Wyoming: *Geological Society of America Bulletin*, v. 85, p. 1733-1740.

**APPENDIX**

Table 4.--Quantitative mineralogy of nahcolitic marlstone in core hole CS

(Values below are in weight percent)

Depth (Meters)	Acid-soluble sodium	Aluminum	Potassium	Silicon	Calcium	Nahcolite	Tauconite	Dolomite	Calcite	K-feldspar	Na-feldspar	Quartz	Kerogen	Total (minerals + kerogen)
561.14--(Dissolution surface)														
561.14-561.75	4.48	4.1	1.5	13.1	5.3	11.4	8.5	21.6	1.5	10.7	14.3	11.3	28.9	108.2
561.75-562.36	1/1.31	3.8	1.6	14.0	4.0	12.9	8.2	12.9	3.0	11.4	11.3	14.8	14.5	99.0
562.36-562.97	11.1	2.3	0.9	7.5	4.9	36.1	7.6	16.6	3.2	6.4	2.4	10.2	23.0	105.6
562.97-563.58	12.3	2.0	0.8	6.6	5.0	40.8	7.1	18.0	2.7	5.7	1.1	9.6	22.3	107.4
563.58-564.18	14.0	1.7	0.6	6.6	4.4	46.7	7.6	15.5	2.6	4.3	---	11.4	23.5	111.6
564.18-564.79	18.0	1.1	0.4	2.7	3.2	62.9	4.9	14.7	---	2.8	---	6.1	14.4	105.9
564.79-565.40	21.0	1.2	0.7	4.7	1.6	71.5	9.0	7.4	---	5.0	---	6.8	4.9	104.5
565.40-566.01	2.44	4.2	2.3	16.4	5.0	4.1	8.3	23.0	---	16.4	10.4	17.4	15.8	95.3
566.01-566.62	17.7	2.0	0.8	7.0	2.7	60.3	7.5	12.4	---	5.7	0.4	11.0	4.2	101.5
566.62-567.23	9.03	3.6	1.5	12.2	4.0	28.1	8.4	18.4	---	10.7	9.7	12.6	8.6	96.4
567.23-567.84	11.0	3.2	1.3	11.2	3.8	36.0	7.2	17.5	---	9.3	9.3	11.6	9.7	100.5
567.84-568.45	1/7.40	4.9	1.7	14.0	3.1	22.6	7.6	14.3	---	12.1	22.4	6.6	15.4	101.1
568.45-569.06	1/1.38	4.5	1.4	14.5	3.4	18.0	8.6	15.6	---	10.0	14.6	11.8	12.3	95.0
569.06-569.67	12.2	3.1	1.3	10.3	3.0	37.7	11.8	13.5	---	9.3	---	16.0	9.7	98.3
569.67-570.28	9.15	4.5	1.7	16.4	4.0	27.4	10.3	18.4	---	12.1	13.5	18.0	13.3	113.0
570.28-570.89	5.75	4.0	1.5	12.2	3.2	13.0	13.7	14.7	---	10.7	---	16.6	13.7	83.2
570.89-571.50	5.70	4.4	2.0	15.9	3.3	16.9	6.9	15.2	---	14.2	16.8	13.3	14.2	92.4
571.50-572.11	4.82	4.7	1.4	15.4	3.4	15.0	4.5	15.6	---	10.0	28.1	7.2	13.9	94.3
572.11-572.72	4.95	4.1	1.5	15.9	3.6	13.7	7.5	16.6	---	12.7	16.1	16.1	15.1	95.7
572.72-573.33	4.82	4.6	1.6	15.4	3.4	13.9	6.4	15.5	---	11.4	22.4	10.2	15.4	95.3
573.33-573.94	7.52	4.6	2.2	15.0	3.5	24.4	5.3	16.1	---	15.7	20.4	8.0	11.9	101.7
573.94-574.55	2.35	6.5	2.3	18.2	3.3	---	14.7	15.2	---	16.4	20.9	14.0	12.2	93.4
574.55-575.16	5.47	4.2	1.5	13.6	5.4	12.6	12.7	24.8	---	10.7	7.7	16.9	11.5	96.9
575.16-575.77	10.5	2.6	0.9	9.4	6.8	31.8	11.3	25.4	3.2	6.4	---	16.0	13.5	107.5
575.77-576.38	2.10	3.9	1.6	14.5	8.1	---	13.2	37.3	---	11.4	3.2	21.4	11.5	98.0
576.38-576.99	4.97	3.3	1.4	12.6	7.0	13.8	7.5	32.2	---	10.0	9.1	14.3	18.9	105.7
576.99-577.60	11.6	2.5	0.6	8.4	6.0	15.3	12.1	27.6	---	4.3	---	15.2	9.3	103.8
577.60-578.21	6.30	3.4	1.0	12.6	5.9	14.9	13.9	27.1	---	7.1	1.0	21.7	14.0	99.7
578.21-578.82	5.80	3.7	1.3	13.6	4.5	15.4	9.9	21.2	---	9.3	9.2	16.8	14.3	96.0
578.82-579.42	5.72	3.6	1.3	13.1	4.9	15.1	9.9	22.5	---	9.3	8.2	16.4	13.7	95.1
579.42-580.03	6.35	3.7	1.6	14.0	4.8	14.8	14.4	22.1	---	11.4	---	22.6	14.7	100.0
580.03-580.64	6.77	3.9	1.6	15.5	7.8	21.0	6.4	15.9	---	11.4	15.5	15.1	14.3	119.6
580.64-581.25	1.95	3.7	1.4	12.6	5.7	2.0	8.8	26.2	---	10.0	10.6	13.2	12.4	83.2
581.25-581.86	1/0.91	5.5	2.5	15.9	4.4	---	5.7	20.2	---	17.8	25.3	4.4	23.0	97.5
581.86-582.47	10.1	3.2	1.5	9.4	3.8	34.4	4.3	17.5	---	10.7	13.2	4.1	18.6	102.8
582.47-583.08	5.60	3.7	1.5	11.7	3.4	16.9	6.1	15.6	---	10.7	14.8	8.0	24.2	96.3
583.08-583.69	11.8	3.1	1.1	7.5	5.6	48.8	2.8	17.6	4.4	7.8	4.1	9.2	8.8	102.5
583.69-584.30	8.17	2.4	1.4	11.2	7.2	25.6	7.3	29.0	2.3	10.0	0.7	17.1	6.4	95.2
584.30-584.91	10.9	1.2	0.7	4.7	2.9	64.7	7.5	13.3	---	5.0	---	6.8	1.8	101.1
584.91-585.52	5.15	3.3	1.4	12.6	6.1	18.2	7.3	28.1	---	10.0	9.4	14.1	20.4	107.4
585.52-586.13	4.65	3.3	1.3	13.6	5.8	10.9	10.4	26.7	---	9.3	4.3	20.1	18.6	100.3
586.13-586.74	4.12	3.3	1.2	12.7	4.8	24.1	9.5	22.1	---	8.5	6.6	16.0	17.0	101.9
586.74-587.35	7.03	4.6	2.2	15.5	5.1	23.5	3.7	23.5	---	15.7	23.1	7.1	20.6	117.2
587.35-587.96	2.60	3.8	1.9	11.7	4.9	5.3	6.2	22.5	---	13.6	9.1	10.1	17.6	86.9
587.96-588.57	2.43	4.6	2.0	15.5	5.4	5.4	6.0	24.8	---	14.2	20.4	9.9	20.8	101.6
588.57-589.18	5.44	4.5	1.4	14.0	3.9	16.2	8.3	14.8	1.7	10.0	19.3	10.3	21.4	100.9
589.18-589.79	18.4	1.1	0.7	2.7	3.2	66.1	1.9	14.7	---	5.0	2.5	3.0	10.3	103.5
589.79-590.40	15.2	1.7	0.7	5.6	5.5	54.8	1.9	25.3	---	5.0	3.4	6.4	7.9	104.4
590.40-591.01	1/8.90	1.7	1.1	7.5	7.8	39.1	4.1	10.9	2.8	7.8	1.6	9.8	11.4	98.5
591.01-591.62	1/1.68	3.3	1.0	12.2	6.4	13.7	10.5	26.5	1.5	7.1	6.2	17.2	16.4	104.3
591.62-592.23	4.88	3.2	1.3	12.6	7.4	12.6	9.0	27.1	3.8	7.8	7.4	16.8	18.9	103.4
592.23-592.84	4.53	3.3	1.1	13.1	7.4	8.5	13.8	29.9	2.3	7.8	---	23.0	19.7	104.9
592.84-593.45	4.63	3.6	1.3	12.6	7.1	11.8	8.8	29.3	1.8	9.3	10.3	13.9	19.2	104.3
593.45-594.06	7.83	2.8	1.0	10.3	7.5	24.0	7.9	27.3	3.9	7.1	6.1	13.2	15.3	104.9
594.06-594.66	6.70	2.5	1.4	11.7	6.6	21.2	5.8	27.4	1.6	10.0	4.4	15.6	15.5	101.3
594.66-595.27	7.10	2.8	1.4	10.8	5.7	21.8	7.1	26.2	---	10.0	4.9	13.3	16.0	99.3
595.27-595.88	6.13	2.4	1.4	11.7	7.2	19.5	5.0	26.6	3.5	10.0	8.8	12.6	14.0	99.7
595.88-596.49	1/0.70	1.4	1.7	7.5	5.6	37.6	4.4	25.8	---	7.1	2.8	9.5	12.8	100.0
596.49-597.10	13.5	2.1	1.1	7.5	5.4	47.3	3.5	24.9	---	7.8	6.7	6.4	15.5	112.0
597.10-597.71	9.45	3.2	1.7	7.4	3.4	37.1	8.7	15.6	---	8.5	15.5	4.0	21.4	101.3
597.71-598.32	1/1.53	3.6	1.4	11.7	3.7	24.4	9.6	17.9	---	10.0	8.1	13.0	15.8	97.9
598.32-598.93	5.17	4.6	1.8	14.9	4.9	11.8	17.5	15.4	---	10.7	11.9	14.9	15.9	95.8
598.93-599.54	9.37	4.3	1.8	14.9	4.7	17.8	11.7	19.3	---	10.0	11.1	15.9	16.4	97.2
599.54-600.15	9.87	3.3	1.7	10.3	3.6	29.7	11.4	16.6	---	8.5	2.6	14.7	12.8	96.2
600.15-600.76	4.93	5.1	1.4	15.4	4.3	6.5	13.7	19.4	---	10.0	16.1	15.4	14.6	96.0
600.76-601.37	5.25	4.7	1.6	13.6	4.0	14.8	11.3	18.4	---	11.4	9.6	15.2	16.4	97.0
601.37-601.98	11.9	3.2	1.4	11.7	3.1	37.8	6.0	14.3	---	10.0	10.9	10.1	14.2	105.3
601.98-602.59	4.17	5.0	1.3	14.5	3.7	10.5	8.4	17.0	---	12.8	21.7	7.8	25.2	103.2
602.59-603.20	2.92	4.6	1.7	15.8	4.1	1.7	12.8	22.1	---	15.1	10.0	21.3	19.9	101.3

Table 4.--Quantitative mineralogy of subcolitic marlstone in core hole CS--continued  
(Values below are in weight percent)

Depth (Meters)	Acid-soluble sodium	Aluminum	Potassium	Silicon	Calcium	Magnesium	Durostone	Dolomite	Calcite	K-feldspar	Na-feldspar	Quartz	Zircon	Total (minerals* kerogen)
605.03-605.64	2.43	3.8	2.0	15.4	6.4	---	15.2	29.4	---	14.2	---	22.7	20.4	103.0
605.64-606.25	4.65	2.9	1.8	12.2	7.0	12.2	8.2	12.2	---	12.8	1.2	17.0	17.5	101.1
606.25-606.86	9.52	2.6	1.4	13.1	6.7	31.7	5.3	10.8	---	10.0	6.3	17.3	17.5	118.8
606.86-607.47	4.79	2.0	1.4	9.4	6.8	14.8	4.6	11.3	---	10.0	1.6	12.4	16.6	85.4
607.47-608.08	4.26	3.9	1.6	13.6	4.9	19.4	---	22.5	---	11.4	27.2	3.1	15.5	99.1
608.08-609.69	2.80	4.8	1.3	15.9	5.9	---	17.5	27.1	---	9.3	6.0	23.9	13.8	97.6
608.69-609.30	1/2.91	4.5	0.8	15.9	5.5	---	18.2	20.5	2.6	5.7	---	5.2	26.8	106.0
609.30-609.90	1.96	4.9	1.6	15.9	6.4	---	12.3	29.4	---	11.4	14.6	16.7	23.9	105.2
609.90-610.51	1.39	4.1	1.9	15.9	6.5	---	8.7	28.1	1.0	13.5	11.2	17.5	24.0	104.1
610.51-611.12	1.71	4.6	1.8	15.9	5.8	---	10.7	26.7	---	12.8	13.1	16.7	23.3	103.3
611.12-611.73	1.88	3.6	1.4	13.1	7.0	---	11.8	31.1	0.6	10.0	4.1	18.7	24.7	101.0
611.73-612.34	1.75	3.9	1.4	14.0	7.2	---	11.0	31.1	---	10.0	6.5	17.6	30.0	110.2
612.34-612.95	6.65	2.5	1.2	9.8	5.9	19.9	7.5	20.5	3.6	8.5	2.5	11.7	26.8	102.5
612.95-613.56	1.73	4.1	1.6	15.0	6.6	---	10.8	27.1	1.8	11.4	9.4	18.3	30.7	109.4
613.56-614.17	7.11	3.0	.8	11.7	5.4	18.8	12.4	24.8	---	5.7	1.1	20.6	20.2	103.7
614.17-614.78	1/1.55	2.9	1.2	11.7	6.4	22.0	9.8	24.6	2.6	8.5	2.3	17.9	17.2	105.0
614.78-615.39	1.91	3.9	1.5	15.4	5.6	7.2	12.3	25.8	---	10.7	5.5	22.3	21.2	104.9
615.39-616.00	3.81	4.1	1.6	15.4	5.4	8.5	9.3	24.8	---	11.4	12.2	17.2	24.1	107.5
616.00-616.61	6.09	3.4	1.2	13.1	5.1	15.7	11.2	20.2	1.8	8.5	4.5	19.4	23.2	104.6
616.61-617.22	6.45	3.6	1.3	13.6	4.9	17.5	10.4	22.5	---	9.3	7.3	18.1	21.9	107.0
617.22-617.83	3.59	3.9	1.5	15.9	6.0	6.4	11.5	24.5	1.7	10.7	6.9	22.4	23.3	107.4
617.83-618.44	1.81	5.0	1.8	16.8	5.9	---	11.3	27.1	---	12.8	15.9	16.7	24.9	102.8
618.44-619.05	2.13	4.9	1.6	16.8	5.5	---	13.3	26.3	---	11.4	12.6	19.9	25.3	107.9
619.05-619.66	1/2.34	4.1	.9	15.0	5.3	5.7	14.7	24.4	---	6.4	7.1	23.1	26.5	107.8
619.66-620.27	2.22	5.0	1.7	15.9	5.8	---	13.9	26.7	---	12.1	11.9	18.0	25.1	107.7
620.27-620.88	3.99	4.4	1.2	15.0	5.2	6.9	13.2	22.0	1.0	8.5	10.7	19.2	23.9	105.5
620.88-621.49	2.30	4.7	1.4	15.5	5.9	---	14.4	27.1	---	10.0	10.0	19.8	25.2	106.6
621.49-622.10	1.16	3.9	1.4	23.0	7.7	---	7.3	5.0	16.5	10.0	15.3	32.3	20.3	106.6
622.10-622.71	1.82	5.2	1.6	14.0	3.2	---	11.4	8.5	3.4	11.4	19.0	9.1	45.2	108.4
622.71-623.32	1.21	4.9	1.4	15.9	2.0	---	7.6	5.4	2.1	10.0	24.4	10.8	(48.6)	103.8
623.32-623.93	2.15	5.1	1.4	20.2	5.2	---	13.5	3.2	11.1	10.0	15.6	26.0	22.3	101.9
623.93-624.54	8.64	1.9	.9	6.6	3.9	29.4	3.7	9.5	4.6	6.4	5.7	6.1	43.6	103.9
624.54-625.14	18.3	0.9	.4	2.8	3.2	65.2	2.8	9.9	3.1	2.8	0.9	3.5	21.9	109.3
625.14-625.75	9.67	2.0	.9	7.0	7.3	33.1	3.8	18.8	8.1	6.4	6.4	6.4	23.4	105.4
625.75-626.36	8.88	2.0	.7	7.5	10.2	28.1	7.4	25.4	11.7	5.0	1.2	12.0	17.3	108.1
626.36-626.97	7.50	2.9	1.0	10.3	8.0	23.5	6.7	27.0	5.3	7.1	9.3	11.9	18.9	108.9
626.97-627.58	16.0	1.5	.8	6.6	3.8	55.8	4.6	12.9	2.5	5.7	0.9	9.3	11.8	103.9
627.58-628.19	1/2.38	4.1	1.2	16.4	6.4	---	14.9	29.4	---	8.5	4.6	26.4	21.5	105.4
628.19-628.80	1.54	3.8	1.6	16.4	7.0	---	9.6	32.2	---	11.4	8.2	21.8	24.4	103.1
628.80-629.41	1.76	4.2	1.6	16.8	6.9	---	11.0	31.7	---	11.4	10.0	21.7	25.8	111.7
629.41-630.02	10.6	2.6	1.2	10.3	5.0	35.9	4.9	23.0	---	5.5	8.4	10.7	19.4	110.8
630.02-630.63	9.24	2.5	1.4	10.8	5.6	31.0	4.7	25.8	---	10.0	6.3	12.3	15.2	105.3
630.63-631.24	5.28	3.6	2.0	13.1	5.5	16.1	5.5	25.3	---	14.2	11.6	10.8	25.6	109.2
631.24-631.85	3.67	4.6	2.0	14.0	5.4	9.5	6.7	24.8	---	14.2	19.1	7.6	26.4	104.4
631.85-632.46	3.85	5.0	1.4	18.2	3.6	---	24.1	16.6	---	10.0	---	32.5	21.3	104.4
632.46-633.07	1/3.80	5.4	1.4	23.0	2.4	---	23.9	11.0	---	10.0	---	42.8	4.9	92.5
633.07-633.68	2.79	5.1	1.7	17.3	4.4	---	16.9	20.2	---	12.1	7.4	24.1	17.6	98.3
633.68-634.29	18.4	1.7	.8	5.6	2.0	64.2	6.4	9.2	---	5.7	---	9.3	10.8	104.6
634.29-634.90	2.74	5.1	1.3	16.8	5.0	---	17.2	23.0	---	9.3	9.6	23.4	22.4	104.8
634.90-635.51	2.41	4.9	1.5	19.6	4.9	---	15.1	22.5	---	10.7	10.1	28.1	23.1	109.6
635.51-636.12	2.65	5.3	1.2	15.9	5.1	---	16.6	24.8	---	8.5	13.2	19.4	25.1	107.7
636.12-636.73	2.69	4.1	1.1	15.9	6.5	---	16.9	29.9	---	7.8	1.8	27.7	18.0	102.1
636.73-637.34	1.27	4.1	2.4	15.9	6.2	---	8.0	28.5	---	17.1	9.3	16.6	19.6	99.0
637.34-637.95	1.72	4.6	1.8	17.3	5.0	---	10.9	23.0	---	12.8	13.0	19.8	22.0	101.4
637.95-638.56	1.80	4.8	1.8	16.3	4.3	---	11.3	22.1	---	12.8	14.0	18.0	22.9	101.1
638.56-639.17	6.33	4.0	1.4	13.6	4.1	18.9	8.8	18.9	---	10.0	13.5	13.4	19.1	101.6
639.17-639.78	1/1.38	5.2	1.7	16.8	4.9	---	8.7	22.5	---	12.1	23.3	12.1	22.4	101.2
639.78-640.39	1/1.78	5.2	1.7	16.8	5.0	---	11.2	23.0	---	12.1	14.8	15.2	21.8	102.1
640.39-640.99	2.28	4.3	1.3	15.9	6.0	---	14.3	27.6	---	9.3	7.1	23.2	18.7	100.1
640.99-641.60	2.26	4.2	1.1	15.4	7.0	---	14.2	32.2	---	7.9	7.7	22.6	22.9	107.4
641.60-642.21	1.96	4.6	2.1	16.8	5.1	---	12.3	23.5	---	15.0	8.3	20.6	23.5	103.4
642.21-642.82	1/2.11	5.0	1.8	16.8	4.7	---	13.2	21.6	---	12.8	12.4	19.1	24.2	103.4
642.82-643.43	1/2.23	5.0	1.6	15.9	4.7	---	14.0	21.6	---	11.4	12.4	18.1	25.1	102.6
643.43-644.04	2.47	5.6	1.4	16.4	4.9	---	15.5	22.5	---	10.0	16.9	17.1	24.8	106.7
644.04-644.65	2.43	5.3	1.4	15.9	4.7	---	15.2	21.6	---	19.0	14.4	17.7	25.1	104.0
644.65-645.25	7.45	3.7	1.2	12.6	3.3	19.0	14.1	17.5	---	8.5	2.2	19.9	21.9	103.2
645.25-645.87	1/2.35	5.0	1.7	15.9	4.7	---	14.7	21.6	---	12.1	10.4	19.1	26.2	104.1
645.87-646.48	2.76	4.9	1.7	15.4	4.9	---	14.2	27.1	---	12.1	10.4	20.0	24.7	103.6
646.48-647.09	2.10	5.5	1.7	15.9	4.5	---	13.2	20.7	---	12.1	18.1	13.8	26.0	103.9
647.09-647.70	3.04	4.7	2.1	15.9	3.8	6.5	7.9	17.5	---	15.0	17.2	12.5	26.9	103.5

Table 4.--Quantitative mineralogy of nahcolitic marlstone in core hole C5--continued

(Values below are in weight percent)

Depth (Meters)	Acid-soluble sodium	Aluminum	Potassium	Silicon	Calcium	Nahcolite	Dawsonite	Dolomite	Calcite	K-feldspar	Na-feldspar	Quartz	Kerogen	Total (minerals+kerogen)
647.70-648.31	1/1.64	5.1	2.0	16.8	4.4	3.9	10.3	20.2	---	14.2	17.4	14.7	25.6	106.4
648.31-649.02		5.05	5.0	1.6	14.0	3.9	15.5	10.1	17.9	11.4	19.5	9.2	23.7	107.3
649.02-649.53		3.37	3.4	1.2	12.6	7.4	5.9	11.0	34.0	9.5	5.0	18.0	27.3	109.8
649.53-650.14	1.67	3.3	1.1	13.1	9.1	---	10.5	38.6	1.8	7.8	5.6	19.1	28.3	111.7
650.14-650.75	1/1.76	3.3	1.1	11.7	8.8	---	11.0	37.3	1.7	7.8	4.6	16.8	28.2	107.5
650.75-651.36	1.77	3.3	1.1	13.1	9.1	---	11.1	40.3	0.9	7.8	4.5	19.9	28.0	112.4
651.36-651.97	1.58	2.9	1.2	13.5	8.7	---	9.9	37.8	1.2	8.5	2.1	22.1	27.7	109.4
651.97-652.58	1.08	3.6	1.6	14.0	8.5	---	6.8	37.1	1.1	11.4	11.9	14.4	28.2	110.9
652.58-653.19	.81	3.5	1.8	23.4	5.4	---	5.1	24.8	---	12.8	12.7	33.0	23.5	112.0
653.19-653.80	2.26	5.7	1.7	19.6	2.5	---	14.2	11.5	---	12.1	18.2	21.6	25.2	102.8
653.80-654.41	1.58	4.4	1.5	14.0	4.7	---	9.9	21.6	---	10.7	14.7	13.0	37.6	107.4
654.41-655.02	1.62	4.2	1.4	13.1	4.5	---	10.1	20.7	---	10.0	12.9	12.7	38.9	105.4
655.02-655.62	1.70	4.0	1.3	14.0	6.1	---	10.6	28.1	---	9.3	10.8	16.6	24.5	99.8
655.62-656.23	1/1.77	4.2	1.7	19.6	5.4	---	4.8	24.8	---	12.1	20.6	19.9	21.8	104.1
656.23-656.84	2.34	6.8	2.3	20.6	1.9	---	14.7	8.7	---	16.4	24.0	17.0	10.4	91.2
656.84-657.45	2.83	6.5	1.7	19.6	2.3	---	17.7	10.6	---	12.1	19.5	20.7	12.9	93.5
657.45-658.06	1/2.13	7.3	2.3	20.6	2.0	---	13.3	9.2	---	16.4	31.2	12.0	13.6	95.8
658.06-658.67	2.58	7.5	1.9	21.6	1.2	---	13.7	5.5	---	13.5	26.2	19.5	12.1	95.5
658.67-659.28	1/3.37	6.3	2.1	18.2	3.0	---	21.1	13.9	---	15.0	8.7	23.3	12.2	94.0
659.28-659.89	2.72	6.4	2.1	18.2	3.0	---	17.0	13.8	---	15.0	17.1	17.5	11.4	91.8
659.89-660.50	3.51	6.5	1.6	18.2	2.2	---	22.0	10.1	---	11.4	12.4	23.1	15.1	94.0
660.50-661.11	1/2.92	6.0	2.0	16.9	3.7	---	19.3	17.0	---	14.2	11.6	18.8	12.4	92.3
661.11-661.72	1.21	6.1	1.8	19.2	2.4	---	7.6	11.0	---	12.8	33.4	7.7	16.4	88.9
661.72-662.33	1/4.20	3.7	2.1	14.0	7.3	9.8	9.5	33.6	---	15.0	4.6	17.1	8.9	98.4
662.33-662.94	1/2.86	5.2	1.7	16.4	5.7	---	17.9	26.2	---	12.1	6.5	22.8	9.8	95.3
662.94-663.55	2.98	5.0	2.0	16.8	5.1	---	19.7	23.5	---	14.2	1.2	25.9	9.7	93.2
663.55-664.16	2.33	5.9	2.2	15.9	4.1	---	14.6	13.9	---	15.7	16.0	12.9	13.1	91.1
664.16-664.77	3.82	4.4	1.1	15.5	6.2	5.3	14.8	25.3	1.7	7.8	8.4	22.4	20.5	106.2
664.77-665.38	4.68	4.0	1.4	14.0	6.2	9.5	14.3	23.5	---	10.0	3.5	21.1	15.2	102.1
665.38-665.99	13.4	2.3	.6	9.4	5.1	42.5	11.1	12.9	5.8	4.3	---	17.3	10.8	104.6
665.99-666.60	6.49	2.6	1.3	9.8	10.7	17.6	10.5	27.5	11.8	9.3	---	15.0	14.6	106.2
666.60-667.21	9.79	2.1	1.2	8.9	9.2	30.4	9.2	33.9	6.2	8.5	---	13.5	7.6	106.4
667.21-667.82	6.77	2.5	1.1	9.4	9.4	26.5	9.5	25.5	9.6	7.8	---	15.0	13.8	107.8
667.82-668.43	7.27	2.2	1.1	9.4	8.8	21.0	9.5	23.2	9.4	7.3	---	15.0	16.1	102.1
668.43-670.26	(No sample)													
670.26-670.86	15.5	2.0	.9	6.6	3.6	51.2	9.3	12.0	2.5	6.4	---	10.0	14.6	106.0
670.86-671.47	15.9	1.3	.7	4.7	6.6	53.8	7.4	15.8	7.9	5.0	---	6.8	10.7	107.4
671.47-672.08	11.3	2.0	1.0	8.0	7.9	36.7	7.9	22.8	7.3	7.1	---	12.5	15.7	110.1
672.08-672.69	9.90	2.8	.9	9.4	7.0	29.2	11.9	25.7	3.0	5.4	---	16.0	18.0	111.2
672.69-673.91	(No sample)													
673.91-674.52	1/1.60	3.9	1.4	12.6	8.0	6.5	10.0	29.4	4.6	10.0	10.3	13.5	24.2	107.4
674.52-675.13	4.47	3.4	1.4	12.6	7.8	11.2	8.8	29.3	3.6	10.0	7.6	15.3	23.1	108.9
675.13-675.74	6.24	3.1	1.2	11.7	7.1	17.7	8.7	25.7	3.9	3.5	6.2	15.3	20.0	105.9
675.74-676.35	3.04	3.8	1.5	13.1	7.8	5.6	9.4	28.5	4.0	10.7	9.7	14.5	23.9	106.3
676.35-676.96	(No sample)													
676.96-677.57	7.14	2.9	1.0	11.2	7.1	20.0	10.4	25.8	3.2	7.1	2.5	17.7	18.7	106.4
677.57-678.18	11.5	2.2	1.0	8.9	5.6	37.7	7.4	19.2	3.5	7.1	1.2	13.6	12.9	102.7
678.18-678.79	5.20	3.2	1.4	10.8	8.0	13.8	8.9	30.5	3.4	10.0	5.5	12.9	19.6	104.6
678.79-679.40	12.2	2.6	1.0	8.4	4.4	40.0	7.8	20.2	---	7.1	4.3	10.4	18.0	107.9
679.40-680.01	10.3	3.7	1.5	10.3	3.4	33.4	7.5	15.6	---	19.7	12.7	6.4	21.1	107.2
680.01-680.62	5.30	3.8	1.8	12.6	4.7	16.4	5.1	21.6	---	12.8	15.6	7.9	19.2	97.7
680.62-681.23	2.80	6.2	2.0	15.4	4.4	4.6	9.7	20.2	---	14.2	19.3	3.6	24.5	106.1
681.23-681.84	1/3.4	3.2	1.1	9.4	1.6	44.0	13.0	7.4	---	7.8	3.8	12.5	16.7	103.1
681.84-682.45	1/0.43	2.4	1.4	7.5	2.4	53.8	2.7	11.0	---	10.9	9.0	3.4	13.9	103.8
682.45-683.06	1/1.48	3.4	1.4	10.9	5.4	26.2	9.3	24.8	---	19.0	6.8	17.0	16.2	105.36
683.06-683.67	(No sample)													
683.67-684.28	13.7	2.6	1.0	8.0	4.3	44.5	9.4	19.8	---	7.1	1.5	11.5	(6.2)	(100.0)
684.28-684.89	16.7	1.7	.8	5.2	3.8	57.5	6.0	17.5	---	5.7	0.7	7.3	11.9	136.1
684.89-685.50	13.9	2.0	.9	6.6	4.7	46.8	6.8	21.6	---	5.4	1.0	9.3	14.2	106.1
685.50-686.10	14.9	2.0	.9	5.6	5.0	50.4	6.9	23.0	---	5.4	0.3	3.4	10.8	107.8
686.10-686.71	15.8	1.7	.9	6.6	4.5	54.1	6.9	20.7	---	5.4	---	10.0	8.4	105.7
686.71-687.32	7.74	2.2	1.6	11.7	6.0	22.8	9.4	27.6	---	11.4	---	17.7	16.4	105.2
687.32-687.93	15.3	1.6	.8	6.6	4.6	52.2	6.3	15.1	3.3	5.7	---	10.4	11.8	104.8
687.93-688.54	15.5	1.7	.9	7.0	4.3	53.2	5.9	19.8	---	6.4	---	10.8	9.7	105.9
688.54-689.15	14.1	1.7	.9	7.0	5.3	47.4	7.1	24.4	---	5.4	---	10.8	10.0	106.1
689.15-689.76	15.1	1.5	.6	5.2	5.4	50.7	7.7	24.9	---	4.3	---	8.4	10.4	106.2
689.76-690.37	8.16	2.6	.8	10.3	7.7	24.7	9.6	24.2	6.0	5.7	2.4	16.7	17.3	107.1
690.37-690.98	10.9	2.2	1.1	9.4	6.6	36.4	5.9	24.7	3.1	7.2	3.3	12.8	12.6	106.6
690.98-691.59	1/7.53	2.5	1.0	10.3	3.3	24.1	6.0	33.7	---	7.1	7.6	12.7	19.7	114.8
691.59-692.20	1/1.52	4.1	1.4	14.0	5.9	9.1	17.1	27.1	---	10.0	12.0	15.3	18.3	102.1



Table 4.--Quantitative mineralogy of nahcolitic marlstone in core hole CS--continued  
(Values below are in weight percent)

Depth (Meters)	Acid-soluble sodium	Aluminum	Potassium	Silicon	Calcium	Nahcolite	Dawsonite	Dolomite	Calcite	K-feldspar	Na-feldspar	Quartz	Kerogen	Total (minerals+kerogen)
692.20-692.81	4.19	4.1	1.8	14.5	5.6	11.0	7.4	25.8	---	12.8	14.3	12.9	18.6	102.8
692.81-693.42	4.79	4.4	2.2	15.0	4.6	14.7	4.8	21.2	---	15.7	19.3	8.7	19.8	104.1
693.42-694.03	5.00	3.9	2.2	13.1	5.0	19.2	3.4	23.0	---	15.7	16.9	6.1	19.9	104.4
694.03-694.64	7.10	3.4	1.9	13.1	5.0	23.0	5.0	23.0	---	13.5	11.1	11.6	18.2	105.2
694.64-695.25	1/0.44	3.6	1.9	13.1	4.8	27.8	2.8	22.1	---	13.5	17.2	7.4	16.6	107.0
695.25-695.86	15.3	2.5	1.2	9.4	3.1	52.3	6.2	14.3	---	8.5	5.0	11.1	11.2	108.6
695.86-696.47	18.0	2.5	.9	6.6	2.0	61.3	7.7	9.2	---	6.4	4.3	7.0	10.5	106.4
696.47-697.08	4.51	5.7	2.1	19.5	1.6	11.2	9.0	7.4	---	15.0	24.8	6.4	28.5	102.3
697.08-697.69	22.8	.7	.3	1.9	.6	01.4	2.6	2.8	---	2.1	0.1	2.6	12.5	104.5
697.69-698.30	20.8	.8	.6	2.3	1.3	74.3	2.9	6.0	---	4.3	---	2.2	14.0	103.6
698.30-698.91	18.6	1.4	.7	4.7	2.8	64.5	5.8	12.9	---	5.0	---	6.8	15.0	110.1
698.91-699.52	1/11.1	2.6	.7	9.8	5.3	35.8	8.2	24.4	---	5.0	5.7	13.8	20.9	113.8
699.52-700.13	1/1.75	3.6	1.3	13.1	7.0	14.3	11.0	32.2	---	9.3	6.3	17.7	15.5	106.2
700.13-700.74	5.60	3.4	1.2	13.1	6.6	13.9	11.2	23.7	3.6	8.5	4.5	19.4	18.6	103.5
700.74-701.34	5.24	3.6	.9	13.6	6.7	12.1	12.1	30.8	---	6.4	7.0	20.2	20.5	109.0
701.34-701.95	9.48	3.3	1.1	10.3	4.8	30.4	7.3	22.1	---	7.9	11.5	9.1	22.9	111.0
701.95-702.56	1/1.43	5.3	2.3	15.5	5.7	---	9.0	26.2	---	16.4	19.8	9.0	29.1	109.4
702.56-703.17	1/1.11	4.4	2.4	15.5	5.9	---	7.9	27.1	---	17.1	14.0	12.5	29.1	106.8
703.17-703.78	1.63	4.8	2.1	14.5	5.9	---	10.2	27.1	---	15.0	14.0	11.7	29.0	107.0
703.78-704.39	2.14	4.4	1.0	13.6	6.9	---	13.4	31.7	---	7.1	11.6	16.5	27.8	108.2
704.39-705.00	2.68	4.4	1.3	14.0	6.8	4.3	9.4	31.3	---	9.3	16.9	12.4	27.4	110.9
705.00-705.61	1.38	4.6	1.6	15.9	7.2	---	3.6	33.1	---	11.4	18.2	14.1	26.9	112.4
705.61-706.22	2.20	4.1	1.3	15.5	6.6	3.5	7.8	30.4	---	9.3	17.0	15.5	27.3	110.7
706.22-706.83	1.54	4.2	1.6	14.0	6.2	---	9.9	28.5	---	11.4	12.3	14.1	32.0	108.1
706.83-707.44	7.91	3.3	1.3	10.8	5.0	24.7	6.9	19.6	1.8	9.3	10.9	9.7	25.5	108.5
707.44-708.05	1/0.45	1.0	.3	3.3	1.9	77.1	2.8	8.7	---	2.1	2.6	3.9	8.2	105.5
708.05-708.66	16.6	2.4	.4	5.6	3.8	57.3	5.7	17.5	---	2.8	10.2	3.1	12.6	109.3
708.66-709.27	6.24	3.7	1.1	12.6	5.9	17.3	9.4	27.1	---	7.8	11.4	14.1	19.5	106.7
709.27-709.88	2.68	4.9	1.4	15.0	5.7	---	16.7	26.2	---	10.0	7.9	20.2	20.8	101.8
709.88-710.49	1.60	4.8	1.7	15.9	5.9	---	10.0	27.1	---	12.1	17.0	14.5	21.1	101.9
710.49-711.10	1/2.03	4.9	1.2	15.9	5.8	---	12.7	26.7	---	9.5	16.4	17.2	21.3	102.9
711.10-711.71	1/1.41	4.9	1.6	15.9	5.1	---	8.8	23.5	---	11.4	20.8	12.4	21.2	98.0
711.71-712.32	1/1.37	5.2	2.2	16.8	5.3	---	8.6	24.4	---	15.7	20.2	12.0	20.0	100.7
712.32-712.93	1/1.37	6.1	2.8	19.2	3.9	---	9.3	17.9	---	19.9	25.5	10.7	16.5	98.8
712.93-713.54	1/1.94	5.8	1.7	18.2	2.6	---	12.2	12.0	---	12.1	22.8	15.4	13.9	88.4
713.54-714.15	2.24	5.2	1.6	18.2	4.8	---	14.0	22.1	---	11.4	14.3	21.8	10.3	93.8
714.15-714.76	1.37	4.8	2.0	15.9	7.0	---	11.1	32.2	---	14.2	13.0	15.8	8.6	95.0
714.76-715.37	1/1.69	4.1	1.7	15.9	6.9	---	10.6	31.7	---	12.1	9.2	19.9	10.7	94.2
715.37-715.98	1/1.44	5.4	1.8	26.2	1.6	---	9.0	7.4	---	12.8	24.0	31.3	15.4	99.9
715.98-716.59	1/2.98	6.7	2.2	20.6	2.3	---	18.0	10.6	---	15.7	17.5	21.9	10.2	93.9
716.59-717.19	2.54	6.0	1.9	19.2	3.5	27.0	15.9	16.1	---	13.5	16.6	19.8	11.3	92.2
717.19-717.80	2.73	8.0	1.9	19.2	1.7	---	17.1	7.8	---	12.8	34.5	9.1	12.4	91.7
717.80-718.41	3.23	7.6	1.7	18.2	2.0	---	20.2	9.2	---	12.1	25.6	13.5	11.6	92.3
718.41-719.02	10.4	4.0	1.4	11.7	1.5	31.4	11.3	6.9	---	10.0	8.9	12.5	16.9	97.8
719.02-719.63	19.1	2.0	.8	4.7	1.5	64.1	3.5	5.9	---	5.7	7.7	1.1	13.2	102.2
719.63-720.24	22.4	.5	.5	1.9	1.4	73.7	14.0	6.4	---	3.6	---	1.4	9.6	109.0
720.24-720.85	20.2	1.1	.6	3.3	2.0	71.7	4.5	9.2	---	4.3	---	4.3	9.7	103.1
720.85-721.46	12.0	2.8	.8	10.3	4.9	38.3	8.5	25.5	---	5.7	6.4	13.9	9.0	105.0
721.46-722.07	6.04	3.1	1.6	10.8	7.7	18.7	5.8	35.4	---	11.4	8.9	9.6	10.3	100.1
722.07-722.68	2.53	4.9	1.6	14.5	7.8	4.7	7.4	35.9	---	11.4	23.3	7.6	15.5	106.1
722.68-723.29	1.71	5.2	1.8	15.9	5.0	---	10.7	27.6	---	12.8	19.0	12.7	18.5	101.3
723.29-723.90	3.43	4.6	1.6	15.4	5.9	7.2	9.1	27.1	---	11.4	17.3	17.7	18.4	104.3
723.90-724.51	3.22	5.1	1.6	15.4	5.8	6.1	9.7	26.7	---	11.4	21.1	11.0	18.6	104.7
724.51-725.12	13.5	3.2	1.0	9.4	4.0	42.2	10.2	18.4	---	7.1	25.1	14.0	13.1	109.2
725.12-725.73	3.71	4.2	1.8	13.1	7.1	10.5	5.2	32.7	---	12.8	19.2	6.5	17.1	104.1
725.73-726.34	1/1.05	5.5	2.2	16.4	4.5	10.9	6.6	20.7	---	15.7	26.7	6.6	19.0	106.2
726.34-726.95	2.43	5.2	2.0	15.9	4.5	---	15.2	21.2	---	14.2	9.4	18.3	20.4	98.8
726.95-727.56	(No sample)													
727.56-728.17	4.22	4.1	1.2	11.7	7.0	14.6	1.4	37.2	---	8.5	29.2	---	28.9	114.9
728.17-728.78	1.52	3.8	1.3	13.1	7.4	5.3	2.4	34.0	---	9.3	27.4	3.2	31.0	110.7
728.78-729.39	1/5.64	3.3	1.0	10.3	6.3	17.3	4.4	29.0	---	7.1	16.9	5.3	27.0	108.4
729.39-730.00	1/0.34	3.6	1.2	11.7	6.5	14.4	1.5	30.4	---	9.5	24.2	2.9	28.2	110.1
730.00-730.61	3.79	3.6	1.4	11.7	6.3	11.9	1.3	31.7	---	10.0	19.5	5.7	29.4	111.0
730.61-731.22	0.10	4.1	1.5	14.9	2.6	---	11.9	39.1	---	19.7	25.4	4.9	24.7	107.0
731.22-731.82	0.11	3.7	1.3	13.1	9.4	---	0.7	38.5	---	9.3	26.9	4.2	26.2	105.0
731.82-732.43	1/0.16	4.0	1.4	14.0	4.1	---	2.3	32.1	3.3	12.8	22.7	6.1	21.4	100.1
732.43-733.04	1.61	5.3	1.7	15.9	6.3	---	11.3	22.0	3.8	12.1	19.5	12.4	23.4	104.9
733.04-733.65	2.51	4.4	1.2	15.5	6.0	---	15.7	22.5	2.8	8.5	9.1	21.4	23.0	102.1
733.65-734.26	1.97	3.6	1.5	12.2	6.2	---	12.3	25.1	1.9	10.7	1.9	17.5	24.1	104.0
734.26-734.87	1.92	4.5	1.3	14.0	7.0	---	12.0	24.3	4.1	9.3	13.1	15.9	26.4	104.4

Table 4.--Quantitative mineralogy of nahcolitic marlstone in core hole C5--continued

(Values below are in weight percent)

Depth (Meters)	Acid-soluble sodium	Aluminum	Potassium	Silicon	Calcium	Nahcolite	Dawsonite	Dolomite	Calcite	K-feldspar	Na-feldspar	Quartz	Kerogen	Total (minerals+kerogen)	
734.87-735.48	0.31	3.6	1.2	14.5	9.0	---	1.9	17.5	2.1	8.5	23.4	9.4	24.7	107.6	
735.48-736.09	0.14	3.3	1.5	15.9	8.7	---	0.9	17.5	1.4	10.7	20.4	13.1	25.0	103.0	
736.09-736.70	0.11	3.6	1.2	13.6	9.5	---	0.7	18.3	2.9	8.5	25.7	5.9	23.8	105.9	
736.70-737.31	0.97	5.1	1.6	18.2	6.0	---	5.1	23.1	2.5	11.4	27.8	12.5	21.2	104.5	
737.31-737.92	1.10	5.0	1.8	14.0	5.1	---	6.9	29.1	---	12.8	24.0	5.2	29.5	105.5	
						Mean	16.3	9.5	22.4	1.0	10.0	10.6	14.2	19.3	103.4
						Standard deviation	19.3	4.3	7.6	2.2	3.2	9.1	6.4	6.9	5.3
						<sup>2/</sup> normalized mean	15.3	9.5	21.1	0.9	9.5	10.0	13.3	14.3	102.00

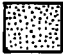






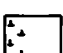
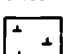
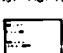

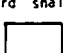
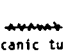

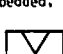
<sup>1/</sup> Acid-soluble sodium was determined on sample after water-soluble nahcolite was removed.

<sup>2/</sup> No sample, assume 0 percent nahcolite.



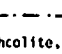
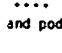


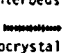

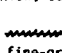
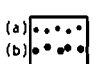
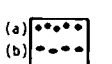


<sup>3/</sup> The mineral averages are calculated to total 100 percent minerals and kerogen, except for the values for nahcolite, dawsonite, and kerogen which are assumed to be correct.

## EXPLANATION FOR PLATES 1 AND 2



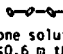
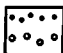

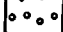
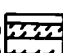
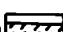
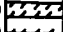
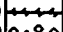
### MARLSTONE AND SILICICLASTIC LITHOLOGIES

-  Sandstone
-  Siltstone
-  Marly siltstone
-  Interbedded sandstone and siltstone
-  Dolomitic siltstone  
Contains clasts of marlstone
-  Shale; part or all may be oil shale
-  Marlstone
-  Marlstone grading to kerogenous marlstone
-  Kerogenous marlstone and minor marlstone
-  Silty kerogenous marlstone
-  Interbedded kerogenous marlstone and shale
-  Blocky kerogenous marlstone
-  Volcanic tuff bed
-  Illitic kerogenous shale; dark brownish gray, fissile to thin-bedded, laminated
-  Core missing


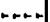
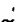
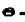
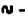
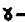

### NAHCOLITE AND ASSOCIATED MINERALS

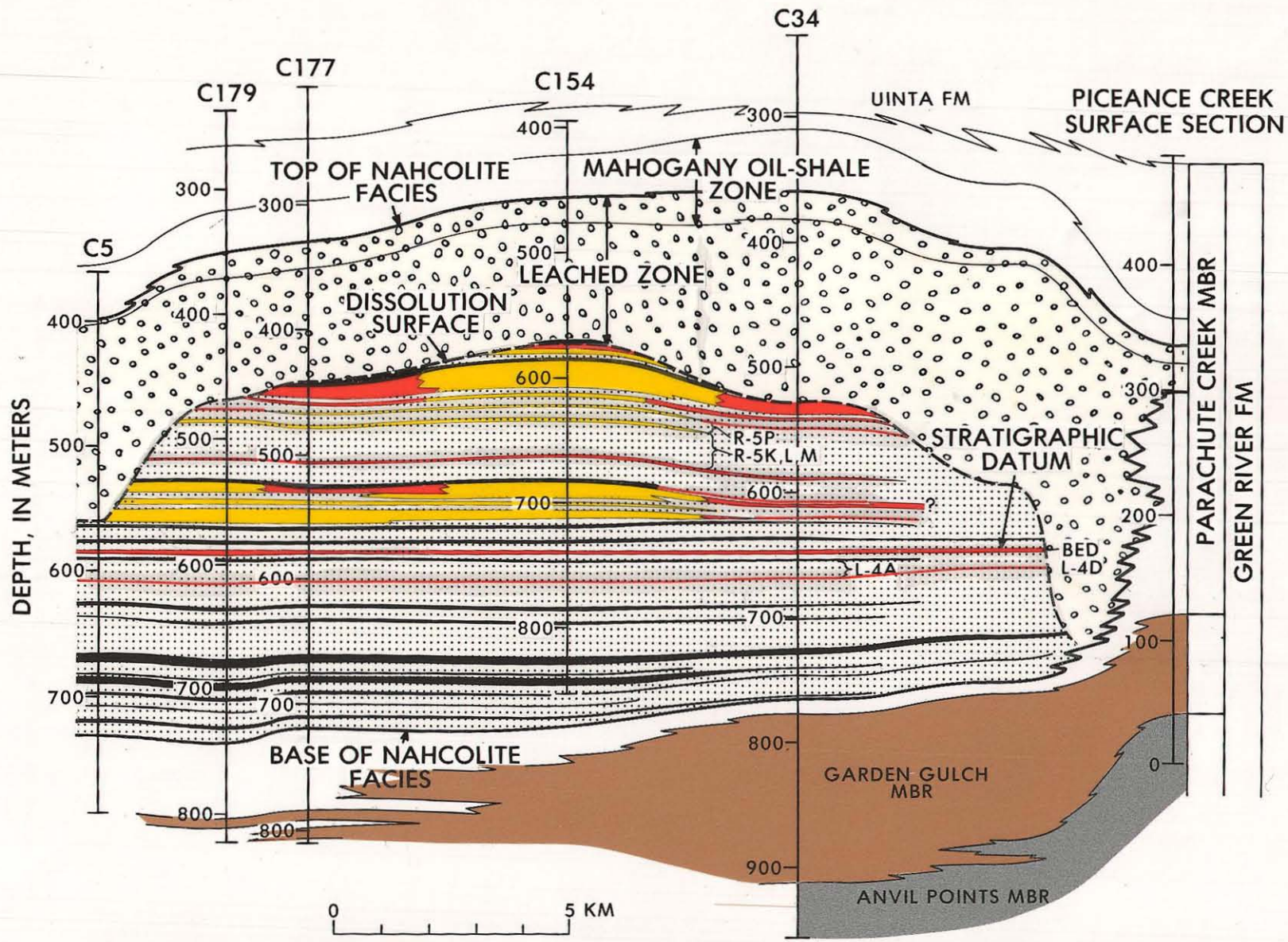
-  Halite and wegscheiderite, includes some marlstone
  -  Halite and nahcolite, bed  $\geq 0.75$  m thick; includes some marlstone
  -  Halite and nahcolite, bed  $< 0.75$  m thick
  -  Patches and pods of halite
  -  White coarse-grained nahcolite; some interbeds of marlstone
  -  Brown microcrystalline nahcolite, bed  $\geq 0.75$  m thick; some interbeds of marlstone
  -  Brown microcrystalline nahcolite, bed  $< 0.75$  m thick
  -  Disseminated fine-grained nahcolite in kerogenous marlstone, bed  $\geq 0.75$  m thick; some nahcolite-free nahcolite
  -  Disseminated fine-grained nahcolite in kerogenous marlstone, bed  $< 0.75$  m thick
  -  Kerogenous marlstone containing scattered nahcolite aggregates (a)  $\geq 8$  cm across and (b)  $\geq 8$  cm across
  -  Kerogenous marlstone containing scattered (a) brown crystals and (b) tan fine-grained pods and lenses of nahcolite
- 3.38/53.0
- Thickness in meters and weight percent nahcolite of selected units
- 8.53/4.26%  $Al_2O_3$
- Thickness of dawsonite-rich marlstone and amount of acid-soluble alumina
- W, wegscheiderite ( $NaHCO_3 \cdot Na_2CO_3$ )  
 T, trona ( $NaHCO_3 \cdot Na_2CO_3 \cdot 2H_2O$ )  
 S, shortite ( $Na_2CO_3 \cdot 2CaCO_3$ )  
 No, northupite ( $Na_2CO_3 \cdot MgCO_3 \cdot NaCl$ )  
 Se, searlesite ( $NaBSi_2O_6 \cdot H_2O$ )
- (a)  I (D, A)  
 (b)  I (D, A)
- Highest (a) or lowest (b) significant occurrence of illite (I), dawsonite (D), or analcime (A); depth in meters

### SOLUTION FEATURES

-  Rubby marlstone or kerogenous marlstone
  -  Marlstone solution breccia  $\geq 0.6$  m thick
  -  Marlstone solution breccia  $< 0.6$  m thick
  -  (a)  (b) 
  -  (a)  (b)  (c) 
- Solution cavities from leaching of nahcolite aggregates; (a)  $\geq 8$  cm across, (b)  $\geq 8$  cm across
- Zone of disseminated crystal cavities (a)  $\geq 0.75$  m thick, (b)  $< 0.75$  m thick; (c) scattered crystal cavities

### ACCESSORY DATA

- C.P. 360.3 m - Core point in meters
-  Fly larvae
-  Laminae of fine-grained crystals (not nahcolite)
-  Fossil fish fragments
-  Ostracodes
-  Carbonaceous fossil plant fragments
-  Unidentified fossil fragments
-  Blebbly and streaked structure
- TD 793.39 m - Total depth in meters



- |  |   |  |   |   |  |   |
|--|---|--|---|---|--|---|
| <div style="border: 1px solid black; width: 40px; height: 20px; margin-bottom: 5px;"></div> DOLOMITIC OIL SHALE<br>WITHOUT NAHCOLITE | <div style="border: 1px solid black; width: 40px; height: 20px; background: repeating-linear-gradient(45deg, transparent, transparent 2px, black 2px, black 4px); margin-bottom: 5px;"></div> WITH NAHCOLITE AGGREGATES | <div style="border: 1px solid black; width: 40px; height: 20px; background: radial-gradient(circle, black 1px, transparent 1px); background-size: 10px 10px; margin-bottom: 5px;"></div> WITH SOLUTION CAVITIES<br>AND BRECCIA | <div style="border: 1px solid black; width: 40px; height: 20px; background-color: #8B4513; margin-bottom: 5px;"></div> FISSILE CLAY SHALE | <div style="border: 1px solid black; width: 40px; height: 20px; background-color: #FFD700; margin-bottom: 5px;"></div> HALITE, NAHCOLITE, AND MARLSTONE | <div style="border: 1px solid black; width: 40px; height: 20px; background-color: #FF0000; margin-bottom: 5px;"></div> WHITE AND BROWN NAHCOLITE | <div style="border: 1px solid black; width: 40px; height: 20px; background: linear-gradient(to right, black 50%, white 50%); margin-bottom: 5px;"></div> DISSEMINATED NAHCOLITE |
|--|---|--|---|---|--|---|



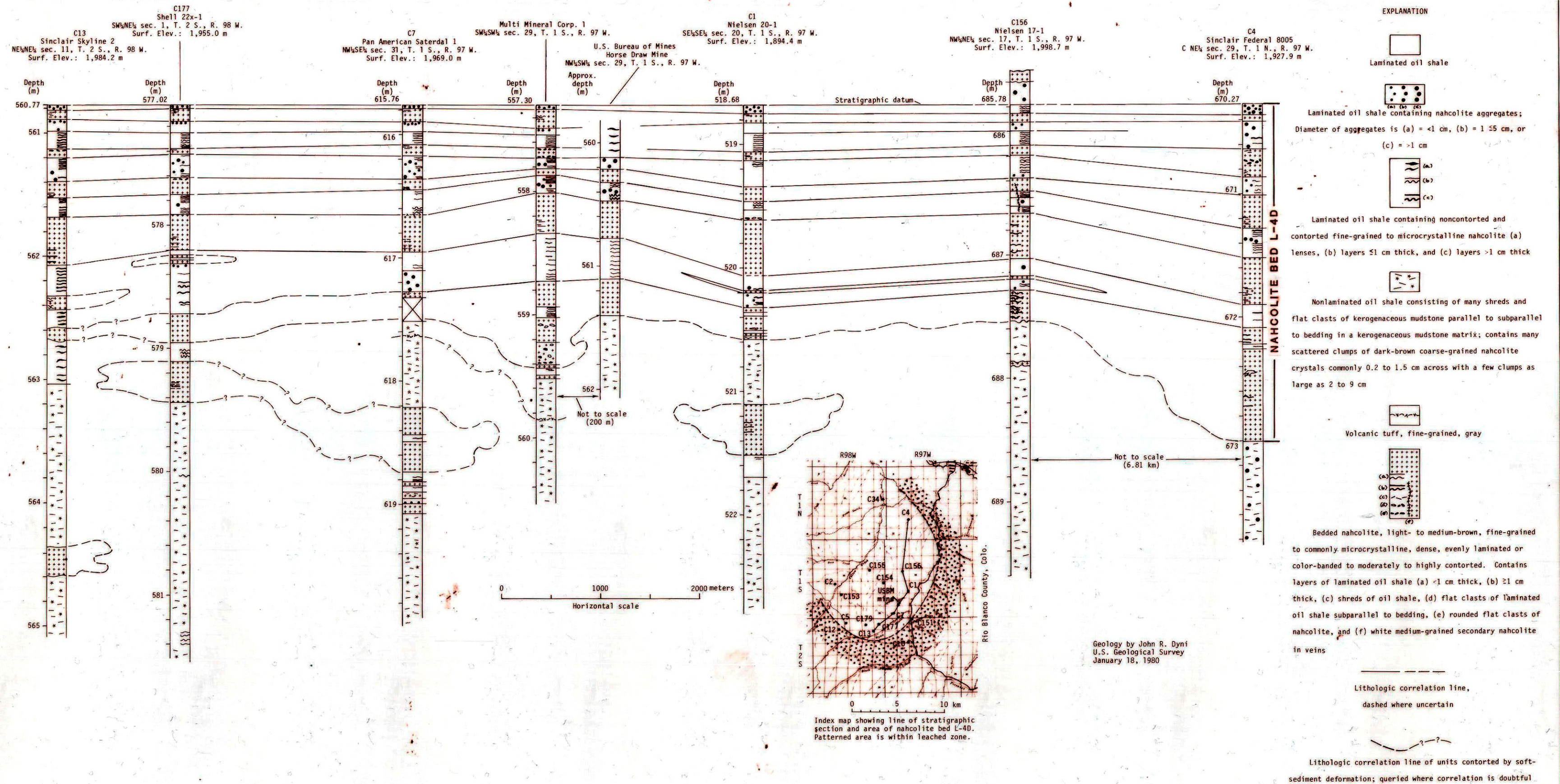


Plate 3. North-south stratigraphic cross section of nahcolite bed L-4D in the northern part of the Piceance Creek Basin, Colorado